# POLYMER-SHELL BONDED PHASE FOR IMPROVING ONLINE LC-MS ANALYSIS OF INTACT PROTEINS, MABS, AND ADCS

by

**Tse-Hong Chen**

**A Dissertation**

*Submitted to the Faculty of Purdue University*

*In Partial Fulfillment of the Requirements for the degree of*

**Doctor of Philosophy**


Department of Chemistry

West Lafayette, Indiana

August 2019

# THE PURDUE UNIVERSITY GRADUATE SCHOOL
# STATEMENT OF COMMITTEE APPROVAL

Dr. Mary J. Wirth, Chair
Department of Chemistry
Dr. Peter T. Kissinger
Department of Chemistry
Dr. Jonathan J. Wilker
Department of Chemistry
Dr. Julia Laskin
Department of Chemistry

**Approved by:**

Dr. Christine A. Hrycyna
Head of the Graduate Program

*To my family and friends*

# ACKNOWLEDGMENTS

First and foremost, I would like to express my deepest gratitude to my research advisor also mentor, Mary Wirth, for her continuous guidance throughout my PhD career. She taught me how to develop critical thinking, design logical experiment, communicate with people, and give attractive presentation, which turned me into a real scientist. It is my greatest honor to be a Dr. Wirth's student! I would like to thank my committee members, Prof. Peter Kissinger, Prof. Jonathan Wilker and Prof. Julia Laskin, for valuable advices on my graduate research.

It is my pleasure to present my appreciation to Dr. Rui Zhang at Western Kentucky University, mentor and advisor of Master's degree, for his patience and moral support to my life of studies. In particular, his kindness and devoted attitude inspire me greatly.

I would like to acknowledge Dr. Pei-Hsun Wei, who introduced Dr. Wirth lab to me and convinced me to join Dr. Wirth group. Then, I am thankful to Dr. Ximo Zhang and Dr. Yiyang Zhou for their strong support on scientific background and instrument at the beginning of my PhD study. I am so grateful to have wonderful present group members: Edwin Alzate, Tyrel Wagner, Charlie Bupp, Yang Yun, and Cameron Schwartz, and past group members: Jonathan Yasosky, John Biechele-Speziale, Rachel Jacobson, and Alexis Huckabee, for their help, collaboration, and time spent together. It is an enjoyable and recallable memories to finish PhD career.

I would like to further thank Dr. Zhaorui (Ray) Zhang and Dr. Thamara Janaratne both in AbbVie, Dr. Cexiong Fu in Shire, and Dr. Bingchuan Wei in Genentech for industry-academia collaborations to enrich and strengthen my pharmaceutical background.

I am sincerely and supremely appreciated my dad and mom for their generous support on both mental and living aspects. I could not make it without my parents.

Finally, I would like to thank my friends in the U.S. and Taiwan as well as a special and gorgeous girl in Wuhan, China, who offers me a lot of joy, encouragement and company. My thesis and degree would not have been successfully completed without their ingenuities and supports.

# TABLE OF CONTENTS

# LIST OF TABLES

# LIST OF FIGURES

# LIST OF ABBREVIATIONS

| | |
|---|---|
| ACN | Acetonitrile |
| ADC | Antibody-drug conjugate |
| mBC | (Chloromethyl)phenyl)dimethylchlorosilane |
| mC1 | Trimethylchlorosilane |
| mC4 | n-Butyldimethylchlorosilane |
| DAR | Drug-to-antibody ratio |
| DFA | Difluoroacetic acid |
| DTT | Dithiothreitol |
| FA | Formic acid |
| HDC | Hydrodynamic chromatography |
| HIC | Hydrophobic interaction liquid chromatography |
| IgG | Immunoglobulin G |
| IPA | Isopropanol |
| mAb | Monoclonal antibody |
| $NH_4OAc$ | Ammonium acetate |
| nRPLC | Native reversed phase liquid chromatography |
| $Me_6TREN$ | Tris 2-(dimethylamino) ethyl amine |
| MS | Mass Spectrometry |
| PDMA | Polydimethylacrylamide |
| PEMA | Polyethylmethacrylate |
| PMMA | Polymethylmethacrylate |
| PPMA | Polypropylmethacrylate |
| PBMA | Polybutylmethacrylate |
| PBzMA | Polybenzylmethacrylate |
| RPLC | Reversed phase liquid chromatography |
| TEM | Transmission electron microscope |
| TFA | Trifluoroacetic acid |
| UHPLC | Ultra-high performance liquid chromatography |

# ABSTRACT

Author: Chen, Tse-Hong (Aaron). PhD
Institution: Purdue University
Degree Received: August 2019
Title: Polymer-Shell Bonded Phase for Improving Online LC-MS Analysis of Intact Proteins, mAbs, and ADCs
Committee Chair: Mary J. Wirth

LC-MS of protein drugs requires new ideas in bonded phase design rather than adapting bonded phases from the realm of small-molecule drugs. The polymer-shell bonded phase is designed to interact with larger molecules and to shield proteins from the silica substrate. The particles consist of a core of solid silica and a shell of dense polymer brush. The polymer layer is thick enough to protect the protein from interactions with silanols to reduce peak tailing. The polymer contains multiple functional groups that introduce more selectivity. This design gives unprecedented LC resolution and MS sensitivity. Our group has developed polymer shell bonded phases for hydrophobic interaction chromatography (HIC-MS) of antibody-drug conjugates (ADCs), hydrophilic interaction liquid chromatography (HILIC-MS) of glycoproteins, and reversed-phase liquid chromatography (RPLC-MS) of monoclonal antibodies. Since HIC is not in-line compatible with MS due to the high salt levels, it is laborious to identify the constituents of HIC peaks. An MS-compatible alternative to HIC is reported here: native reversed phase liquid chromatography (nRPLC). This employs a mobile phase 50 mM ammonium acetate for high sensitivity in MS, and elution with a gradient of water/isopropanol. The nRPLC-MS data show that all ADC species, ranging from drug-to-antibody ratios of 1 to 8, remained intact and native on the column. As we adapt this concept to intact proteins, we find that lysozyme and α-chymotrypsinogen A are both eluted in their native conformations. We also use the polymer-shell concept to resolve IgG1 free thiol variants by RPLC-MS with 0.5% formic acid. Since there are always other variants besides the intended ones, the need for high MS sensitivity is desired to distinguish subtle mass change between disulfide bond and free thiols. Overall, MS sensitivity increases 10X relative while all of the thiol variants are well resolved by the polymethylmethacrylate bonded phase.

# CHAPTER 1. INTRODUCTION

## 1.1 Monoclonal antibodies and antibody-drug conjugates

Monoclonal antibody (mAbs) are constructed of two heavy polypeptide chains (~50 kDa each) and two light polypeptide chains (~25 kDa each), having molecular weight approximately 150 kDa, structure shown in Figure 1-1. Heavy chain contains approximately 450-550 amino acids and light chain is 210-220 amino acids.[1-3] mAbs are effective treatment for many chronic and malignant diseases such as cancer therapy, immunotherapy, and solid tumor. In this regard, it is also called immunoglobulin, which selectively binds with antigen binding sites by complementarity-determining regions (CDRs). For example, rituximab has been approved to treat Hodgkin's lymphoma, chronic lymphocytic leukemia, rheumatoid arthritis, etc, and trastuzumab is used to treat breast cancer, which are both manufactured by Genentech. [4-8]

Antibody-drug conjugates (ADCs) consist of recombinant monoclonal antibodies convalently conjugated with highly potent agents (known as payloads or warheads) via a linker. They exploit specific binding properties through CDRs to selectively deliver cytotoxic payloads to cancer cells over non-malignant cells, resulting in maximized efficacy and minimized systemic toxicity. The vast majority of the cytotoxic warheads of the ADCs currently in clinical trials are conjugated to either lysine or cysteine residues on the antibody[9-11]. For instance, Genentech further discovered that the function of emtansine, a small chemical drug, and conjugated it with trastuzumab to increase the efficacy of the treatment on breast cancer[12]. There are three generations of ADCs; lysine conjugate ADCs, cysteine conjugated ADCs, and site-specific ADCs.[9, 13-15] In this work, cysteine conjugated ADCs will be introduced in the next chapter, which involves the conjugation through partially reduced cysteine groups to generate up to eight reactive free thiols [16-18], which results in heterogeneous mixture of antibody with drug population ranging from 0 to 8. As a result, drug-to-antibody ratio (DAR) is used to evaluate the discrepancy between the number of cytotoxic small-molecule drugs covalently attached to an antibody and the mixture is described as average DAR.

## 1.2 Silanols on silica particles

Chromatographic nonlinear peak tailing never goes away no matter how pure the silica is. This situation causes the reduced efficiency of separation especially for proteins, presenting in Figure 1-2. The phenomenon is attributed to dissociated silanols ($SiO^-$) or called active silanols. Therefore, Dr. Wirth and her group members started doing single-molecule spectroscopy to track separation pattern on C18/silica surfaces using AFM and fluorescence microscope.[19-23] The cause of peak tailing and peak asymmetry from silaonls (SiOH) and $SiO^-$ can be explained from bi-Langmuir adsorption isotherm to understand the slower desorption kinetics.[20] The experimental results showed that the retention time of C18 surface is three order of magnitude shorter than the retention time of active silanols. Moreover, the equilibrium constant of silanol sites are 500-fold greater than the equilibrium constant of C18 sites. To be consideration of proteins and peptides, tailing and broadening are more severe because of the hydrogen bonding between amine groups and silanols on silica. As a result, hydroxylation of silica surface to construct hydrogen bonds to each silanol is pivotal.

Two decades ago, Type B silica was invented to improve the quality of chromatographic separation science by increasing the density of silanols, approximately 8 μmol/$m^2$.[24, 25] A high density of silanols prefers to form hydrogen bond network better with each other rather than with the analyte. Recently, annealing of silica has been studied to reduce the concentration of the dissociated silanols and improves peak tailing in RPLC.[26] For the chromatographic aspect, additives, modifiers, and salts in mobile phases are applied to protonate silanol groups to avoid analyte-silanol interaction.

## 1.3 Online LC/MS

Liquid chromatography (LC) coupled with mass spectrometry (MS) is a powerful analytical tool to perform qualitative and quantitative analysis and characterization. Offline LC-MS is performed by fractionating samples from LC, exchanging buffer for samples, and preparing samples for MS. Those procedures are redundant and laborious, which normally take days to achieve whole offline LC-MS analysis. Nonetheless, fraction collection and buffer exchange may risk samples of temperature stress, pH stress, light stress, and so on. These situations will bias results from analysis. Therefore, online LC-MS draws people attention since sample can be

separated by LC and directly analyzed by MS, which shorten the analysis time from days to hours as well as reduced the deviation of analysis. However, there are several challenges in LC-MS analysis. [27]

- Insufficient dynamic range of LC separation since analyte may be poorly retained or strongly retained.
- Some analytes with no UV absorbance will be missed by most commonly used UV detector of LC.
- Analytes are complicated to cause co-elution with multiple components within one peak.
- In the aspect of small molecule separation, chiral compounds with multiple chiral centers are complex.
- Matrix effects are associated with MS-incompatible mobile phases to prevent analyte from analyzing by MS.

Matrix effects obstruct online LC-MS mainly since adducts in mobile phase result in MS signal suppression by interference of ionization efficiency, and thus it affects MS characterization and identification dramatically including deviation of mass accuracy or less ion abundance of false negative results.[28-30] For instance, sodium ion, a nonvolatile metal ion, has stronger ion paring effect and causes vanish of charged droplet.[31, 32] The common methods to overcome matrix effects are solid-phase extraction, dilution, or purification by resin.[33-35] Recently, multi-dimensional LC are established to resolve the matrix effect from salt such as the first dimension LC is ion exchange (IEX) or hydrophobic interaction chromatography (HIC) method, which require the use of salt; the second dimension is reversed-phase liquid chromatography (RPLC) to desalt and directly couples the second dimension to MS.[36] In addition, trifluoroacetic acid (TFA) are a gold standard for RPLC separation to introduce the highest RPLC resolution but also a well-known ion suppression acidic modifier. New apparatus is invented by Regeneron Analytical group to modify the desolvation gas from TFA to a MS-compatible acid vapor, propionic acid and isopropanol (IPA).[37] Consequently, better separation science to advance directly online LC-MS is required in both material and instrumentation fields.

## 1.4 Research objectives

Traditionally, the better LC resolution is, the worse MS sensitivity is. With common pH range of 2 to 8 for HPLC mobile phases, amino groups carry positive charges and isolated silanols may be negatively charged since pKa of silanols is 4.5, so electrostatic interaction is absolutely strong. A postulated mechanism of interaction between proteins and $SiO^-$ are shown in Figure 1-3. Instead of improving silanol endcapping or exploring surface morphology, a dense and thick layer of polymer is coated on silica surface to protect the protein from negatively charged interactions with silanols to reduce peak tailing (Figure 1-4). In this thesis, I am going to introduce polymer-shell technology to screen surface silanols and prevent proteins from the silica surface. Furthermore, polymer envelops protein to increase selectivity. This idea enables the LC separation using MS-compatible mobile phases to solve matrix effect from the LC and to improve online LC-MS platform to alleviate laborious work, time consuming, and cost of material use. Overall chromatographic resolution is better and most importantly, the design avoids trade-off between LC resolution and MS sensitivity.

## 1.5 References


1. Janeway, C. A. J.; Travers, P.; Walport, M., Immunobiology: The Immune System in Health and Disease. 5th edition. New York: Garland Science; 2001. The structure of a typical antibody molecule. Garland Science: New York, 2001.

2. Rosati, S.; Yang, Y.; Barendregt, A.; Heck, A. J., Detailed mass analysis of structural heterogeneity in monoclonal antibodies using native mass spectrometry. Nat Protoc **2014,** 9 (4), 967-76.

3. Sukupolvi-Petty, S.; Austin, S. K.; Engle, M.; Brien, J. D.; Dowd, K. A.; Williams, K. L.; Johnson, S.; Rico-Hesse, R.; Harris, E.; Pierson, T. C.; Fremont, D. H.; Diamond, M. S., Structure and function analysis of therapeutic monoclonal antibodies against dengue virus type 2. J Virol **2010,** 84 (18), 9227-39.

4. Weiner, L. M.; Dhodapkar, M. V.; Ferrone, S., Monoclonal antibodies for cancer immunotherapy. Lancet **2009,** 373, 1033-1040.

5. Strome, S. E.; Sausville, E. A.; Mann, D., A mechanistic perspective of monoclonal antibodies in cancer therapy beyond target-related effects. Oncologist **2007,** 12 (9), 1084-95.

6. Christiansen, J.; Rajasekaran, A. K., Biological impediments to monoclonal antibody–based cancer immunotherapy. Molecular Cancer Therapeutics **2004,** 11, 1493-1501.

7. Lipman, N. S.; Jackson, L. R.; Trudel, L. J.; Weis-Garcia, F., Monoclonal Versus Polyclonal Antibodies: Distinguishing Characteristics, Applications, and Information Resources. ILAR Journal **2005,** 46, 258-268.

8. Scott, A. M.; Allison, J. P.; Wolchok, J. D., Monoclonal antibodies in cancer therapy. Cancer Immunity **2012,** 12, 14-22.

9. Tsuchikama, K.; An, Z., Antibody-drug conjugates: recent advances in conjugation and linker chemistries. Protein Cell **2018,** 9 (1), 33-46.

10. Flygare, J. A.; Pillow, T. H.; Aristoff, P., Antibody-drug conjugates for the treatment of cancer. Chem. Biol. Drug. Des. **2013,** 81 (1), 113-21.

11. Peters, C.; Brown, S., Antibody-drug conjugates as novel anti-cancer chemotherapeutics. Biosci. Rep. **2015,** 35 (4).

12. Barok, M.; Joensuu, H.; Isola, J., Trastuzumab emtansine: mechanisms of action and drug resistance. Breast Cancer Research **2014,** 16, 209-221.

13. Thomas, A.; Teicher, B. A.; Hassan, R., Antibody–drug conjugates for cancer therapy. The Lancet Oncology **2016,** 17 (6), e254-e262.

14. Flygare, J. A.; Pillow, T. H.; Aristoff, P., Antibody-drug conjugates for the treatment of cancer. Chem Biol Drug Des **2013,** 81 (1), 113-21.

15. Diamantis, N.; Banerji, U., Antibody-drug conjugates--an emerging class of cancer treatment. Br J Cancer **2016,** 114 (4), 362-7.

16. Behrens, C. R.; Ha, E. H.; Chinn, L. L.; Bowers, S.; Probst, G.; Fitch-Bruhns, M.; Monteon, J.; Valdiosera, A.; Bermudez, A.; Liao-Chan, S.; Wong, T.; Melnick, J.; Theunissen, J. W.; Flory, M. R.; Houser, D.; Venstrom, K.; Levashova, Z.; Sauer, P.; Migone, T. S.; van der Horst, E. H.; Halcomb, R. L.; Jackson, D. Y., Antibody-Drug Conjugates (ADCs) Derived from Interchain Cysteine Cross-Linking Demonstrate Improved Homogeneity and Other Pharmacological Properties over Conventional Heterogeneous ADCs. Mol. Pharmaceutics **2015,** 12 (11), 3986-98.

17. Sanderson, R. J.; Hering, M. A.; James, S. F.; Sun, M. M. C.; Doronina, S. O.; Siadak, A. W.; Senter, P. D.; Wahl, A. F., In vivo Drug-Linker Stability of an Anti-CD30 Dipeptide-Linked Auristatin Immunoconjugate. Clin. Cancer Res. **2005,** 11, 843-852.

18. Sun, M. M. C.; Beam, K. S.; Cerveny, C. G.; Hamblett, K. J.; Blackmore, R. S.; Torgov, M. Y.; Handley, F. G. M.; Ihle, N. C.; Senter, P. D.; Alley, S. C., Reduction-Alkylation Strategies for the Modification of Specific Monoclonal Antibody Disulfides. Bioconjugate Chem. **2005,** 16, 1282-1290.

19. Ludes, M. D.; Wirth, M. J., Single-Molecule Resolution and Fluorescence Imaging of Mixed-Mode Sorption of a Dye at the Interface of C18 and Acetonitrile/Water. Analytical Chemistry **2002,** 74, 386-393.

20. Wirth, M. J.; Legg, M. A., Single-Molecule Probing of Adsorption and Diffusion on Silica Surfaces. Annual Review of Physical Chemistry **2007,** 58 (1), 489-510.

21. Wirth, M. J.; Ludes, M. D.; Swinton, D. J., Spectroscopic Observation of Adsorption to Active Silanols. Analytical Chemistry **1999,** 71, 3911-3917.

22. Smith, E. A.; Wirth, M. J., pH dependence of tailing in reversed-phase chromatography of a cationic dye: measurement of the strong adsorption site surface density. Journal of Chromatography A **2004,** 1060 (1-2), 127-134.

23. Wirth, M. J.; Smith, E. A.; Anthony, S. R., Measurement and simulation of tailing zones of a cationic dye in analytical-scale reversed phase chromatography. Journal of Chromatography A **2004,** 1034 (1-2), 69-75.

24. Zhuravlev, L. T., The surface chemistry of amorphous silica. Zhuravlev model. Colloids and Surfaces A: Physicochemical and Engineering Aspects **2000,** 173, 1-38.

25. Kohler, J.; Kirkland, J. J., Improved Silica-Based Column Packings for High-Performance Liquid Chromatography. Journal of Chromatography A **1987,** 385, 125-150.

26. Newby, J. J.; Legg, M. A.; Rogers, B.; Wirth, M. J., Annealing of silica to reduce the concentration of isolated silanols and peak tailing in reverse phase liquid chromatography. J Chromatogr A **2011,** 1218 (31), 5131-5.

27. Zhang, K.; Wang, J.; Tsang, M.; Wigman, L.; Chetwyn, N., Two-Dimensional HPLC in Pharmaceutical Analysis. Am. Pharm. Rev. **2013,** 16, 39-44.

28. Cappiello, A.; Famiglini, G.; Palma, P.; Trufelli, H., Matrix Effects in Liquid Chromatography-Mass Spectrometry. Journal of Liquid Chromatography & Related Technologies **2010,** 33 (9-12), 1067-1081.

29. Srneraglia, J.; Baldrey, S. I.-.; Watson, D., Matrix Effects and Selectivity Issues in LC-MS-MS. Chromatogaphia **2002,** 55, S95-S99.

30. Zhou, W.; Yang, S.; Wang, P. G., Matrix effects and application of matrix effect factor. Bioanalysis **2017,** 9, 1839-1844.

31. Banerjee, S.; Mazumdar, S., Electrospray ionization mass spectrometry: a technique to access the information beyond the molecular weight of the analyte. Int J Anal Chem **2012,** 2012, 282574.

32. Panuwet, P.; Hunter, R. E., Jr.; D'Souza, P. E.; Chen, X.; Radford, S. A.; Cohen, J. R.; Marder, M. E.; Kartavenka, K.; Ryan, P. B.; Barr, D. B., Biological Matrix Effects in Quantitative Tandem Mass Spectrometry-Based Analytical Methods: Advancing Biomonitoring. Crit Rev Anal Chem **2016,** 46 (2), 93-105.

33. Chambers, E.; Wagrowski-Diehl, D. M.; Lu, Z.; Mazzeo, J. R., Systematic and comprehensive strategy for reducing matrix effects in LC/MS/MS analyses. J Chromatogr B Analyt Technol Biomed Life Sci **2007,** 852 (1-2), 22-34.

34. Cappiello, A.; Famiglini, G.; Palma, P.; Pierini, E.; Termopoli, V.; Trufelli, H., Overcoming Matrix Effects in Liquid Chromatography-Mass Spectrometry. Analytical Chemistry **2008,** 80, 9343-9348.

35. Hall, T. G.; Smukste, I.; Bresciano, K. R.; Wang, Y.; McKearn, D.; Savage, R. E., Identifying and Overcoming Matrix Effects in Drug Discovery and Development. In Tandem Mass Spectrometry - Applications and Principles, Prasain, J., Ed. InTech: Rijeka, Croatia, 2012.

36. Valeja, S. G.; Xiu, L.; Gregorich, Z. R.; Guner, H.; Jin, S.; Ge, Y., Three dimensional liquid chromatography coupling ion exchange chromatography/hydrophobic interaction chromatography/reverse phase chromatography for effective protein separation in top-down proteomics. Anal Chem **2015,** 87 (10), 5363-5371.

37. Wang, S.; Xing, T.; Liu, A. P.; He, Z.; Yan, Y.; Daly, T. J.; Li, N., Simple Approach for Improved LC-MS Analysis of Protein Biopharmaceuticals via Modification of Desolvation Gas. Anal Chem **2019,** 91 (4), 3156-3162.

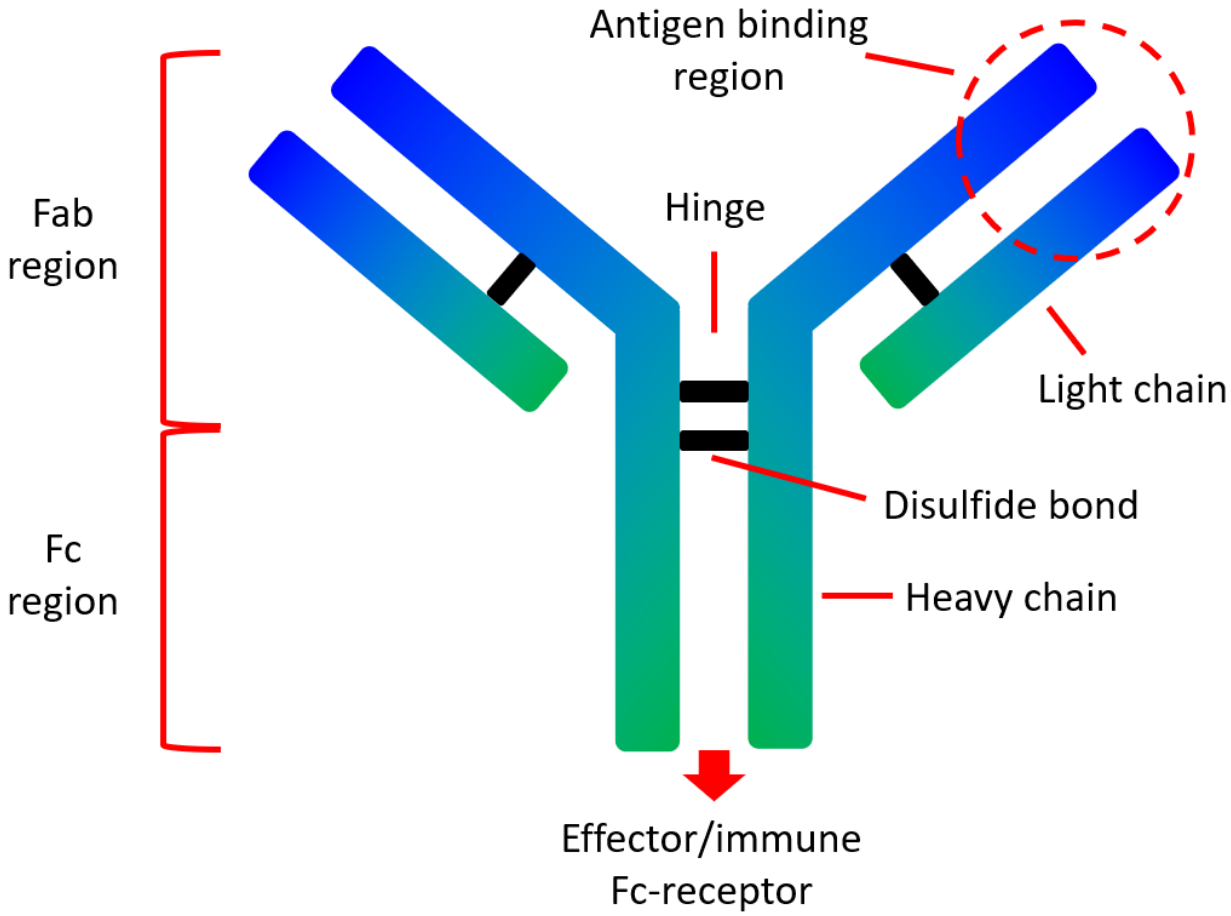


Figure 1-1 Stypical structure of monoclonal antibody (mAb)

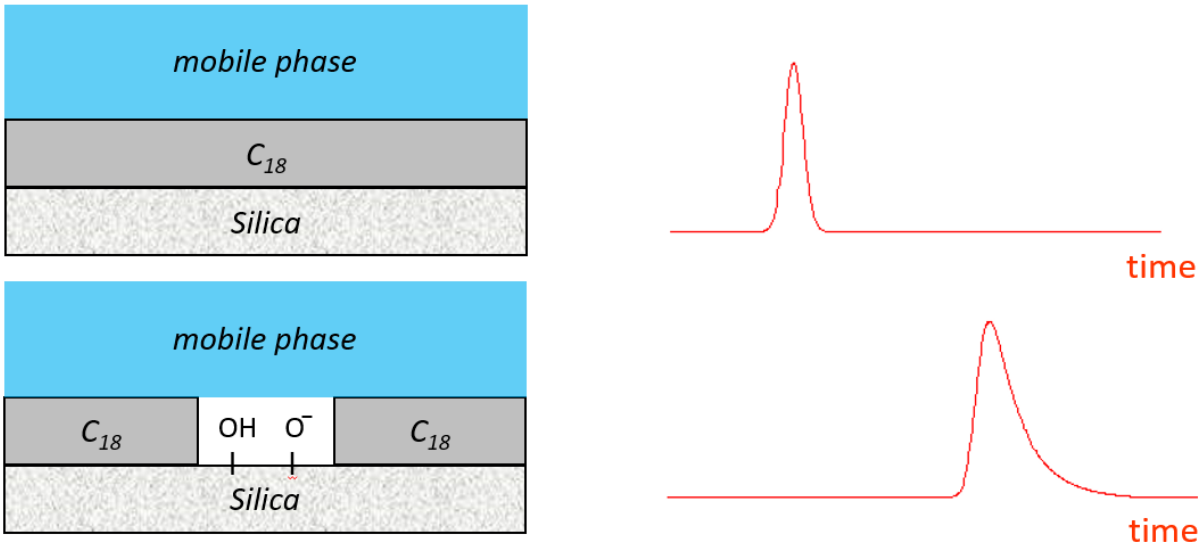


Figure 1-2 (Top panel ) Schematic representation of fully silylated silica surface, resulting a perfect Guassian peak. (Bottom panel) The realistic silica surface with silanols, causing peak tailing (ref. 20).

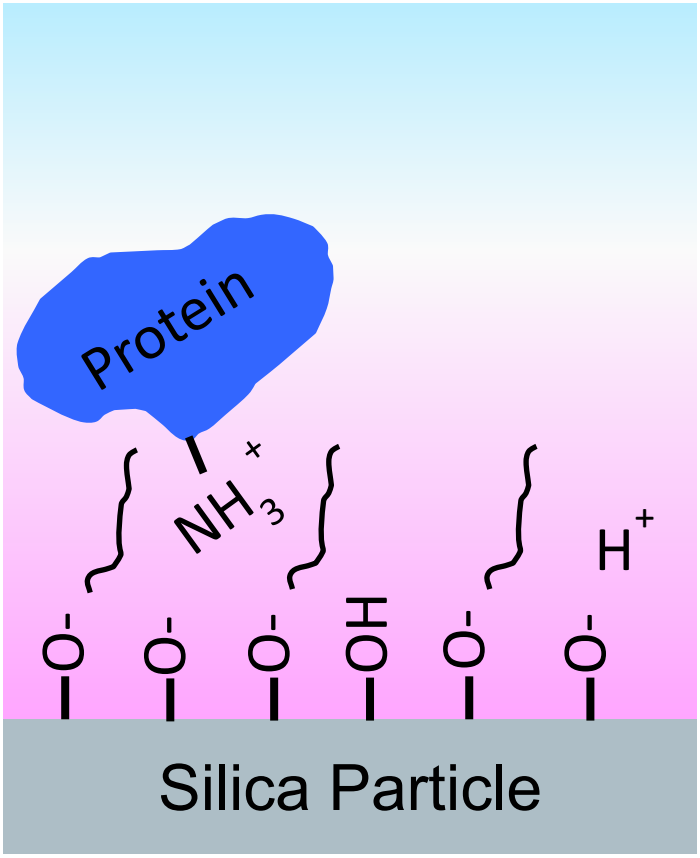


Figure 1-3 Depiction of silica surface with silanols (SiOH), dissociated silanols ($SiO^-$), modified silanols and postulated mechanism of protein adsorption to dissociated silanol groups on silica. The Si are drawn in black bonds and the mobile phase is drawn in pink to light blue.

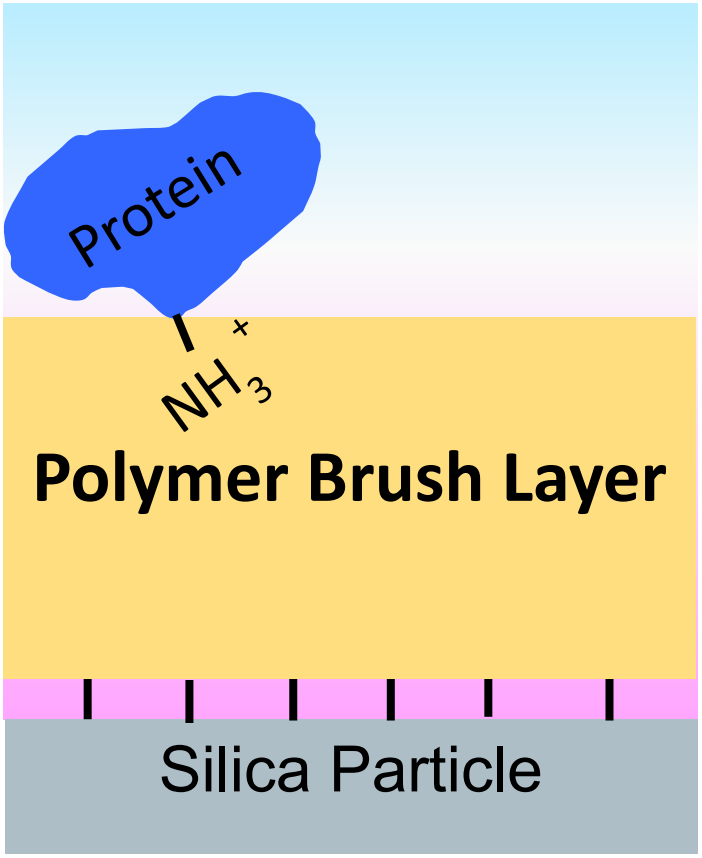


Figure 1-4 Depiction of silica surface coated with a polymer brush layer to keep proteins away from silica surface to reduce charge interactions.

# CHAPTER 2. NATIVE REVERSED-PHASE LIQUID CHROMATOGRAPHY: A TECHNIQUE FOR LCMS OF INTACT ANTIBODY-DRUG CONJUGATES AND PHARMACEUTICAL PROTEINS

A version of this chapter has been published by *Analytical Chemistry*. Reprinted with permission from Tse-Hong Chen, Yun Yang, Zhaorui Zhang, Cexiong Fu, Qunying Zhang, Jon D. Williams and Mary J. Wirth, Native Reversed-Phase Liquid Chromatography: A Technique for LCMS of Intact Antibody–Drug Conjugates. *Analytical Chemistry* **2019**, *91* (4), 2805-2812. DOI: 10.1021/acs.analchem.8b04699. 

## 2.1 Abstract

The synthesis of antibody-drug conjugates (ADCs) using the interchain cysteines of the antibody inherently gives a mixture of proteins with varying drug-to-antibody ratio. The drug distribution profiles of ADCs are routinely characterized by hydrophobic interaction chromatography (HIC). Since HIC is not in-line compatible with mass spectrometry (MS) due to the high salt levels, it is laborious to identify the constituents of HIC peaks. An MS-compatible alternative to HIC is reported here: native reversed phase liquid chromatography (nRPLC). This novel technique employs a mobile phase 50 mM ammonium acetate for high sensitivity in MS, and elution with a gradient of water/isopropanol. The key to the enhancement is a bonded phase giving weaker drug-surface interactions compared to the noncovalent interactions holding the antibody-drug conjugates together. The hydrophobicity of the bonded phase is varied and the least hydrophobic bonded phase in the series, polymethylmethacrylate, is found to resolve the intact constituents of a model ADC (Ab095-PZ) and a commercial ADC (brentuximab vedotin) under the MS-compatible conditions. The nRPLC-MS data show that all species, ranging from drug-to-antibody ratios of 1 to 8, remained intact in the column. Another desired advantage of the nRPLC is the ability of resolving multiple positional isomers of ADC that are not well resolved in other chromatographic modes This supports the premise that lower hydrophobicity of the bonded phase is the key to enabling online nRPLC-MS analysis of antibody-drug conjugates.

## 2.2 Introduction

Antibody-drug conjugates (ADCs) are highly selective and potent chemotherapeutics for the treatment of different types of cancer, inspired by Paul Ehrlich[1]. An ADC consists of a recombinant monoclonal antibody (mAb) covalently conjugated with a drug via a hydrophilic linker. The mechanism exploits specific binding of tumor-expressed antigens and delivers covalently conjugated cytotoxic payloads to cancer cells selectively over non-malignant cells, resulting in greater efficacy and minimized systemic toxicity. Four ADCs are currently on the market: Adcetris® (brentuximab vedotin) from Seattle Genetics for the treatment of relapsed Hodgkin's lymphoma and systemic anaplastic large-cell lymphoma, Kadcyla® (trastuzumab emtansine), from Genentech for the treatment of metastatic breast cancer[2-4], Mylotarg® (gemtuzumab ozogamicin) from Pfizer for acute myeloid leukemia and Besponsa® (inotuzumab ozogamicin) also from Pfizer for acute lymphoblastic leukemia. More than 60 ADCs have been advanced into clinical trials for cancer treatment,[3] and there are currently more than 65 ADCs in clinical evaluation to target different hematologic malignancies and solid tumors[3, 5]. The vast majority of the cytotoxic warheads of the ADCs currently in clinical trials are conjugated to either lysine or cysteine residues on the antibody,[6-8] with most using cysteine residues.[9] Drug loading in the ADCs is an important design parameter that needs to be characterized.[10]

Liquid chromatography separation of cysteine-conjugated ADCs to characterize the drug loading distribution is the topic of this paper. Taking IgG1, for example, a common conjugation approach entails partial reduction of four interchain disulfide bonds to generate up to eight reactive thiol groups.[11-13] This conjugation scheme yields a mixture of species ranging from 0 to 8 drugs per antibody, which is a broad distribution. The different drug loadings have been reported to affect the pharmacokinetics, stability, and clearance of ADCs.[14-18] Native SEC-MS is a rapid technique for determining the distribution of drug loads, where the SEC serves to de-salt the sample rather than separate the components and relies solely on MS for characterization and quantitation.[19] The technique skews the distribution toward lower drug load due to ion suppression and sub-optimal recovery of species with higher drug load.[20] Pretreatment by enzymatic cleavage of the hydrophobic drug from the ADC, which leaves the hydrophilic linker attached as a tag, reduces the skewing but does not eliminate it.[21] Consequently, chromatographic separations are used for quantitative ADC characterization. Reversed-phase liquid chromatography coupled to mass

spectrometry (RPLC-MS) is used to determine the average drug-to-antibody ratio (DAR) by separating the denatured subunits of the reduced ADC,[22] but this approach loses information about the drug load distribution.[23] Hydrophobic interaction chromatography (HIC) is a non-denaturing separation[24-26] that is currently the gold standard for resolving the drug distribution of ADCs.[27] A gradient of decreasing salt concentration is used for elution,[28, 29] and the high initial concentration and low volatility of the salts prevent its direct coupling to mass spectrometry for peak identification.[30-34]

The Ge and Alpert groups were the first to show that HIC-MS of intact proteins is possible with volatile salts.[26, 35] In their papers, MS-compatible ammonium acetate salt was used, with a gradient decreasing from 1 M to 20 mM, concurrent with a gradient of increasing acetonitrile in water from 0 to 50%. Since $NH_4OAc$ has weaker kosmotropic properties than the typical HIC salts of $(NH_4)_2SO_4$ and $Na_2HPO_4$, they used a bonded phase with increased hydrophobicity, and their results demonstrated that the proteins maintained their native forms. HIC-MS has not yet been reported for intact ADCs.

The considerations for HIC-MS of ADCs are different from that of natural proteins. The conjugated drug of an ADC is far more hydrophobic than the solvent-exposed surface of a native protein, as demonstrated by the elution time increasing with increasing drug load in HIC of ADCs. In light of this, the concept behind our work is that a fixed, low concentration of MS-compatible salt, e.g., 50 mM $NH_4OAc$, might give retention of ADCs on hydrophobic columns since less salting-out would be needed. If so, the question then is whether a mild organic additive, isopropanol, can be made to desorb the ADC from the stationary phase without dissociating the noncovalently bound subunits of the antibody. The strategy is to decrease the hydrophobicity of the bonded phase so that less organic component is needed for elution, thereby avoiding the dissociation of the antibody into subunits [36]. This is the opposite of the strategy used by Chen and co-workers[26, 35] since ADCs present a different problem than mAbs, which are more hydrophilic than ADCs. The other difference from the prior work is that the salt concentration is fixed at low level while the organic component is increased, which would make this a reversed-phase separation. Hence the proposed new method is a non-denaturing version of reversed-phase liquid chromatography (RPLC), and we refer to it as native reversed-phase liquid chromatography (nRPLC).

The purpose of this work is to test the idea that a bonded phase with sufficiently low hydrophobicity would enable a new technique, nRPLC-MS, for separating intact ADCs and determining their molecular weights by in-line coupled mass spectrometry. The method is evaluated using both a model ADC and a commercial ADC, where each ADC has a drug mimic or drug coupled to cysteines of the mAb using a hydrophilic linker.

## 2.3 Materials and methods

### 2.3.1 Materals

Nonporous silica particles (1500 nm) were purchased from Superior Silica (Tempe, AZ). Empty stainless-steel columns (2.1 mm I.D., 50 mm length), reservoirs (4.6 mm I.D., 150 mm), and frits (0.5 µm pore diameter) were purchased from Isolation Technologies (Middleboro, MA). Stainless-steel tubing, ferrules, and internal nuts were all purchased from Valco Instruments (Houston, TX). Silanes, i.e., (chloromethyl)phenyl)dimethylchlorosilane (+99%) and trimethylchlorosilane (+99%), were purchased from Gelest (Morrisville, PA). Methyl methacrylate (MMA, 99%), sodium ascorbate (≥99%), butylamine (99.5%), $NH_4OAc$ (99.99%), ammonium sulfate ($(NH_4)_2SO_4$, ≥99%), sodium phosphate ($Na_3PO_4$, 96%), and ammonium hydroxide were purchased from Sigma–Aldrich (St. Louis, MO). Other chemical used included trifluoroacetic acid (TFA, 99%), difluoroacetic acid (DFA, 98%) and copper(II) chloride (CuCl2, 99%) from Acros Organics (Morris Plains, NJ), tris(2-dimethylaminoethyl)amine ($Me_6$TREN, +99%) from Alfa Aesar (Haverhill, MA), and formic acid (FA, 99.5%+, LC/MS grade), acetonitrile (ACN), and 2-propanol (IPA) from Fisher Scientific (Hampton, NH). Ultrapure water was obtained from a Milli-Q system (MilliporeSigma, Darmstadt, Germany.)

IgG1 Ab095 was conjugated with drug-linker mimic PZ in-house at AbbVie (North Chicago, IL) as a model ADC. Brentuximab vedotin was obtained from Seattle Genetics. Both ADCs were prepared at 1 mg/mL in $NH_4OAc$ or $(NH_4)_2SO_4$ with final concentration 0.8–1.0 M.

### 2.3.2 UHPLC column preparation

The silica particles were modified as described earlier[37]. Briefly, the silica particles were calcined at 600 °C for 12 h, then annealed at 1050°C for 3 h, and rehydroxylated overnight in 1.0 M $HNO_3$. Particles were then rinsed in ultrapure water and dried in a 60 °C vacuum oven. SEM

showed that the particles decreased in diameter to 1.2 μm from the heating steps. Freshly rehydroxylated silica particles were suspended in a dry toluene solution containing 2% (v/v) of (chloromethyl)phenyl)dimethylchlorosilane and 0.1% (v/v) of butylamine. The solution was refluxed for 3 h and then rinsed by dry toluene. The particles were then endcapped by suspending in another dry toluene solution containing 2% (v/v) of trimethylchlorosilane and 0.1% (v/v) of butylamine and refluxed for 3 h. The silylated, endcapped particles were then rinsed with dry toluene and allowed to dry in a 60 °C vacuum oven for 2 h.

For polymer growth, each monomer was dissolved in 40:60 $H_2O$/IPA (v/v) in a 50 mL round bottom flask for a final concentration of 2.5 M. Two other solutions were made: 1) a solution containing 40 mg of $CuCl_2$ and 80 μL $Me_6$TREN, and 2) a solution containing 20 mg sodium ascorbate. These were also prepared in 2.0 mL of 40:60 $H_2O$/IPA. Afterwards, the Cu/$Me_6$TREN solution was added to the round bottom flask, followed by the sodium ascorbate solution. The resulting solution was poured into a plugged reservoir column of 4.6 mm × 150 mm. A 2.1 mm × 50 mm column was packed with 0.24 g of silylated, endcapped particles suspended in acetonitrile. The reservoir and column were connected in series. A high-pressure pump, LabAlliance Series 1500 HPLC Pump (Laboratory Alliance of Central New York, LLC, Syracuse, NY) was used for packing and modification. The reaction solution from the reservoir was pumped into the column starting at 200 μL/min until the reaction mixture dripped from the end of the column. The flow rate was then lowered to 100 μL/min, and the polymerization reaction was allowed to proceed for a range of reaction times from 40 to 85 min for optimization. After reaction, the freshly packed column polymethylmethacrylate (PMMA) was rinsed with water for 20 min at 100 μL/min.

### 2.3.3 UHPLC

The columns and mobile phases for the various separations are summarized in Table 2.1.

A Thermo Accela UHPLC system (Thermo-Scientific, Waltham, MA, USA) was used for the development of nRPLC separations at the Purdue lab. Lab-made nRPLC columns (2.1 × 50 mm, 1.2 μm nonporous silica particles coated with various polyalkylmethacrylates were used as the analytical columns. A commercial column, MabPac HIC-Butyl (4.6 × 100 mm, 5 μm nonporous), from Thermo Scientific (Waltham, MA) was used under both HIC and nRPLC conditions for comparison since both have polymeric surfaces. UV absorbance wavelength was

set to 280 nm. The flow rate was 100 μL/min for all cases. The column temperature was 30 °C and the injection volume was 3 μL.

A TSKgel Butyl-NPR column (4.6 × 35 mm, 2.5 μm, Tosoh, King of Prussia, PA) was used for HIC at the AbbVie site, with an Agilent 1200 HPLC (Agilent, Santa Clara, CA). The system is routinely used for HIC separations of ADCs to calculate DAR. With the mobile phase given in Table 1, the gradient started with 90% MPA, decreased to 75% MPA in 2 min followed by a gradient to 0% MPA in 10 min and was held for 2 min before re-equilibrium. The flow rate was 0.8 mL/min and column temperature was set to 25 °C.

### 2.3.4 LC-MS

For RPLC-MS of the reduced ADC, this was generated in the Purdue lab by adding 1,4-dithiothreitol (DTT), a Thermo Accela UHPLC was used with a Thermo MabPac RP column (2.1 x 50 mm, 4 um, supermacroporous polymer particles) (Thermo-Scientific, Waltham, MA, USA), and the column was coupled to a Thermo LTQ Velos mass spectrometer (Thermo-Scientific, Waltham, MA, USA). With the mobile phase given in Table 1, the gradient started with 27% with MPB2, increased to 43% MPB2 in 15 min and returned to 27% MPB2 for re-equilibrium. Flow rate was 0.2 mL/min and column temperature was 80 °C. Peak identities were assigned by matching deconvoluted masses with theoretical masses.

For RPLC-MS of the non-reduced ADC (no DTT), a Supelco Bioshell A400 Protein C4 column (2.1 x 100 mm, 3.4 μm, Sigma-Aldrich, St. Louis, MO) was used in the AbbVie lab. With the mobile phase given in Table 1, the the gradient started with 90% MPA3, ramped to 69% MPA3 in 1 min followed by a decrease to 52% MPA3 in 13 min and returned to original condition for re-equilibrium. Flow rate was 0.3 mL/min and column temperature was 70 °C. The ADC samples were analyzed using an Acquity UPLC H-Class coupled to a Synapt G2 Si mass spectrometer (Waters, Milford, MA). Peak identities were assigned by matching deconvoluted masses with theoretical masses.

For online nRPLC-MS analysis, the polymethylmethacrylate (PMMA) column made in the Purdue lab was used at AbbVie, where the LC-MS system was a Waters Acquity UPLC H-Class coupled to a Xevo G2 qTOF mass spectrometer (Waters, Milford, MA). With the mobile phase given in Table 1, the gradient started with 0% MPB4, held for 2 min, ramped to 15% MPB4 in 3

min followed by a gradient to 50% MPB4 in 15 min and held at 50% MPB4 for 6 min before re-equilibrium. Flow rate was reduced to 0.07 mL/min. Column temperature was 30 °C. For MS condition, capillary voltage was 3.00 kV, Sample cone voltage was 85V, trap collision energy was set to 60 V, source temperature was 140 °C and desolvation temperature was 500 °C. The high sampling cone voltage was used to improve resolution and sensitivity in raw MS spectra, but this more prone to cause in-source fragmentation.

## 2.4 Results and discussions

A model ADC was synthesized by AbbVie, with the chemical structure of the linker and drug portions depicted in Figure 2-1a. The structure is similar to that of the commercial ADC, Brentuximab, also studied here, with its structure depicted in Figure 2-1b. These are both cysteine-conjugated ADCs using a similar, typical hydrophilic linker with coupling to the mAb cysteines via the maleimide group. The figure shows that the drug mimic for the AbbVie model ADC and the drug for brentuximab vedotin are quite hydrophobic, each with a log P in excess of 3, where P is the partition coefficient for octanol/water.

ADCs can be characterized with respect to their average DAR by fully reducing the ADCs with DTT and then separating the subunits by RPLC. Sketches to indicate labeling for intact ADCs and the various subunits are given in Figure 2-2a. The RPLC chromatogram for the reduced AbbVie model ADC Ab095-PZ is shown in Figure 2-2b. The mass spectrum of each peak (Figure 2-3) was used to assign each of the six peaks to the subunit, as labeled in the chromatogram. The first two peaks are light chains without (L0) or with (L1) one drug+linker, and the latter four peaks are heavy chains with 0, 1, 2 and 3 drug+linker attachment(s). The average DAR calculated from the relative peak areas is 3.9. The RPLC chromatogram of Ab095-PZ without DTT reduction (i.e., non-reduced RPLC) is shown in Figure 2-2c. The peak assignments from MS show that the model ADC was only partially reduced during the conjugation process, as expected. The results demonstrate that in conventional RPLC, without interchain disulfide bond linkages, the ADC dissociates into subunits. The value of this chromatogram is that it can be later compared to that for native RPLC with DTT absent. The HIC chromatogram of Ab095-PZ, using a commercial HIC-Butyl column and typical HIC salt gradient, is shown in Figure 2-2d. As is common practice, an isopropanol gradient was superimposed on the salt gradient to attain full elution of the ADC

constituents. The species with higher drug loading gave multiple peaks, and this is shown later to be due to partial resolution of positional isomers. Mass spectrometry cannot be used to identify the peaks of Figure 2-2d because the conventional HIC salts suppress ionization and causes adduct formation, as discussed earlier. One can make tentative peak assignments based on typical drug loading profile for ADCs with an average DAR of 3.9, as indicated in Figure 2-2d.

The proposed strategy described earlier to enable native RPLC-MS is to use no more than 50 mM $NH_4OAc$. This amount of salt is normally reached at the end of a salt gradient for online HIC-MS;[25, 26, 38] therefore, there is now little value in even running a salt gradient in RPLC mode. Despite this low level of salt, the same commercial HIC column as used for the HIC of Figure 2-2d (Thermo MabPac HIC-Butyl column) was found to give virtually no elution of the ADC; the retention to the column is too strong for elution. This indicates that the lower kosmotropic power of 50 mM $NH_4OAc$ gives more retention than the higher kosmotropic power of 50 mM sodium phosphate of Figure 2-2d. The strong retention with 50 mM $NH_4OAc$ is attributed to irreversible adsorption of the hydrophobic drug rather than to salting out of the intact ADC. The HIC stationary phase, which is said to be made of butyl groups, is thus too hydrophobic for use with isocratic 50 mM $NH_4OAc$, i.e., the hydrophobic interactions between ADC and bonded phase surface are stronger than the intramolecular hydrophobic interactions within the ADC. This inspires the proposed strategy to make the bonded phase less hydrophobic so that the free energy barrier for protein desorption is lower than the free energy barrier for protein denaturation.

Native RPLC chromatograms of model ADC Ab095-PZ using isocratic 50 mM $NH_4OAc$ with a gradient of 0-50% isopropanol are shown in Figure 2-4a-d for a series columns with decreasing bonded phase hydrophobicity, including polymethyl-, polyethyl-, polypropyl- and polybutylmethacrylate. The recovery and resolution are progressively higher with lower hydrophobicity, consistent with less denaturation of the ADCs lower mobile phase strength. Polymethylmethacrylate, with the lowest hydrophobicity, gives a chromatogram similar to that of the native HIC chromatogram of Figure 2-2d, suggesting that intact ADCs are indeed eluted under mild organic phase content without dissociation. The chromatogram is quite different from than that of the denaturing RPLC case of Figure 2-2c, again arguing that the ADCs are not dissociated. The downside of the nRPLC separation of the ADCs in Figure 2-4is that the native antibody, i.e., the species having no conjugated drug, D0, has low retention. This is an inherent outcome of the nRPLC strategy, where the designed retention mechanism is based on the hydrophobic interaction

between the exposed/or partially exposed hydrophobic drug with the bonded phase. To increase the retention of D0 species, some mixed-mode copolymer could potentially be used with minimal effect on retention of the hydrophobic drug.

The results presented in Figure 2-4 used a reaction time of 70 min for polymer growth, which was based on an optimization. The column performance with varying polymer growth time is presented in Figure 2-5for polymethylmethacrylate, under the same chromatographic condition as for Figure 2-4. The LC resolution and recovery reaches a maximum for 70 min reaction time. It is not surprising that the bonded phase must reach certain thickness to diminish the undesired electrostatic interactions with the surface, hence the initial improvement in separation with thickness. Further increasing the reaction time to 85 min attains limited increase of resolution and suffered from loss in protein recovery. One can speculate that polydispersity is beginning to effect the separation for the long reaction time since termination occurs throughout the reaction. The morphology of the bonded phase will eventually change from a brush-like layer to a loosely packed polymer strands as the reaction time increases. Excessively long, isolated polymer chains could cause protein denaturation. Overall, the nRPLC column performance is rather sensitive to the polymer reaction time, and given that only a few reaction times were tested, it is possible that higher peak resolution can be obtained by fine-tuning the reaction time. Optimization of other reaction conditions, such as monomer concentration, copper (II) concentration, and temperature, all of which affect growth rate and polydispersity of the polymer, could also give improved LC performance.

Mass spectrometry is used to test whether the constituents of the ADC peaks are intact vs. dissociated under nRPLC conditions for the column with polymethylmethacrylate grown for 70 min. Figure 2-6a shows the nRPLC chromatogram for the AbbVie model ADC using the polymethylmethacrylate column, now with the gradient adjusted for faster elution. The peaks are labeled in detail based on the mass of the most prevalent protein for each peak. The raw mass spectral data are given in Figure 2-6b. By extracting high mass range (extracted in chromatogram not shown), it was confirmed that the unconjugated species (D0) was barely retained and was nearly co-eluting with the injection peak. The small peak in the chromatogram of Figure 2-6a eluting at 10 min was identified as D1. In Figure 2-6b, the first mass spectrum assigned the peak at 13 min as D2 based on deconvoluted mass, which gives the mass (149,380 Da) corresponding to that expected for D2 (theoretical mass: 147,640+2x859). There are three peaks for D4, labeled

as D4(1), D4(2) and D4(3) in the order of elution, and Figure 2-2a showed that there are theoretically four positional isomers for D4. Of note, the positional isomers of D4 that result from conjugation of the upper vs lower cysteine pairs in the hinge region likely co-elute since they are only subtly different in structure. Similarly, D6 gives two peaks when there are expected to be three, but again, as illustrated in Figure 2-2a, two cases differ only by position on the heavy chain (upper hinge cysteine conjugation vs. lower hinge cysteine conjugation). It is novel for a HIC column to resolve different D4 and D6 isoforms from one another, and the separation on this polymethylmethacrylate under nRPLC mode could be advantageous in process understanding and quality control. The mass spectrum of the larger of the two D6 peaks is given in Figure 2-6b. It shows some peak overlap with D4, as indicated by the light blue lines in Figure 2-6b. The mass spectrum of the peak labeled D8 indicates it to be mainly D8 with some overlap from D5, D6 and D7. No peaks due to fragments were observed. It is noteworthy that all ADC mass spectra demonstrated a native-like charge envelope distribution with charge state from 24 to 33, which further supports the conclusion of native RPLC.

Representative mass spectra of model ADC over a wider range of mass-to-charge ratio (m/z) are given in Figure 2-7a. All spectra show strong signals from a heretofore unexpected L1 fragment (light chain plus drug), despite the absence of corresponding species (ADC minus L1) in the higher mass range for intact ADC. This at first seems to contradict the claim of intact ADC elution during the discussion of Figure 2-6 for the higher mass range. Our conclusion is that this L1 signal in Figure 2-7 arises from two circumstances: 1) in-source fragmentation of the ADC after elution due to the rather high sampling cone voltage and 2) a greater ionization efficiency of the L1 fragment to make its signal appear disproportionately strong compared to that of the intact ADC. If the signal strength were proportional to abundance, there would be a significant amount of ADC-L1 detectable in the higher range of m/z. Therefore, the large peaks for L1 must be due to greater ionization efficiency. In addition, if L1 dissociated from the ADC on the column, the EIC based on L1 would not be correlated with the UV chromatogram. The only reasonable way for the subunits of the ADC to travel together throughout the separation is for the ADC to be intact. An extracted ion chromatogram (EIC) for the L1 fragment is shown in Figure 2-7b, in comparison with the same chromatogram using UV detection. It is clear that the chromatograms closely track one another for the two different modes of detection. Further, the exceptions prove the rule: the blue arrows in Figure 2-7b show a D4 peak that is increased and a D4 peak that is decreased for

EIC of L1. These are consistent with the expectation that one D4 should have two L1 species and one should have none. The inset images in Figure 2-7b depict the structures of the positional isomers. D4(2) has twice as many light chains with drug compared to D4(1), which would make its signal increase for EIC of L1. Likewise, D4(3) has no light chain with drug, hence signal would decreases for EIC of L1. The EIC supports the conclusion that L1 dissociated post-column and all ADCs remained intact throughout the nRPLC separation. It is remarkable that D8, with fully reduced interchain disulfide bonds between subunits, eluted intact.

The native RPLC-MS strategy was also tested for a commercial ADC, brentuximab vedotin, which is a well-characterized commercial ADC, with an average DAR of 4.0, comparable to that of the AbbVie model ADC.[39] HIC was performed to compare DAR profiles of the two ADCs. The results are provided in Figure 2-8, confirming that the DAR profiles of these two ADCs are qualitatively similar. The chromatograms show that the D0 peak elutes later for brentuximab vedotin, indicating that the brentuximab (mAb of brentuximab vedotin) sequence is more hydrophobic than that of the AbbVie model ADC. This is offset by the drug of brentuximab vedotin being less hydrophobic than the drug-linker of the AbbVie model ADC, with its lower octanol/water partition coefficient, log P = 3.01, for MC-VC-MMAE compared to that of the AbbVie model drug, log P = 3.35. The elution times of peaks with higher drug load in HIC are similar in both chromatograms: 10 min.

The DAR values were calculated from the integration of peaks of the signal at 280 nm. Figure 2-9 shows the DAR profiles comparison between HIC method from Figure 2-8a and nRPLC method from Figure 2-6a. The average DAR are 3.80 and 3.84, respectively. The good agreement on average DAR values indicates that nRPLC method is comparable. Furthermore, at similar target DAR values point out the nRPLC is a promising technique for quantitative characterization of ADC drug load distribution.

The nRPLC chromatogram for brentuximab vedotin, using the same polymethylmethacrylate column and separation conditions as for the AbbVie model ADC, is given in Figure 2-10a. The chromatogram is similar to that for the AbbVie model ADC, with differences in relative peak heights and a small extra peak before D6. The D0 species is now slightly retained in nRPLC, owing to the greater hydrophobicity of the mAb that was noted using HIC. All ADC peaks elute somewhat earlier in nRPLC for brentuximab vedotin, consistent with the lower

hydrophobicity of the drug. The mass spectra, detailed in Figure 2-10b, show that the D2 peak and the first D4 peak, D4(1), are intact, with no loss of L1. The other two D4 peaks, D4(2) and D4(3), show some loss of one or two light chains with drug (D4-L1 and D4-2xL1), in addition to the intact forms being observed. Overall, the results show that it is much easier to lose L1 from brentuximab vedotin than it is from the AbbVie model ADC.

As was done with the AbbVie model ADC to distinguish on-column vs. in-source dissociation, Figure 2-11a shows representative mass spectra over wider range of m/z for brentuximab vedotin. The relative signals from the L1 fragment are much stronger than those of the AbbVie model ADC, again illustrating the greater ease of loss of L1 for brentuximab vedotin. To determine whether L1 dissociated on-column or in-source, the EIC for the L1 fragment is shown in Figure 2-11b, in comparison with the same chromatogram using UV detection. As with the case for the AbbVie model ADC, the UV and extracted ion chromatograms closely track one another. The lack of an L1 background across the chromatogram confirms that all of the ADCs remain intact throughout the course of the nRPLC separation. As with the AbbVie model ADC, the L1 fragment signal is more pronounced in the D4(2) position than the latter peak D4(3), indicated by the blue arrows. As with the case for the AbbVie model ADC, the relative abundances of the L1 fragment peaks are likely associated with same two factors: a) the L1 molar ratio in the positional isomer: 1, 2, 0, for D4(1), D4(2) and D4(3), respectively; and b) strength of the noncovalent interaction between L1 and heavy chain in the MS source. These two factors reflect on the L1 fragment peak abundance in the order of D4(2)>D4(1)>>D4(3). The Comparison of EIC and UV chromatograms again supports the conclusion that nRPLC elutes intact brentuximab vedotin species. The greater loss of L1 in the source for brentuximab vedotin relative to the AbbVie model ADC indicates that the noncovalent interactions between light and heavy chains are weaker for brentuximab vedotin than that of the AbbVie model ADC Ab095-PZ.

## 2.5 Conclusions

A novel protein chromatography technique intersecting HIC and RPLC modes was developed, termed native reverse-phase liquid chromatography, nRPLC. nRPLC employs the solvent elution model and MS compatibility of RPLC, while preserving the native form of protein and ADC as in HIC. This new nRPLC technique is an alternative to HIC for ADCs when in-line

coupling of MS is desired by virtue of using only 50 mM $NH_4OAC$. The nRPLC method eluted intact ADCs for both a model ADC from AbbVie and a commercial ADC from Seattle Genetics. Key to this chromatographic advance was lower hydrophobicity of the bonded phase to make drug-surface hydrophobic interactions weaker than the intramolecular hydrophobic interactions that maintain the noncovalent complexes. Inherent to this strategy of designing retention only for interactions between the attached drug and chromatographic surface is that the D0 species has little retention at this stage in column development. The column gives partial resolution of positional isomers, thereby providing additional characterization beyond what is typically obtained using HIC. The lesser number of peaks in HIC permits full resolution of the ADC based on drug loading, which enables precise calculation of DAR. With its greater resolution of positional isomers that currently overlap, nRPLC will be a companion rather than a replacement for HIC until resolution is improved. Longer nRPLC columns, refinement of polymer growth conditions and optimization of separation conditions could lead to sufficient resolution to determine DAR while also characterizing positional isomers. To our knowledge, this is the first time that intact ADCs made from reduced cysteines have been separated based on DAR using an MS-compatible mobile phase.

## 2.6 Further studies

nRPLC has been further studied for smaller proteins, for example, lysozyme, α-chymotrypsinogen A (α-chymo. A), cytochrome C and myoglobin. PMMA column has been applied for lysozyme and α-chymo. A under nRPLC condition. The gradients used for elution are detailed along with the results. Figure 2-12a, b both chromatograms show non-retained peak of lysozyme and α-chymo. A. This phenomenon is attributed to the native form of protein usually has hydrophilic surface and buries hydrophobic part inside of the structure. The HIC separation mechanism in this case differs from the mechanism in ADCs since ADCs perform hydrophobic interaction with stationary phase via small and hydrophobic payloads. This result obviously indicates that more hydrophobic surface is required. In order to investigate a suitable stationary phase, with varying hydrophobicity of bonded phase has been tested same as Figure 2-4. However, none of bonded phase in Figure 2-4 gives us an acceptable chromatogram. In this regard, the benzyl methacrylate (BzMA) has been selected for nRPLC separation of proteins.

The polymerization of BzMA is similar as polymerization of MMA. The difference parts are 1 M BzMA and 20:80 $H_2O$/IPA were used. The reason to have changes on monomer concertation and organic uses is BzMA is relatively more hydrophobic and the self-polymerization and fast polymerization in reaction solution have been found. The lower monomer concentration and higher organic are required to perform controllable polymerization. Figure 2-13 shows nRPLC separation using PBzMA 90 min column. By calculating of time for stacking and gradient delay, both lysozyme and α-chymo. A elute out at IPA approximate 30%. The deconvoluted mass spectra show both proteins are intact and raw mass spectra show both proteins are native. The was mass spectra are comparable with published article by Ying Ge's group[26].

Cytochrome C and myoglobin are then examined under nPRLC using PBzMA. Cyctochrome C and myoglobin are proteins with heme-centered group. Those proteins are relatively fragile due to an open environment of binding pocket for heme. The folding and unfolding behavior of myoglobin has been studied[40], which could be highly related to pH, resulting in the difference solubility of heme in aqueous solution. The basic pH accelerates the release of heme and directly interrupts the structure of heme-protein complex. Although at the low pH, protein structure tends to be unfolded, in return, it prevents the dissociation of the heme from protein and the heme-protein structure will be wholesome. In this regard, we use ammonium formate at pH 5.5 instead of ammonium acetate at pH 7 for both cases of cytochrome C and myoglobin. As we expected, we do see cytochrome C and myoglobin are denatured under certain amount of organic use, shown in Figure 2-14. Cytochrome C in Figure 2-14a has a similar retention time as lysozyme and α-chymo. A. however, the raw mass spectra show gradual denaturation along with the peak from 10.5 min to 12 min. At 10.5 min, 5+ to 7+ demonstrates the charge states are native, but in the same peak to 12 min, the charge states shift to down scale from 8+ to 12+, which represents the cytochrome C is partially denatured[41]. The denaturing property results from the intolerance of relatively high organic. Myoglobin in Figure 2-14b, is highly retained on PBzMA and elutes at 50% IPA. Consequently, the raw mass spectrum also shows partially denatured form of myoglobin from charge state from 1x+ to 1x+. Gratefully, the charge envelop well describes that the myoglobin does not lose heme under nRPLC condition[40].

## 2.7 References


1. Hughes, B., Antibody-drug conjugates for cancer: poised to deliver? *Nature reviews. Drug discovery* **2010,** *9* (9), 665-7.

2. Thomas, A.; Teicher, B. A.; Hassan, R., Antibody–drug conjugates for cancer therapy. *Lancet Oncol.* **2016,** *17* (6), e254-e262.

3. Beck, A.; Goetsch, L.; Dumontet, C.; Corvaia, N., Strategies and challenges for the next generation of antibody-drug conjugates. *Nature reviews. Drug discovery* **2017,** *16* (5), 315-337.

4. Polakis, P., Antibody Drug Conjugates for Cancer Therapy. *Pharmacological reviews* **2016,** *68* (1), 3-19.

5. Lambert, J. M.; Berkenblit, A., Antibody-Drug Conjugates for Cancer Treatment. *Annu. Rev. Med.* **2018,** *69*, 191-207.

6. Tsuchikama, K.; An, Z., Antibody-drug conjugates: recent advances in conjugation and linker chemistries. *Protein & cell* **2018,** *9* (1), 33-46.

7. Flygare, J. A.; Pillow, T. H.; Aristoff, P., Antibody-drug conjugates for the treatment of cancer. *Chemical biology & drug design* **2013,** *81* (1), 113-21.

8. Peters, C.; Brown, S., Antibody-drug conjugates as novel anti-cancer chemotherapeutics. *Bioscience reports* **2015,** *35* (4).

9. Jain, N.; Smith, S. W.; Ghone, S.; Tomczuk, B., Current ADC Linker Chemistry. *Pharmaceutical Research* **2015,** *32* (11), 3526-3540.

10. Hamblett, K. J.; Senter, P. D.; Chace, D. F.; Sun, M. M. C.; Lenox, J.; Cerveny, C. G.; Kissler, K. M.; Bernhardt, S. X.; Kopcha, A. K.; Zabinski, R. F.; Meyer, D. L.; Francisco, J. A., Effects of drug loading on the antitumor activity of a monoclonal antibody drug conjugate. *Clinical Cancer Research* **2004,** *10* (20), 7063-7070.

11. Behrens, C. R.; Ha, E. H.; Chinn, L. L.; Bowers, S.; Probst, G.; Fitch-Bruhns, M.; Monteon, J.; Valdiosera, A.; Bermudez, A.; Liao-Chan, S.; Wong, T.; Melnick, J.; Theunissen, J. W.; Flory, M. R.; Houser, D.; Venstrom, K.; Levashova, Z.; Sauer, P.; Migone, T. S.; van der Horst, E. H.; Halcomb, R. L.; Jackson, D. Y., Antibody-Drug Conjugates (ADCs) Derived from Interchain Cysteine Cross-Linking Demonstrate Improved Homogeneity and Other Pharmacological Properties over Conventional Heterogeneous ADCs. *Molecular pharmaceutics* **2015,** *12* (11), 3986-98.

12. Sanderson, R. J.; Hering, M. A.; James, S. F.; Sun, M. M. C.; Doronina, S. O.; Siadak, A. W.; Senter, P. D.; Wahl, A. F., In vivo Drug-Linker Stability of an Anti-CD30 Dipeptide-Linked Auristatin Immunoconjugate. *Clin. Cancer Res.* **2005,** *11*, 843-852.

13. Sun, M. M. C.; Beam, K. S.; Cerveny, C. G.; Hamblett, K. J.; Blackmore, R. S.; Torgov, M. Y.; Handley, F. G. M.; Ihle, N. C.; Senter, P. D.; Alley, S. C., Reduction-Alkylation Strategies for the Modification of Specific Monoclonal Antibody Disulfides. *Bioconjug. Chem.* **2005,** *16*, 1282-1290.

14. Ducry, L., *Antibody-Drug Conjugates*. Humana Press: New York City, NY, 2013; Vol. 1045.

15. Shen, B. Q.; Xu, K.; Liu, L.; Raab, H.; Bhakta, S.; Kenrick, M.; Parsons-Reponte, K. L.; Tien, J.; Yu, S. F.; Mai, E.; Li, D.; Tibbitts, J.; Baudys, J.; Saad, O. M.; Scales, S. J.; McDonald, P. J.; Hass, P. E.; Eigenbrot, C.; Nguyen, T.; Solis, W. A.; Fuji, R. N.; Flagella, K. M.; Patel, D.; Spencer, S. D.; Khawli, L. A.; Ebens, A.; Wong, W. L.; Vandlen, R.; Kaur, S.; Sliwkowski, M. X.; Scheller, R. H.; Polakis, P.; Junutula, J. R., Conjugation site modulates the in vivo stability and therapeutic activity of antibody-drug conjugates. *Nat. Biotechnol.* **2012,** *30* (2), 184-9.

16. Adem, Y. T.; Schwarz, K. A.; Duenas, E.; Patapoff, T. W.; Galush, W. J.; Esue, O., Auristatin antibody drug conjugate physical instability and the role of drug payload. *Bioconjug. Chem.* **2014,** *25* (4), 656-64.

17. Boswell, C. A.; Mundo, E. E.; Zhang, C.; Bumbaca, D.; Valle, N. R.; Kozak, K. R.; Fourie, A.; Chuh, J.; Koppada, N.; Saad, O.; Gill, H.; Shen, B. Q.; Rubinfeld, B.; Tibbitts, J.; Kaur, S.; Theil, F. P.; Fielder, P. J.; Khawli, L. A.; Lin, K., Impact of drug conjugation on pharmacokinetics and tissue distribution of anti-STEAP1 antibody-drug conjugates in rats. *Bioconjug. Chem.* **2011,** *22* (10), 1994-2004.

18. Lyon, R. P.; Bovee, T. D.; Doronina, S. O.; Burke, P. J.; Hunter, J. H.; Neff-LaFord, H. D.; Jonas, M.; Anderson, M. E.; Setter, J. R.; Senter, P. D., Reducing hydrophobicity of homogeneous antibody-drug conjugates improves pharmacokinetics and therapeutic index. *Nat. Biotechnol.* **2015,** *33* (7), 733-5.

19. Valliere-Douglass, J. F.; McFee, W. A.; Salas-Solano, O., Native Intact Mass Determination of Antibodies Conjugated with Monomethyl Auristatin E and F at Interchain Cysteine Residues. *Analytical Chemistry* **2012,** *84* (6), 2843-2849.

20. Firth, D.; Bell, L.; Squires, M.; Estdale, S.; McKee, C., A rapid approach for characterization of thiol-conjugated antibody-drug conjugates and calculation of drug-antibody ratio by liquid chromatography mass spectrometry. *Analytical biochemistry* **2015,** *485*, 34-42.

21. Chen, J.; Yin, S.; Wu, Y. J.; Ouyang, J., Development of a Native Nanoelectrospray Mass Spectrometry Method for Determination of the Drug-to-Antibody Ratio of Antibody-Drug Conjugates. *Analytical Chemistry* **2013,** *85* (3), 1699-1704.

22. Wiggins, B.; Liu-Shin, L.; Yamaguchi, H.; Ratnaswamy, G., Characterization of cysteine-linked conjugation profiles of immunoglobulin G1 and immunoglobulin G2 antibody-drug conjugates. *J. Pharm. Sci.* **2015,** *104* (4), 1362-72.

23. Fekete, S.; Veuthey, J. L.; Beck, A.; Guillarme, D., Hydrophobic interaction chromatography for the characterization of monoclonal antibodies and related products. *Journal of pharmaceutical and biomedical analysis* **2016,** *130*, 3-18.

24. J.Alpert, A., High-performance hydrophobic-interaction chromatography of proteins on a series of poly(alkyl aspart-amide)-silicas. *J. Chromatogr. A* **1986,** *359*, 85-97.

25. Xiu, L.; Valeja, S. G.; Alpert, A. J.; Jin, S.; Ge, Y., Effective protein separation by coupling hydrophobic interaction and reverse phase chromatography for top-down proteomics. *Anal. Chem.* **2014,** *86* (15), 7899-906.

26. Chen, B.; Peng, Y.; Valeja, S. G.; Xiu, L.; Alpert, A. J.; Ge, Y., Online Hydrophobic Interaction Chromatography-Mass Spectrometry for Top-Down Proteomics. *Anal. Chem.* **2016,** *88* (3), 1885-91.

27. Wiggins, B.; Liu-Shin, L.; Yamaguchi, H.; Ratnaswamy, G., Characterization of Cysteine-Linked Conjugation Profiles of Immunoglobulin G1 and Immunoglobulin G2 Antibody-Drug Conjugates. *Journal of Pharmaceutical Sciences* **2015,** *104* (4), 1362-1372.

28. McCue, J. T., Theory and Use of Hydrophobic Interaction Chromatography in Protein Purification Applications. *Methods Enzymol.* **2009,** *463*, 405-414.

29. J.A. Queiroz, C. T. T., J.M.S. Cabral, Hydrophobic interaction chromatography of proteins. *J. Biotechnol.* **2001,** *87* (143-159).

30. Géza Rippel, L. S., Hydrophobic interaction chromatography of proteins on an Alkyl-Superose column. *J. Chromatogr. A* **1994,** *664*, 27-32.

31. Christine Machold, K. D., Rainer Hahn, Alois Jungbauer, Hydrophobic interaction chromatography of proteins I. Comparison of selectivity. *J. Chromatogr. A* **2002,** *972*, 3-19.

32. Xia, F.; Nagrath, D.; Garde, S.; Cramer, S. M., Evaluation of selectivity changes in HIC systems using a preferential interaction based analysis. *Biotechnology and bioengineering* **2004,** *87* (3), 354-63.

33. To, B. C.; Lenhoff, A. M., Hydrophobic interaction chromatography of proteins. II. Solution thermodynamic properties as a determinant of retention. *J. Chromatogr. A* **2007,** *1141* (2), 235-43.

34. Baca, M.; De Vos, J.; Bruylants, G.; Bartik, K.; Liu, X.; Cook, K.; Eeltink, S., A comprehensive study to protein retention in hydrophobic interaction chromatography. *J Chromatogr. B.* **2016,** *1032*, 182-188.

35. Chen, B. F.; Lin, Z. Q.; Alpert, A. J.; Fu, C. X.; Zhang, Q. Y.; Pritts, W. A.; Ge, Y., Online Hydrophobic Interaction Chromatography-Mass Spectrometry for the Analysis of Intact Monoclonal Antibodies. *Anal. Chem.* **2018,** *90* (12), 7135-7138.

36. Bobaly, B.; Beck, A.; Veuthey, J. L.; Guillarme, D.; Fekete, S., Impact of organic modifier and temperature on protein denaturation in hydrophobic interaction chromatography. *Journal of pharmaceutical and biomedical analysis* **2016,** *131*, 124-132.

37. Huang, X.; Wirth, M. J., Surface-Initiated Radical Polymerization on Porous Silica. *Anal. Chem.* **1997,** *69* (22), 4577-4580.

38. Valeja, S. G.; Xiu, L.; Gregorich, Z. R.; Guner, H.; Jin, S.; Ge, Y., Three dimensional liquid chromatography coupling ion exchange chromatography/hydrophobic interaction chromatography/reverse phase chromatography for effective protein separation in top-down proteomics. *Anal Chem* **2015,** *87* (10), 5363-5371.

39. Janin-Bussat, M. C.; Dillenbourg, M.; Corvaia, N.; Beck, A.; Klinguer-Hamour, C., Characterization of antibody drug conjugate positional isomers at cysteine residues by peptide mapping LC-MS analysis. *J. Chromatogr. B* **2015,** *981*, 9-13.

40. Sogbein, O. O.; Simmons, S. A.; Konermann, L., Effects of pH on the Kinetic Reaction Mechanism of Myoglobin Unfolding Studied by Time-Resolved Electrospray Ionization Mass Spectrometry. *J. Am. Soc. Mass Spectrom* **2000,** *11*, 312-319.

41. May, J. C.; Jurneczko, E.; Stow, S. M.; Kratochvil, I.; Kalkhof, S.; McLean, J. A., Conformational Landscapes of Ubiquitin, Cytochrome c, and Myoglobin: Uniform Field Ion Mobility Measurements in Helium and Nitrogen Drift Gas. *Int J Mass Spectrom* **2018,** *427*, 79-90.

42. McCalley, D. V., Effect of buffer on peak shape of peptides in reversed-phase high performance liquid chromatography. *Journal of Chromatography A* **2004,** *1038* (1-2), 77-84.

43. McCalley, D. V., Study of overloading of basic drugs and peptides in reversed-phase high-performance liquid chromatography using pH adjustment of weak acid mobile phases suitable for mass spectrometry. *Journal of Chromatography A* **2005,** *1075* (1-2), 57-64.

Table 2.1. Summary of HPLC columns and their applications

| **Column** | **Application** | **Mobile Phase A; B** |
|---|---|---|
| Thermo MabPac RP | RPLC, reduced ADC | $H_2O$+0.1% DFA; ACN + 0.1% DFA |
| Supelco Bioshell A400 | RPLC, non-reduced ADC | $H_2O$+0.1% FA+0.015%TFA; ACN + 0.1% FA +0.015%TFA |
| Thermo-HIC butyl | HIC, ADC (Purdue) | 50 mM $Na_3PO_4$+1 M $(NH_4)_2SO_4$, pH 7; 50 mM $Na_3PO_4$+30% IPA, pH 7 |
| Tosoh TSKgel Butyl | HIC, ADC (AbbVie) | 25 mM $Na_3PO_4$+1.5 M $(NH_4)_2SO_4$, pH 7; 25 mM $Na_3PO_4$+25% IPA, pH 7 |
| PMMA, nonporous | nRPLC, ADC | 50 mM $NH_4OAc$, pH 7; 50 mM $NH_4OAc$+50% IPA, pH7 |

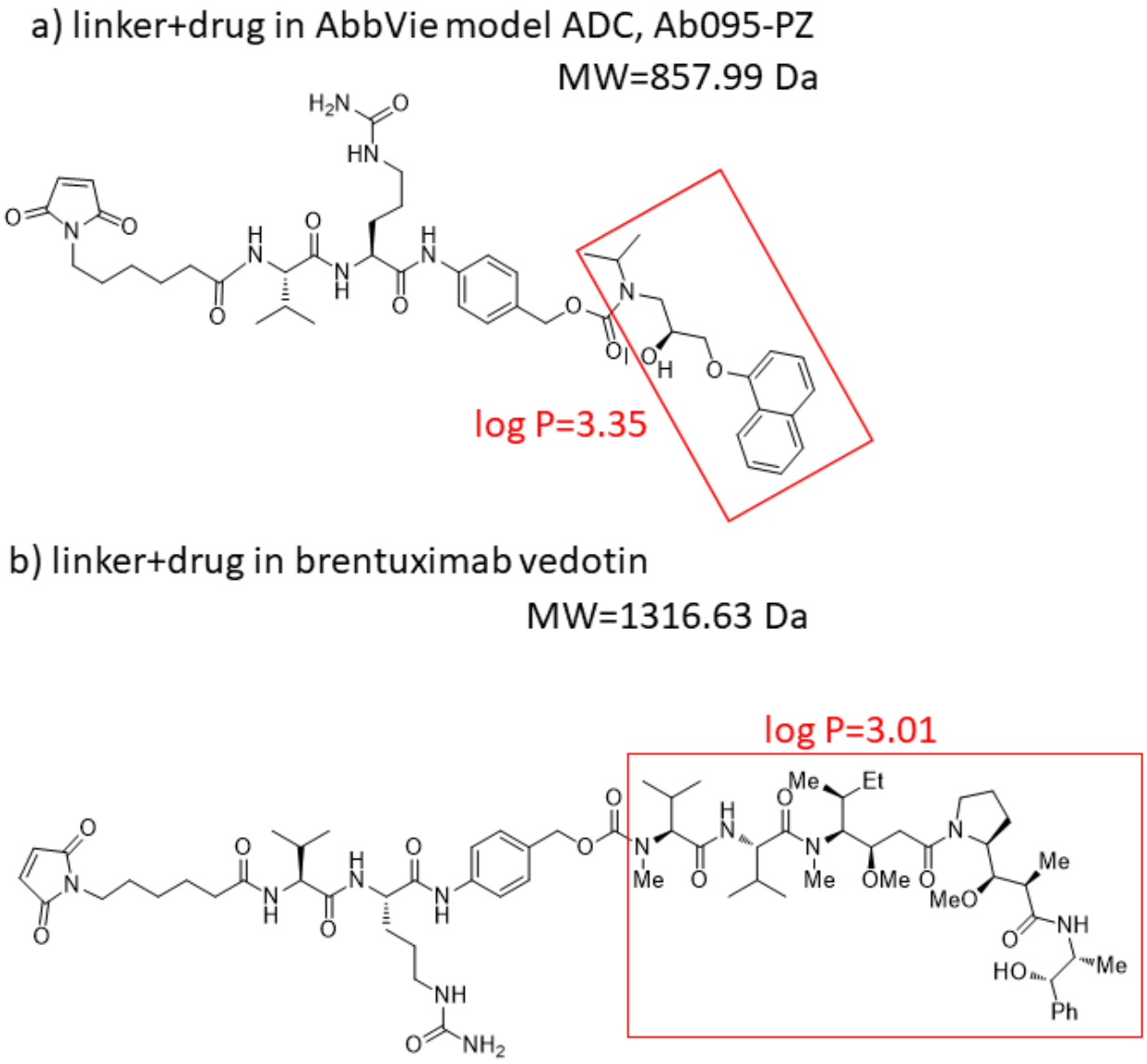


Figure 2-1 Chemical structures of linker-drug combination for a) the AbbVie model ADC, Ab095-PZ and b) brentuximab vedotin. Each drug or drug mimic part is in the red square, and its hydrophobicity is expressed by log P, where P represents the octanol/water partition coefficient.

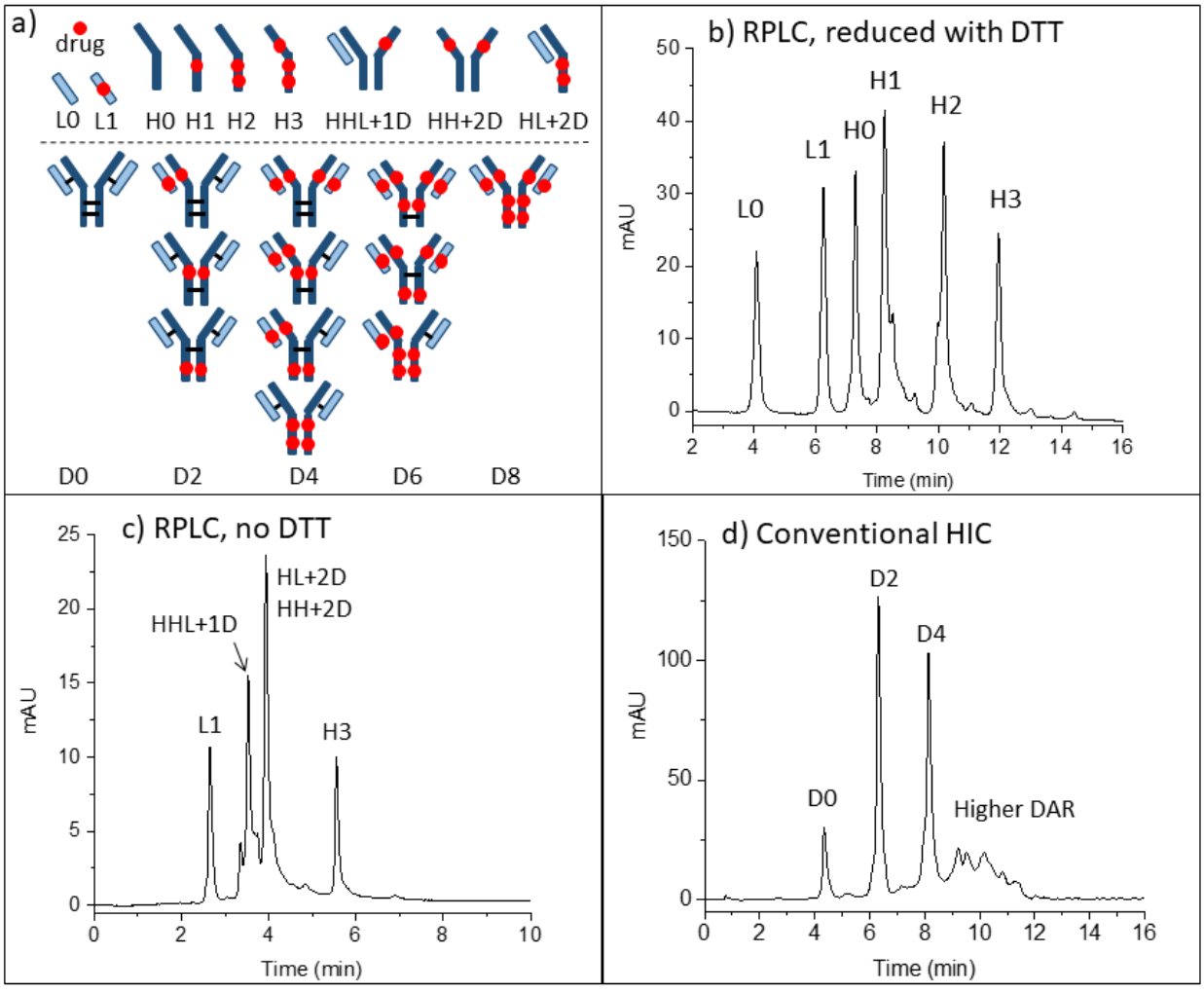


Figure 2-2 a) Sketches explain abbreviations for peak assignments. b) RPLC of the model ADC after reduction with DTT. c) RPLC of the model ADC without DTT. d) HIC of the intact ADC with tentative peak assignments. Condition are in supporting information.

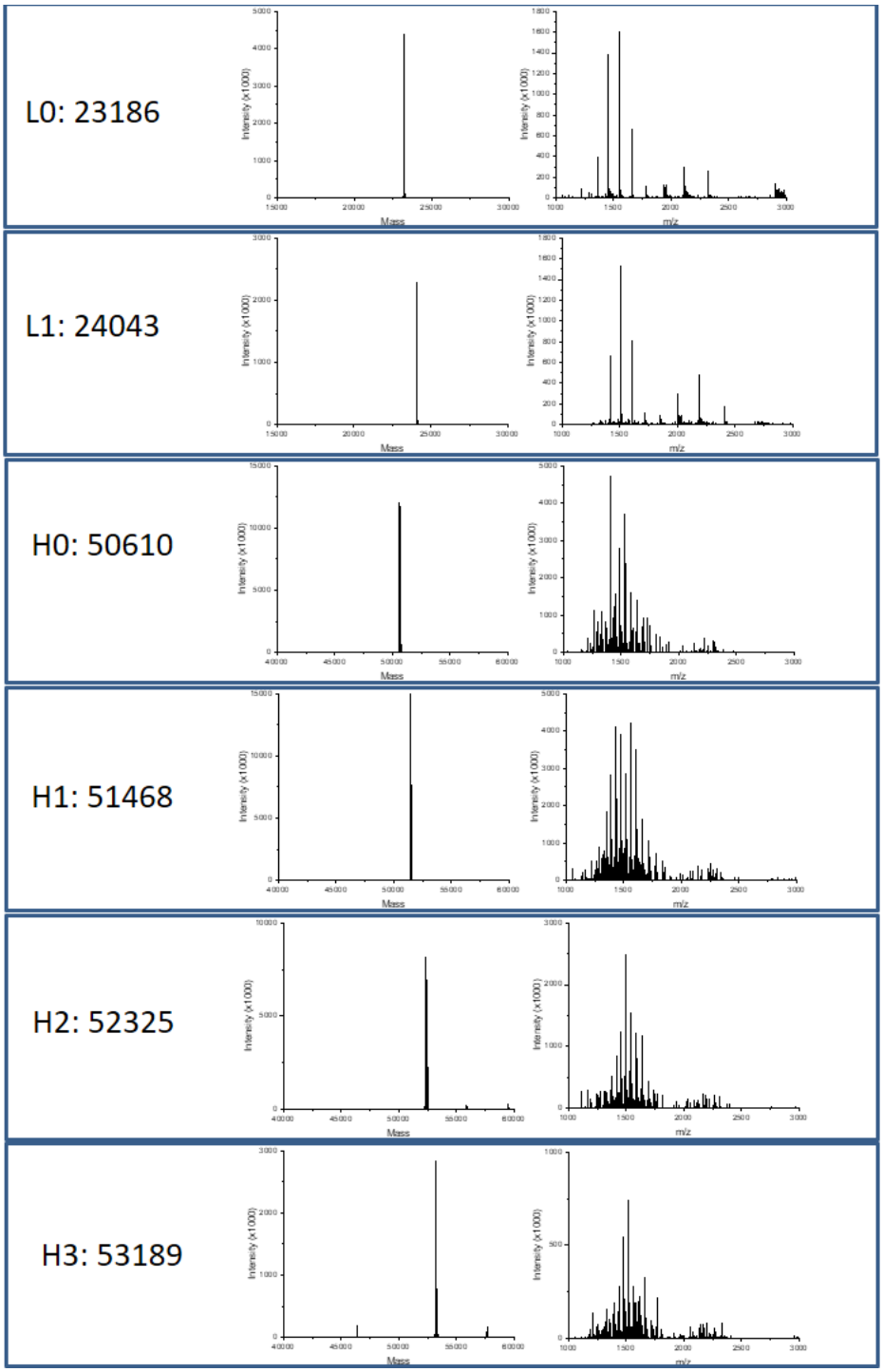


Figure 2-3 Raw mass spectra (right) and deconvoluted mass spectra (left) for each peak in the chromatograms of Figure 2-2b.

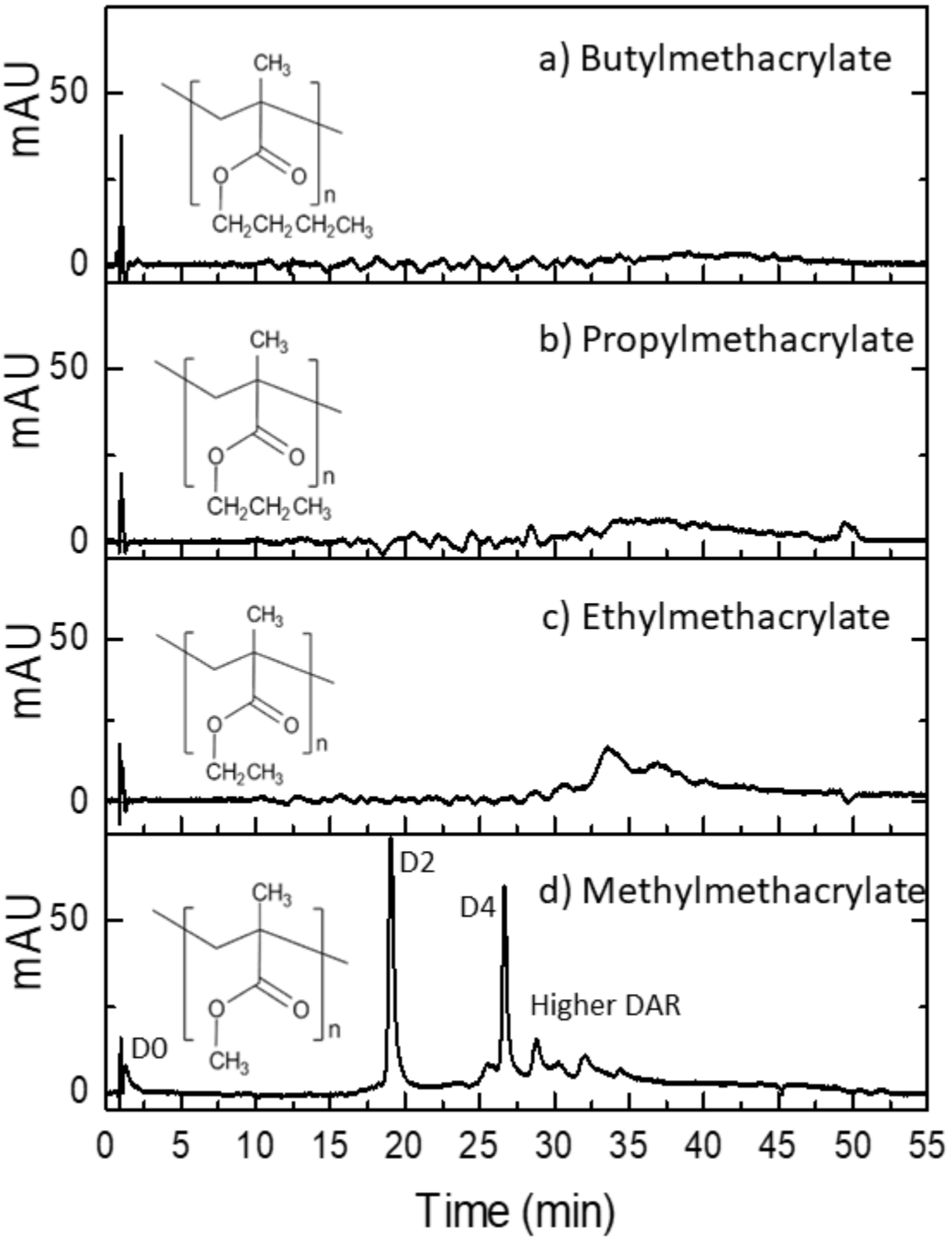


Figure 2-4 nRPLC of AbbVie model ADC with varying hydrophobicity of bonded phase, as denoted by the structures. Gradient conditions are A: 50 mM $NH_4OAc$, pH 7, B: 50 mM $NH_4OAc$, 50% IPA, pH 7, 0-100 %B /40 min, 100 %B /5 min, 100 µL/min, 30 °C. The same tentative labels as for the HIC chromatogram of Figure 2-2d are made due to the similarity.

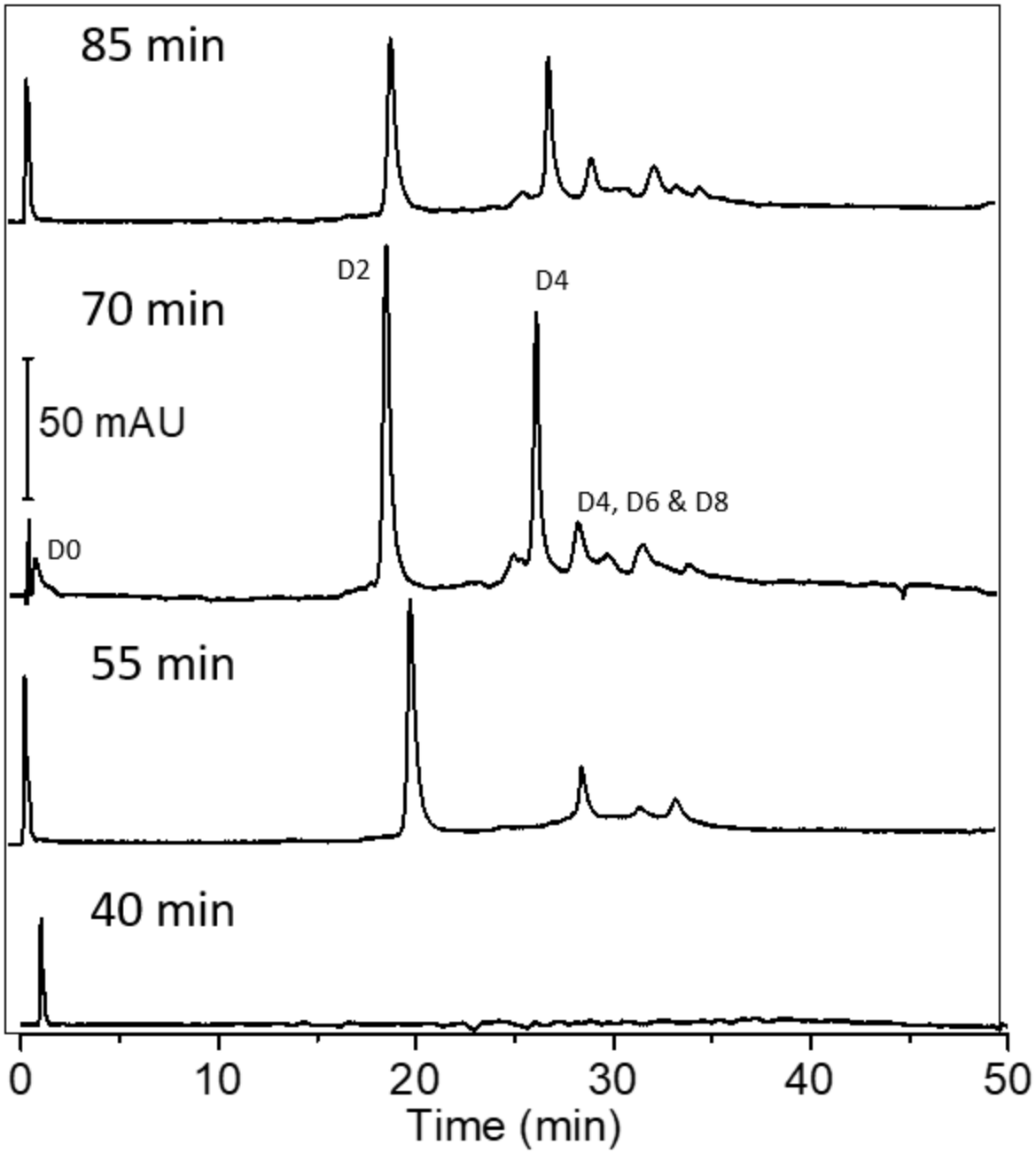


Figure 2-5 nRPLC chromatogram for varying PMMA growth time using the same non-denaturing conditions as in, showing that the 70 min growth time is optimal with respect to resolution and recovery. Polymer growth time is labeled in each panel.

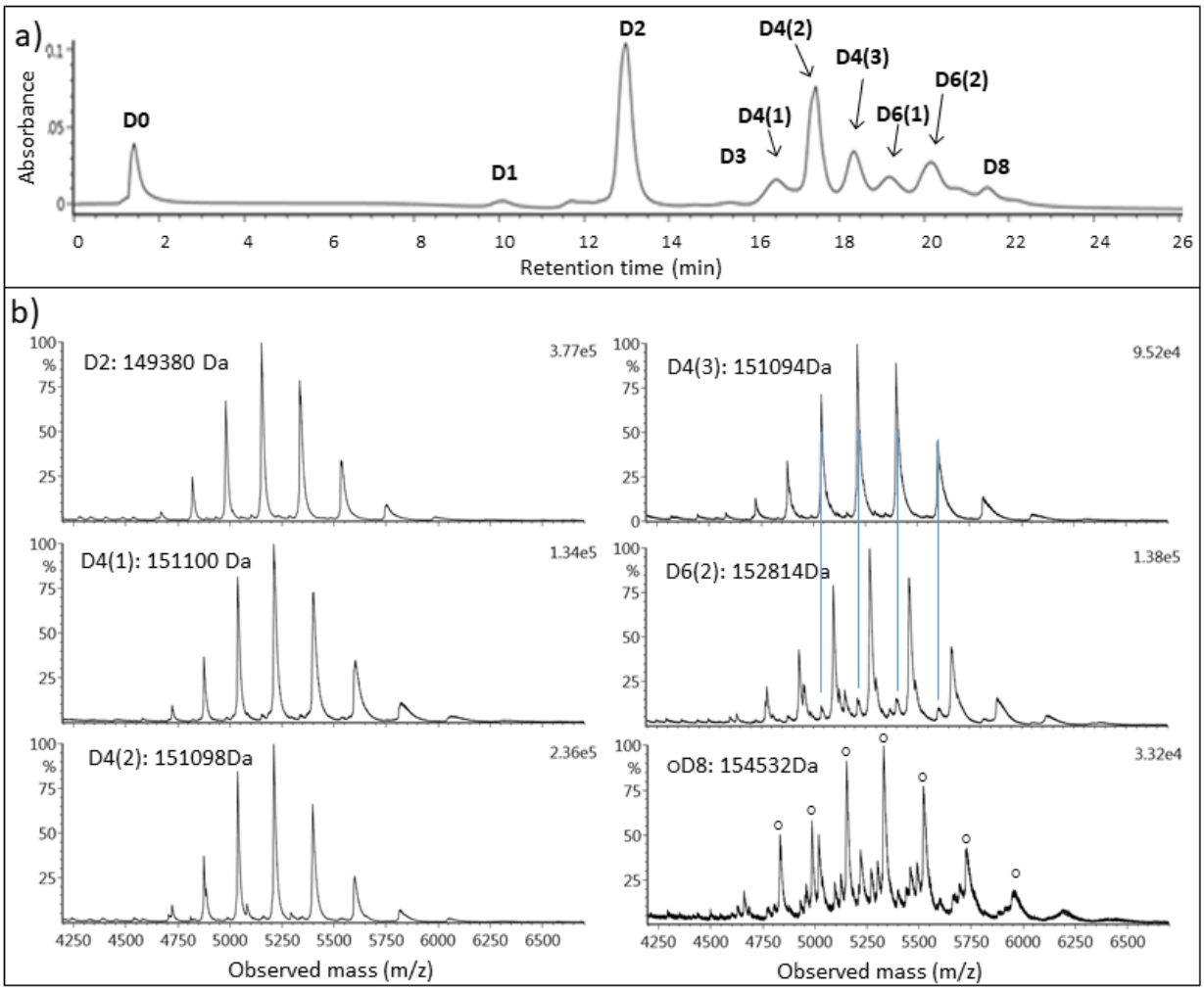


Figure 2-6 a) nRPLC of the AbbVie model ADC Ab095-PZ, with peaks labeled based on the mass spectra. Gradient: 0 to 4.5% IPA/water over 3 min., then 4.5 to 50% IPA/water over 20 min. Detection at 280 nm. b) Raw mass spectra for peaks as labeled, with the molecular weight based on deconvoluted mass spectra for peak ID. The blue lines show that extra peaks are from overlap.

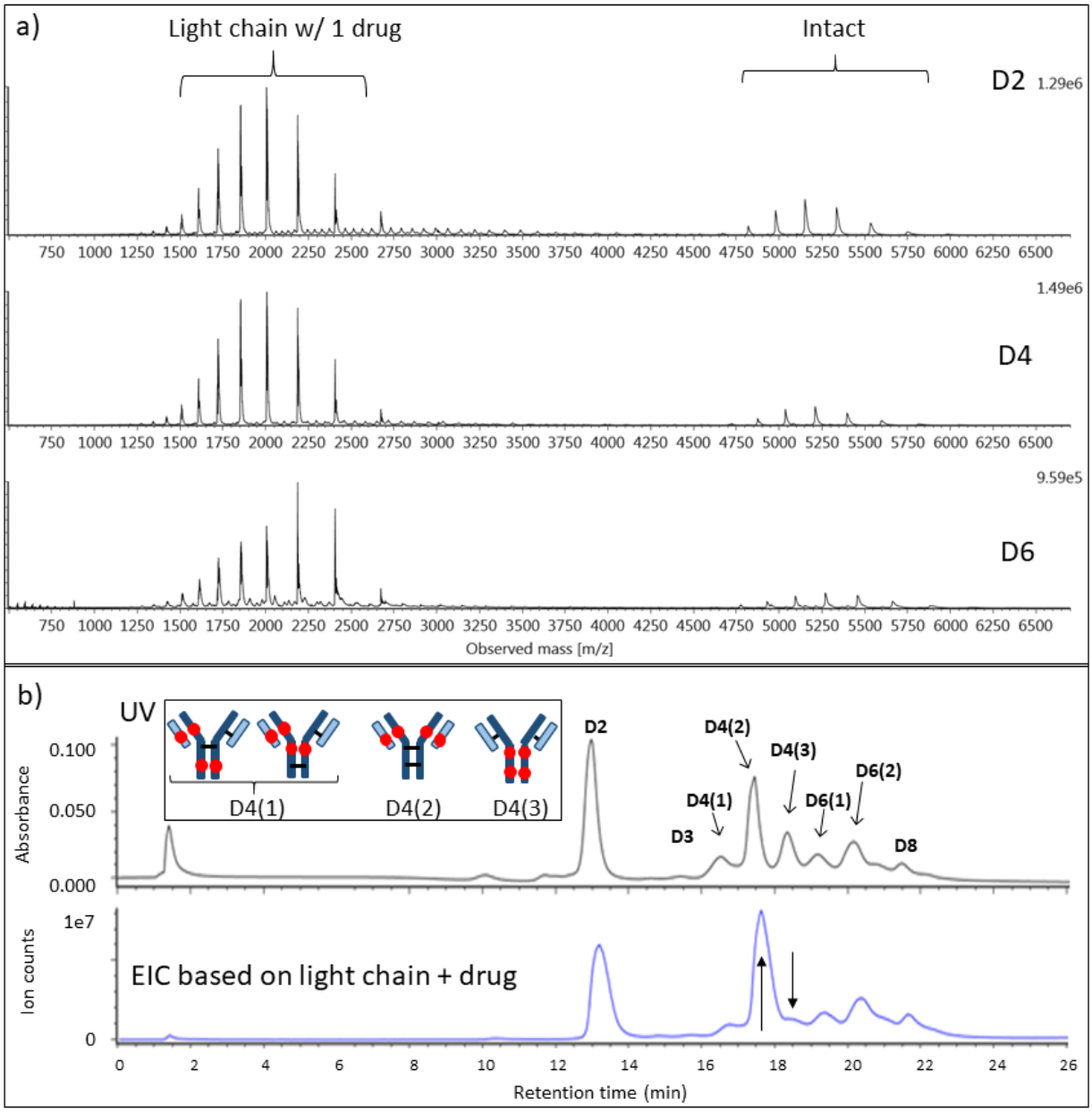


Figure 2-7 Evidence that light chain dissociates in MS source for AbbVie model ADC. a) Full-range raw mass spectra show large signals for light chain+drug, but no significant signals for ADC minus light chain+drug. b) Chromatogram with UV detection (top) and EIC based on light chain+drug (bottom). The blue arrows point to two peaks that changed intensities, and the inset depicts the structures for the isomers consistent with these intensity changes.

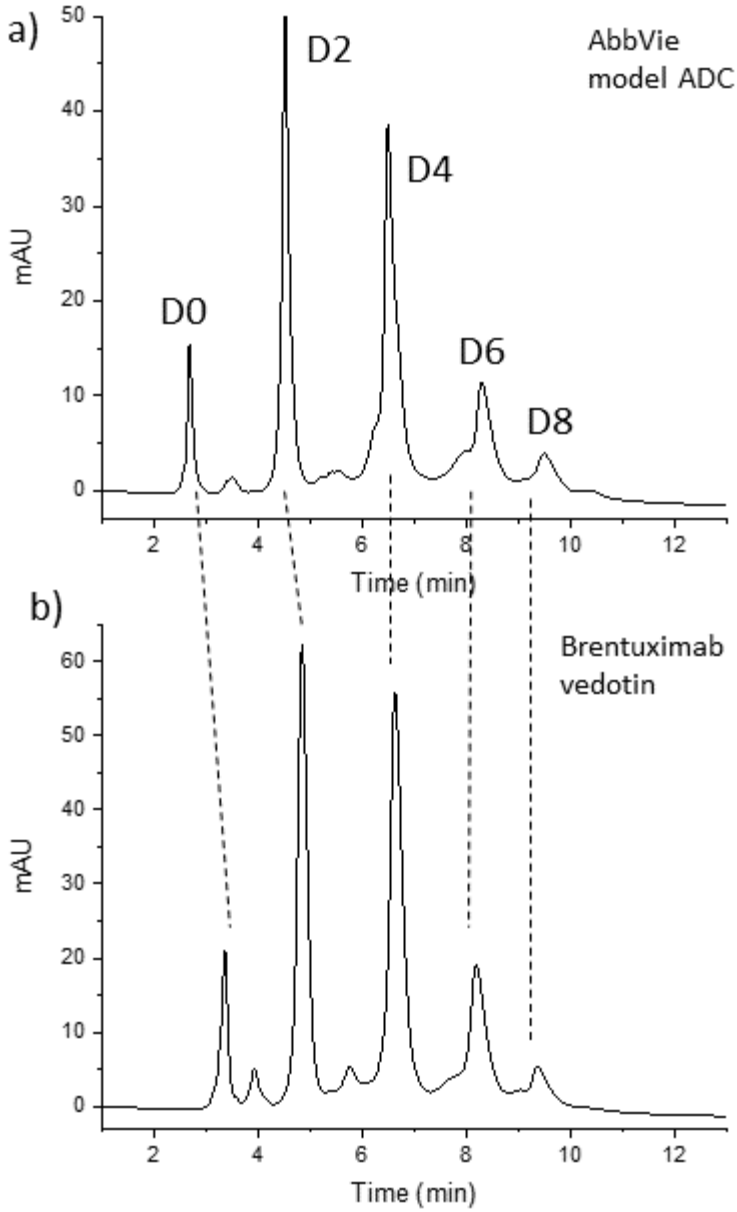


Figure 2-8 HIC separation of a) model ADC and b) commercial ADC Brentuximab vedotin. The dashed lines illustrate that the greater hydrophobicity of the mAb itself for Brentuximab vedotin. Tosoh TSKgel Butyl-NPR, 4.6x35mm, 2.5 um. MPA: 1.5M ammonium sulfate, 25 mM sodium phosphate pH 7.0; MPB: 25 mM sodium phosphate pH 7.0 with 25% IPA; Flow rate: 0.8 mL/min; Column temp: 25 °C

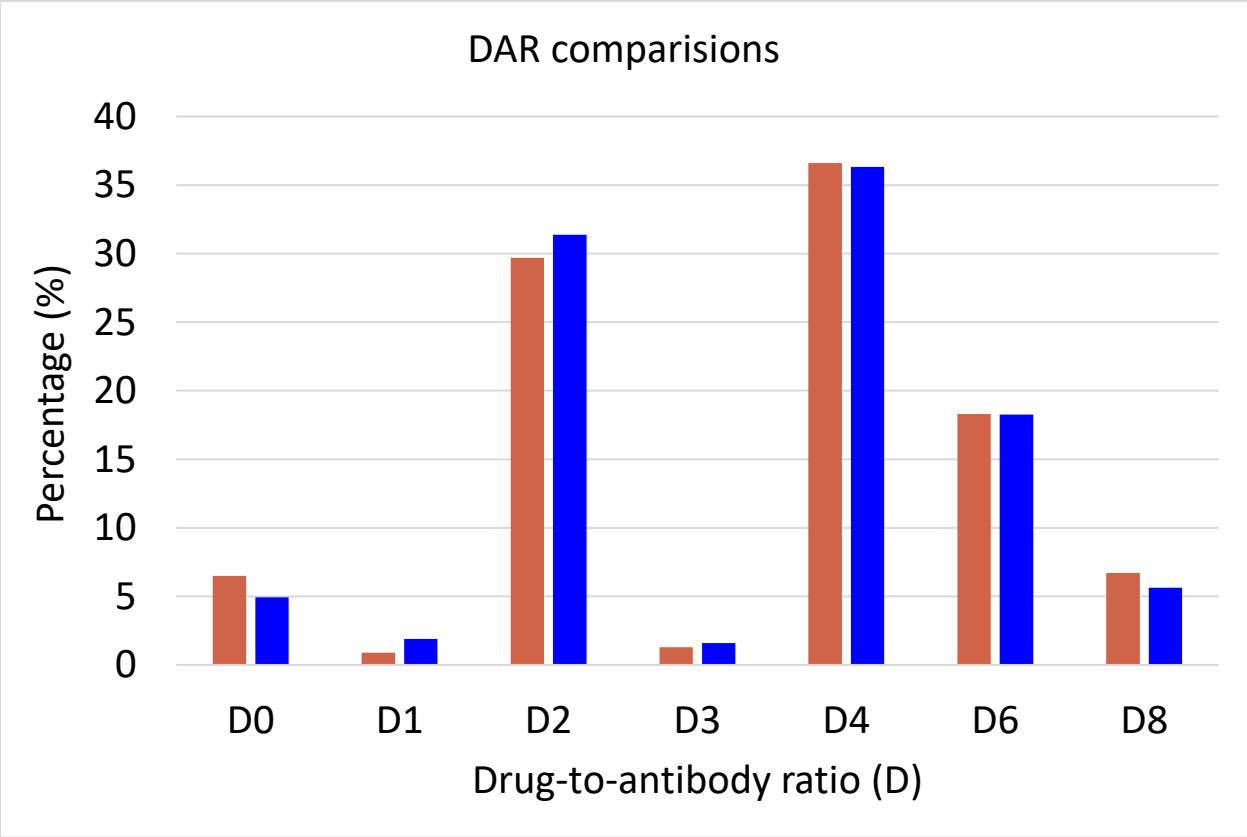


Figure 2-9 The comparison of drug-to-antibody ratio of model ADC. a) Orange bars were integrated peak area from Figure 2-8a, HIC separation from Tosoh TSKgel Butyl-NPR column. b) Blue bars were integrated peak area from Figure 2-6a, nRPLC separation from PMMA column.

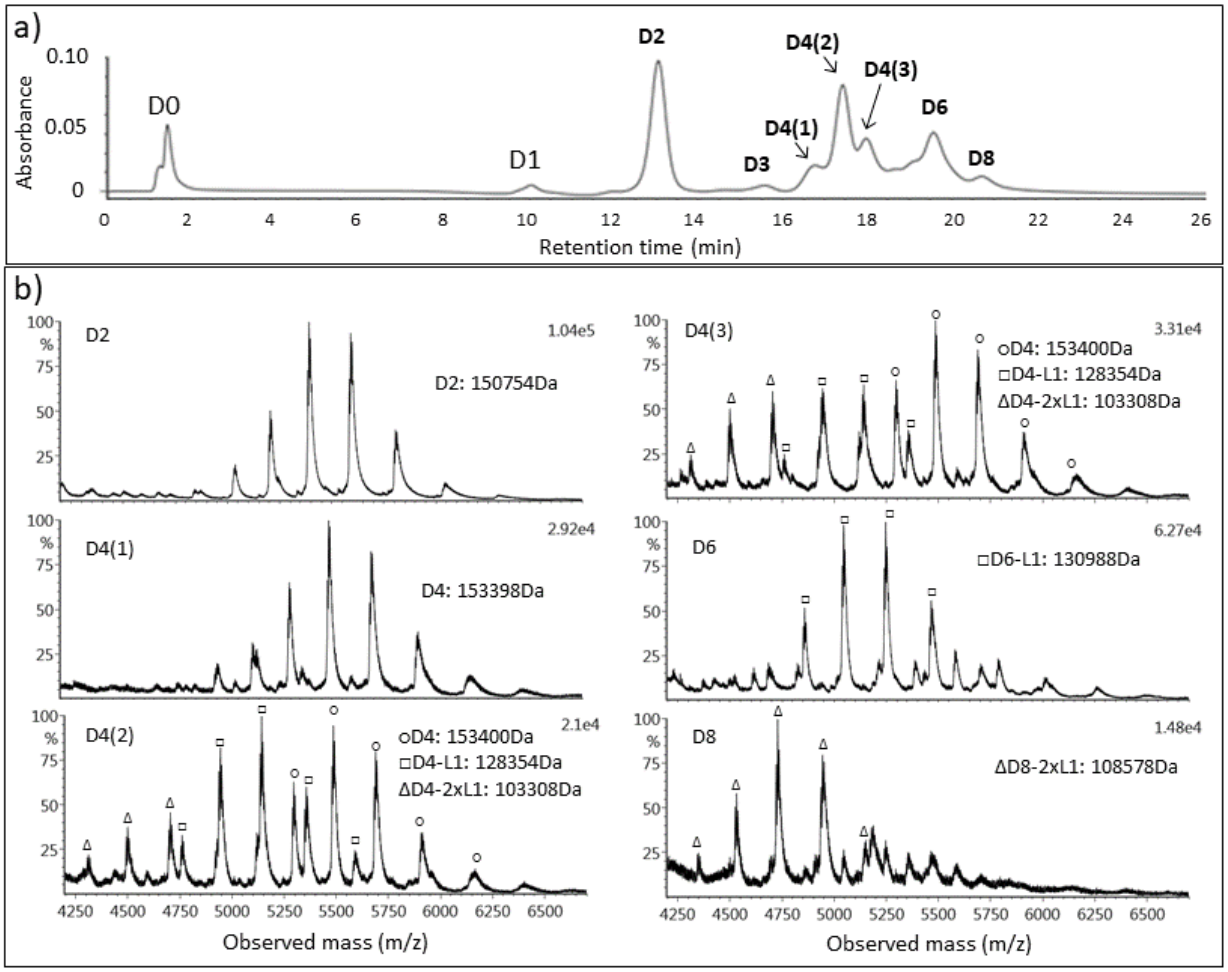


Figure 2-10 nRPLC and mass spectra for commercial ADC: brentuximab vedotin. a) nRPLC with detection at 280 nm. Conditions same as for Figure 2.6. b) Raw mass spectra for D2, D4(1,2,3), D6, D8, with the molecular weight based on deconvoluted mass spectra.

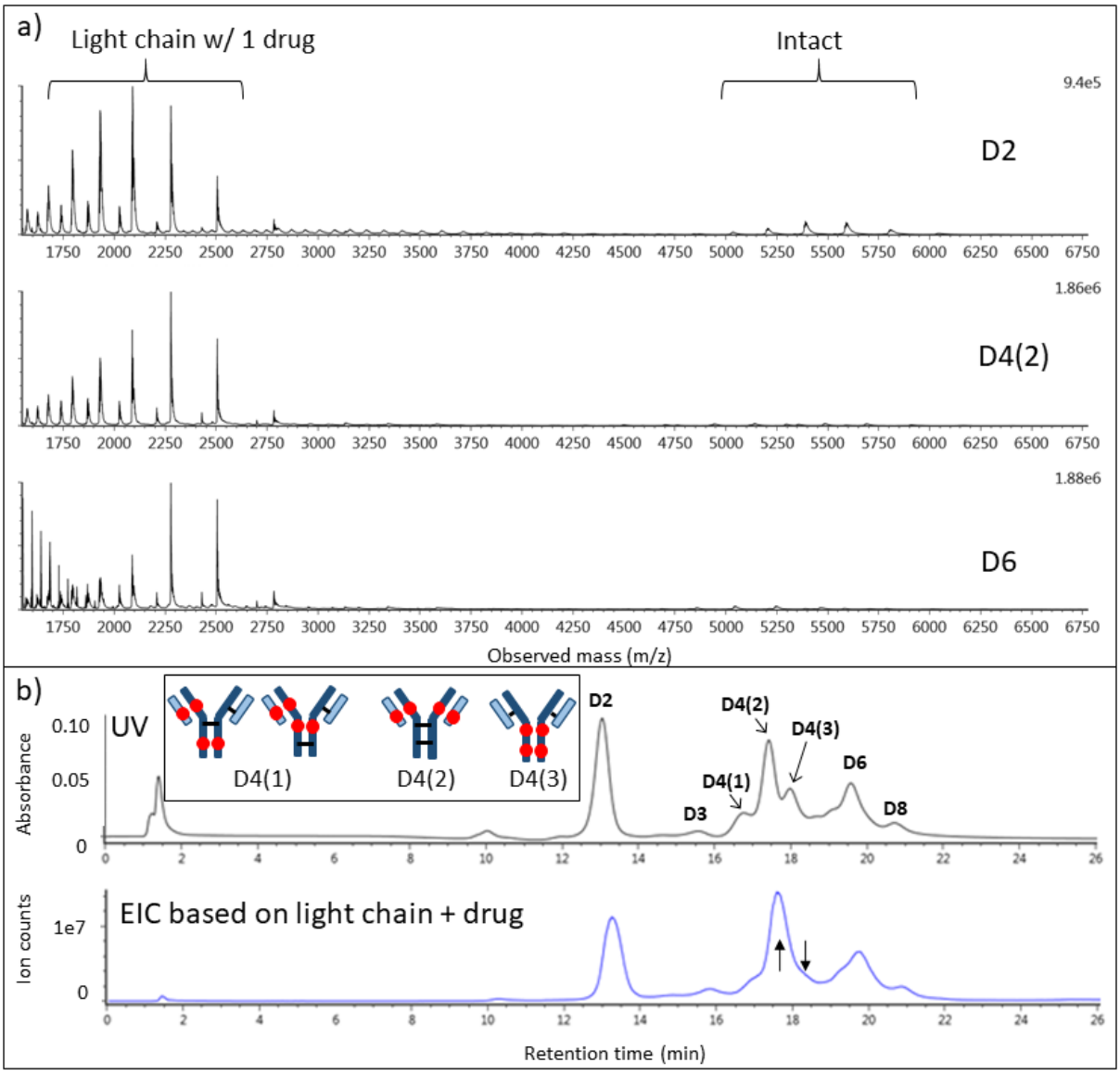


Figure 2-11 a) LCMS data for brentuximab vedotin, analogous to Figure 5. a) Full-range raw mass spectra show even stronger signals for light chain+drug than observed for the AbbVie model ADC. b) Chromatogram for UV detection (top) approximately tracks that of EIC for signal of light chain+drug, again indicating light chain+drug dissociated after separation. Again, the blue arrows show two peaks that changed intensities, and the inset depicts the structures for the D4 isomers that are consistent with these changes.

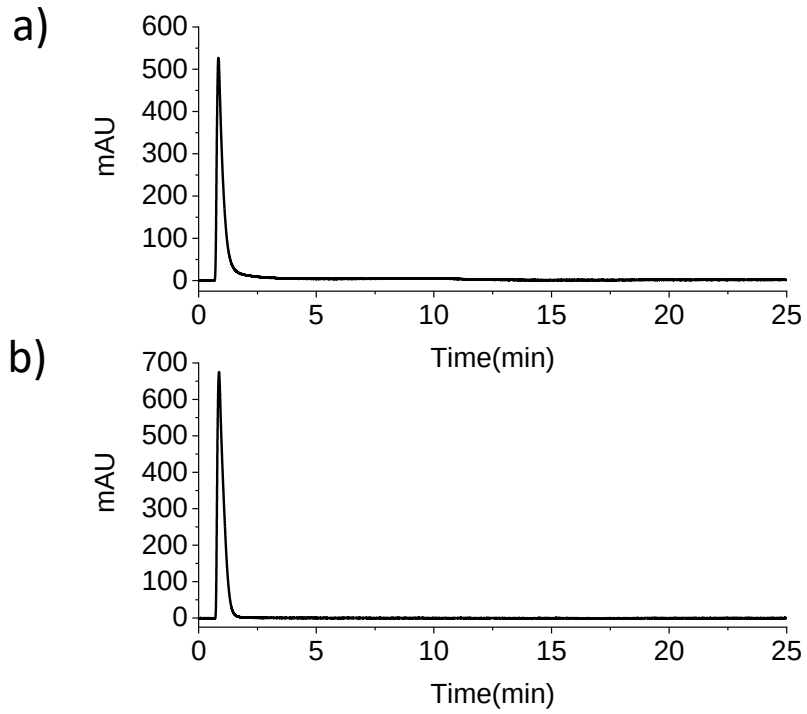


Figure 2-12 nRPLC of a) lysozyme, and b) α-chymotrypsinogen A using PMMA with the 70 min growth time. Gradient conditions are A: 50 mM $NH_4OAc$, pH 7, B: 50 mM $NH_4OAc$, 50% IPA, pH 7, 0-100 %B /10 min, 100 %B /5 min, 100 µL/min, 25 °C. Injection amount is 3 µg. Chromatograms are shown with baseline subtraction.

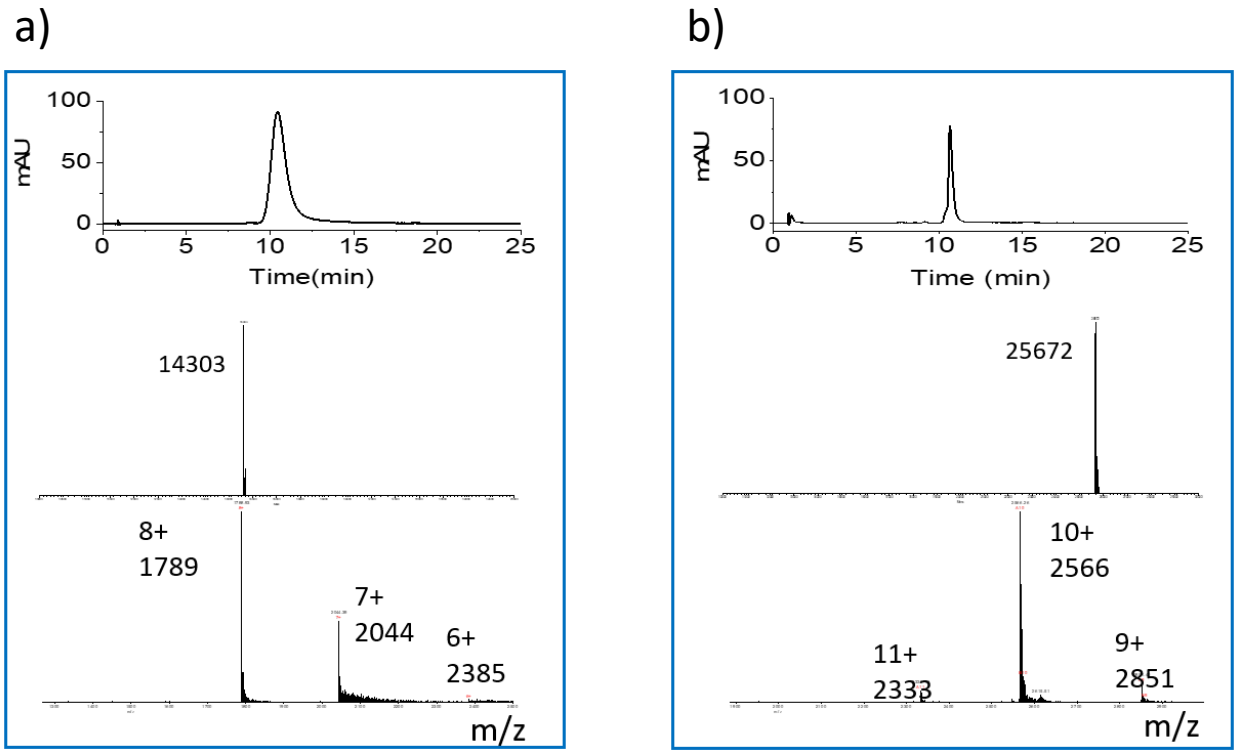


Figure 2-13 nRPLC of a) lysozyme, and b) α-chymotrypsinogen A using PBzMA with the 90 min growth time. Gradient conditions are same as Figure 2-12. Chromatograms are shown with baseline subtraction.

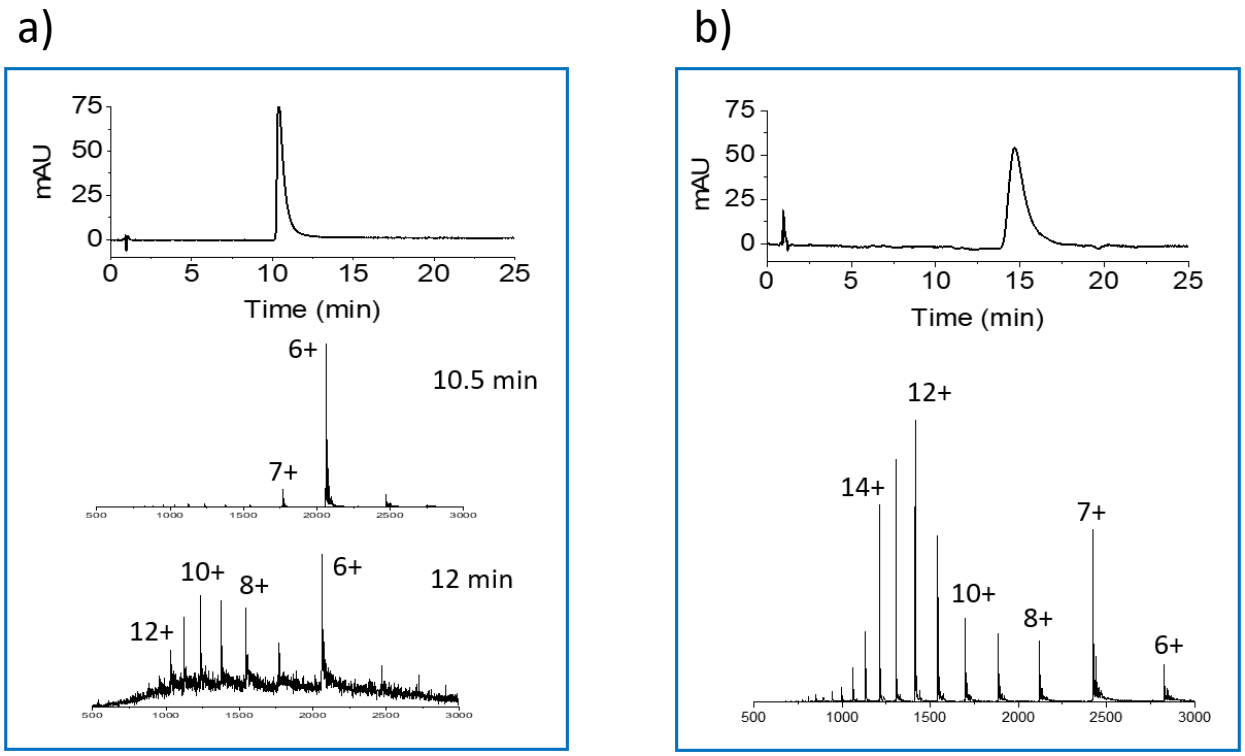


Figure 2-14 nRPLC of a) cytochrome C, and b) myoglobin using PBzMA with the 90 min growth time. Gradient conditions are A: 50 mM $NH_4HCOO$, pH 5.5, B: 50 mM $NH_4HCOO$, 50% IPA, pH 5.5, 0-100 %B /10 min, 100 %B /5 min, 100 µL/min, 25 °C. Injection amount is 3 µg. Chromatograms are shown with baseline subtraction.

# CHAPTER 3. POLYMER LAYER TO SHIELD SURFACE CHARGES: ALLOWING FOR RPLC-MS WITH 0.5% FORMIC ACID AS ADDITIVE

## 3.1 Abstract

A polymethylmethacrylate bonded phase was studied for its ability to screen surface charge in RPLC-MS for improving LC resolution with formic acid. The separation of IgG1 free thiol variants was used to test LC resolution and MS sensitivity. For silane monolayers, LC resolution is shown to decrease two-fold when using 0.5% formic acid place of 0.1% trifluroacetic acid, losing the ability to resolve free thiol variants. The polymer behaves oppositely, resolving the free thiol variants with 0.5% formic acid, but not with 0.1% trifluoroacetic acid. Chromatograms show that increasing polymer thickness gives sharper peaks, supporting the notion of shielding surface charge. The lower resolution for the polymer with trifluoroacetic acid is associated with marked loss of protein recovery, which is indicated by decreasing recovery with increased ratio of trifluoroacetic:formic acids at constant pH. This is attributed to wetting of the polymer by the mobile phase when trifluoroacetic acid is used, as wetting makes the mobile and stationary phases more similar. Overall, using 0.5% formic acid instead of 0.1% trifluoroacetic acid, MS sensitivity increases 10X relative while all of the thiol variants are well resolved by the polymethylmethacrylate bonded phase.

## 3.2 Introduction

The liquid chromatography coupled with mass spectrometry (LC-MS) is one of the most powerful and reliable analytical technique for protein characterization in pharmaceutical industry.[1, 2] Based on statistical data of the methods used for monoclonal antibody (mAb) from Food and Drug Administration (FDA), LC-MS based workflow becomes a dominant implement for analysis of biopharmaceuticals and biosimilars.[3] Although the LC-MS platform has been improved, intact protein separation from LC and mass analysis from MC are still challenging due to their large molecule size, complicated structure, complex interactions with other molecular systems, solubility, low ionization efficiency, sparse signal among charge states, which result in poor LC resolution and MS sensitivity[4, 5].

Monoclonal antibody therapies for cancer has dramatically increased since 1990 and global sales revenue reaches $75 billion since 2013.[6] There are over 300 mAb candidates currently in pharmaceutical pipelines.[6] One key factor comparing antibodies and small-molecule drugs is specific targeting, which selectively target malignant cells with less toxic to biological system.[7-9] In breast cancer, for example, the first approved mAb, trastuzumab from Genentech, showed targeting specific HER-2 receptors to achieve clinical benefits.[10] Another key factor is that mAb is able to trigger immune responses against tumor cells to maximize therapeutic effects.[7] By blocking a PD-1/PD-L1 pathway to activate immunotherapy to battle tumors has been aggressively studied recently. For instance, pembrolizumab from Merck has successfully triggered immune system by inhibiting PD-1.[11] Currently, immunoglobulin G1 (IgG1) is the most abundant and used as mAb drugs effectively.[12, 13]

Structural heterogeneity of IgG1 causes different effector functions and its complexity requires bioanalytical techniques severely under intact level.[14] Thiol and disulfide variant of cysteines are important post-translational modification (PTM) of IgG1. Free thiol could induce the antibody aggregation, activity, and stability, which may significantly impact biological function[15-19]. Multiple bioanalytical methods have been developed to identify free thiols: Ellman's assay[20], fluorescent labeling[21, 22], and sodium dodecyl sulfate polyacrylamide gel electrophoresis (SDS-PAGE)[23]. However, those methods are strongly time-consuming and labor-intensive. Since changes in disulfide bond and existence of free thiol could conduct protein conformational changes and induce protein hydrophobicity changes, reversed-phase liquid chromatography (RPLC) could thus be applied.[24-27] Furthermore, RPLC method performs high selectivity and has become the most common identification and quantification separation method to chemical modification of mAbs at intact level[28]. Recently, Protein Analytical Chemistry Group in Genentech published characterization and identification of free thiol variants and unpaired cysteines using RPLC-MS.[29-31] In these articles, 0.1% trifluoroacetic acid (TFA) was used to achieve baseline separation of five peaks including three major thiol forms on complementarity determining regions (CDR) and two minor thiol forms on other positions. However, TFA is not very MS-friendly due to strong ion pairing effect, which suppresses ionization efficiency and reduce MS sensitivity enormously.[5, 32, 33] Moreover, TFA can reduce protein recovery, lower chromatographic selectivity, and broaden peak width because of ion pairing.[34-36] On the contrary, formic acid (FA) has no ion pairing effect and yields higher MS response[37, 38]. Nonetheless, FA inevitably reduces LC resolution and

sacrifices information from more hydrophilic components[31, 39]. By compromising the LC resolution and MS ion response, a mixer of 0.1% FA and 0.025% TFA is an acceptable alternative and offers similar LC resolution to 0.1% TFA only and better MS sensitivity. Due to only +2 Da mass shift resulted from the reduction of disulfide to a pair of free thiols in the mAb, the deconvoluted spectra did not show desirable mass difference from 2-4 Da.[31] Although the N-*tert*-butylmaleimide-alkylated free thiols allow the more obvious mass shift and provide additional hydrophobicity to free thiol variants, 0.08% TFA is still required to get better baseline separation.[30] Additionally, the observed mass is still not accurate and also alkylation the labeling degree and conformational change may be concerned. As a result, it is an urgent need to develop a label-free RPLC-MS method to characterize IgG1 free thiols with accomplishment of both LC resolution and MS sensitivity.

In this study we report RPLC-MS using polymer-shell bonded phases for separating for free thiol variants on intact IgG1 with 0.5% formic acid (FA) without the use of TFA, which baseline resolves more free thiol variants and shows 1000X ion abundance higher than using TFA solely. This polymer-shell technology allows LC directly coupled with MS. The polymer layer is thick enough to screen surface charges from dissociated silanols. The polymer stationary phase is evaluated using both MS-compatible and MS-incompatible mobile phases, where has the highest LC resolution and greatest MS sensitivity using formic acid.

## 3.3 Materials and methods

### 3.3.1 Materials

Nonporous silica particles (1500 nm) were purchased from Superior Silica (Tempe, AZ). Empty stainless-steel columns (2.1 mm I.D., 50 mm length), reservoirs (4.6 mm I.D., 150 mm), and frits (0.5 µm pore diameter) were purchased from Isolation Technologies (Middleboro, MA). Stainless-steel tubing, ferrules, and internal nuts were all purchased from Valco Instruments (Houston, TX). Silanes, i.e., (chloromethyl)phenyl)dimethylchlorosilane (+99%) and trimethylchlorosilane (+99%), were purchased from Gelest (Morrisville, PA). Methyl methacrylate (MMA, 99%), benzyl methacrylate (BzMA, 98%) sodium ascorbate (≥99%), butylamine (99.5%), and ammonium hydroxide were purchased from Sigma–Aldrich (St. Louis, MO). Other chemical used included trifluoroacetic acid (TFA, 99%), difluoroacetic acid (DFA,

98%) and copper(II) chloride ($CuCl_2$, 99%) from Acros Organics (Morris Plains, NJ), tris(2-dimethylaminoethyl)amine ($Me_6$TREN, +99%) from Alfa Aesar (Haverhill, MA), and formic acid (FA, 99.5%+, LC/MS grade), isopropanol (IPA), and acetonitrile (ACN) from Fisher Scientific (Hampton, NH). Ultrapure water was obtained from a Milli-Q system (MilliporeSigma, Darmstadt, Germany.)

IgG1 sample was obtained by courtesy of Genentech, Inc. Before injected onto column, the original 30 mg/mL IgG1 sample was diluted to 1 mg/mL with PBS 1x buffer (pH 7.2).

### 3.3.2 UHPLC column preparation

The silica particles were modified as described earlier[40]. Briefly, the 1.5 μm silica particles were calcined at 600 °C for 12 h, then annealed at 1050°C for 3 h. SEM showed that the particles decreased in diameter to 1.2 μm from the calcining and annealing steps. After heating steps, the silica particles were rehydroxylated overnight in 10% $HNO_3$, and then rinsed in ultrapure water and dried in a 60 °C vacuum oven. Freshly rehydroxylated silica particles were suspended in a dry toluene solution containing 2% (v/v) of (chloromethyl)phenyl)dimethylchlorosilane and 0.1% (v/v) of butylamine. The solution was refluxed for 3 h and then 2% (v/v) of trimethylchlorosilane was added for endcapping and refluxed for 3 h. The silylated, endcapped particles were then rinsed with dry toluene and allowed to dry in a 60 °C vacuum oven for 2 h.

For packing a column, a 2.1 mm × 50 mm column was packed with 0.24 g of silylated, endcapped particles suspended in acetonitrile. The reservoir (4.6 mm × 150 mm) and column were connected in series. For polymer growth, methylmethacrylate monomer was dissolved in 40:60 $H_2O$/IPA (v/v) in a 50 mL round bottom flask for a final concentration of 2.5 M. Two other solutions were made in 2.0 mL of 40:60 $H_2O$/IPA: 1) a solution containing 40 mg of $CuCl_2$ and 80 μL $Me_6$TREN, and 2) a solution containing 20 mg sodium ascorbate. Afterwards, the Cu/$Me_6$TREN solution was added to the round bottom flask, followed by the sodium ascorbate solution. The resulting solution was poured into a plugged reservoir. A high-pressure pump, LabAlliance Series 1500 HPLC Pump (Laboratory Alliance of Central New York, LLC, Syracuse, NY) was used for packing and modification. The reaction solution from the reservoir was pumped into the column starting at 200 μL/min until the reaction mixture dripped from the end of the column. The flow rate was then lowered to 100 μL/min, and the polymerization reaction was allowed to proceed for a range of reaction times from 0, 20, 40, 60 and 80 min for optimization.

After reaction, the freshly packed column PMMA was rinsed with IPA/water for 20 min at 100 μL/min.

For another bonded phase, the polymerization of benzyl methacrylate was conducted with 20:80 $H_2O$/IPA (v/v) in a 50 mL round bottom flask for a final concentration of 1.0 M and polymer growth time was 90 min or otherwise noted.

### 3.3.3 UHPLC

A Waters Acquity UPLC I-Class (Waters, Milford, MA) was used for the optimization of RPLC separations. Lab-made RPLC columns (2.1 × 50 mm, 1.2 μm nonporous silica particles coated with polymerization time varied PMMA) were used as the analytical columns. Mobile phase A (MPA) and B (MPB) were water and acetonitrile, with different percentage of TFA, DFA, and FA as acidic modifiers. The acidic modifiers and gradients used for elution are detailed along with the results. UV absorbance wavelength was set to 280 nm. The optimal flow rate and column temperature were investigated: 0.1 mL/min at 50 $^{o}$C. The injection amount of IgG1 was 2 μg.

A commercially available AdvancedBio RP-mAb Diphenyl column (2.1 × 50 mm. 3.5 μm, 450 Å, Agilent, Santa, Clara, CA, USA) was used for comparison. Mobile phase A (MPA) and B (MPB) were water and acetonitrile, with different percentage of FA as an acidic modifier. The acidic modifiers and gradients used for elution are detailed along with the results. The optimized flow rate was 100 μl/min and column temperature was 75 °C. The injection amount of IgG1 was 2 μg. The UV detection was 280 nm.

### 3.3.4 LC-MS

For online RPLC-MS, Waters Acquity UPLC I-Class was coupled directly to a Thermo LTQ Velos mass spectrometer with electrospray interface. The electrospray ionization (ESI) spray voltage was set in positive mode at 3.8 kV. Sheath and auxiliary gas pressure was 40 arb and 5 arb, respectively. All spectra were obtained in the m/z range of 1000 – 3800, which included nearly all of intact IgG1 charge envelope while excluding low m/z noise. The gradients and acidic modifiers used for elution are detailed along with the results.

## 3.4 Results and discussions

Figure 3.1 shows the three major forms of free thiol variants on Genentech IgG1. To distinguish such small mass shift from +2 Da and +4 Da by one pair or two pairs of free thiols based on molecular mass of IgG, 150 kDa is absolutely challenging. Therefore, baseline resolved RPLC separation and sufficient ion abundance MS sensitivity is highly required. Diphenyl columns with wide pore are commonly used for RPLC separation for mAbs and free thiols[26, 31]. Agilent AdvancedBio RP-mAb Diphenyl column (2.1 × 50 mm. 3.5 μm, 450 Å) has been selected to make comparison of LC separation using different mobile phase composition in order to evaluate our lab-made polymer-shell columns. Monoclonal antibody is a relatively large size protein, which has around 11 nm by 11 nm in diameter. The larger pore size will be beneficial for separation since it will not be trapped by smaller pore size. By running same condition (6% ACN/ 3 min, 0.6 mL/min at 75 °C), 450 Å pore size performs much better chromatographic resolution than 300 Å pore size used in Liu's article.[31] In Figure 3-2a and b, the above mentioned Agilent column was used for separations of Genentech IgG1 using 31-46% ACN within 50 min in both 0.5% FA (blue) and 0.1% TFA (red) systems in order to get fair comparison of peak width, protein recovery, and peak selectivity. Additional 5% ACN is required to elute IgG1 out under TFA condition in both Figure 3-2a and b because TFA ion pairing effect makes the protein more hydrophobic, increasing elution time selectively[41]. In addition to retention time increase, selectivity between two major peaks shows greater in TFA than in FA, which agrees with increasing ion-pairing hydrophobicity increases selectivity[42]. Apparently, no matter acidic modifier is FA or TFA, 75 °C (Figure 3-2b) is better than 50 °C (Figure 3-2a). This result further proves that TFA has strong ion pair effect, which sometimes induces lower protein recovery and thus, higher temperature is required[34]. With similar functional group, phenyl group, polybenzylmethacrylate (PBzMA) was first selected to test IgG1 (Figure 3-2c). The gradient was 27 to 42% ACN within 50 min at 50 °C in both TFA and FA conditions. Agilent diphenyl and PBzMA both stationary phases have phenyl groups but former one performed ideal separation under 75 °C and later one is 50 °C. This difference could be ascribed by faster mass transfer by polymer shell due to owing to screening surface charges better and flexible polymer brush layer. Again, due to affinity of TFA for hydrophobic sites on protein, retention is longer. In return, TFA gives better peak selectivity. FA chromatogram of PBzMA is similar to FA chromatogram of Agilent Diphenyl column with better resolving minor peaks. In contrast, PBzMA using TFA

resolves total 8 peaks comparing with 5 peaks in Liu's article. Although the selectivity in Figure 3-2c is a little worse than in Figure 3-2b, most of peaks are still baseline resolved. PBzMA performs extraordinary separation on Genentech IgG1, yet the LC condition is 0.1% TFA, MS-unfriendly. According to previous published result, polymethylmethacrylate (PMMA) bonded-phase has remarkable separations on antibody-drug conjugates using MS-friendly condition[40]. Therefore, we further tested PMMA column for Genentech IgG1. The gradient slope is the same as others, 15% ACN within 50 min and since methylmethacrylate is less hydrophobic than benzylmethacrylate, 19-34% ACN was used. Surprisingly, under FA condition, PMMA column resolves total 8 peaks shown in Figure 3-2d, which the peak assignment is comparable to PBzMA column under TFA condition. It is seldom to have similar separation performance between FA and TFA. Peaks are then broader with FA due to silanol dissociation.[43] TFA result from PMMA on the contrary gives low protein recovery and LC resolution. Based on the larger retention time shift from FA to TFA than PBzMA and Agilent Diphenyl, speculation is that protein gets enmeshed inside PMMA with TFA due to protein hydrophobicity. Overall, lower resolution (~ 2X lower) and efficiency are generated when using FA instead of TFA. However, FA enables directly coupled RPLC to MS. PMMA column is the selected candidate for extended investigations.

Apart from column evaluation, we valued systematically other chromatographic factors for PMMA PMMA column. Previous works on IgG1 found out temperature plays a critical role to significantly impact recovery and resolution[31]. Besides, other works discovered protein will generally have a faster mass transfer between stationary phase and mobile phase at higher temperature.[44] So here we varied temperature in dependent of protein recovery and resolution. Temperature has been varied from 30-70 °C with the identical separation condition detailed in Figure 3-3. Chromatograms are of the same separation window time ($\Delta t$ = 14 min), but shifted along time axis to align the first major peak. Two vertical dashed lines indicate the distance between two largest peaks in 30 °C chromatogram and horizontal dashed line on each chromatogram points out the baseline shift before and after IgG1 elution. PMMA column displays no issue on baseline shift even if temperature is 30 °C, which specifies PMMA surface is not sticky to proteins, signaling a fast mass transfer at low temperatures. This is a big advantage to minimize antibody on-column degradation at high temperature[45]. Figure 3-4a plots total protein recovery along with the increase of temperature from 30 °C to 70 °C. The protein recovery is measured by integral of all peaks and normalized by highest integral value, 50 °C. The normalized result shows

level-off after temperature reaches 50 °C. Figure 3-4b plots the distance between major peaks as a function of temperature from 30 °C to 70 °C. Obviously, the distance is narrower, decreasing from 2.92 min (30 °C) to 2.00 min (70 °C). This observation suggests that higher temperature introduces more hydrophobic conformation and relatively decreases hydrophobicity difference between variants as the original hydrophobicity difference between free thiols is subtle. Although the selectivity is worse with higher temperature, the overall chromatographic resolution is better with higher temperature. In addition to resolution, protein recovery is another concern. In this regard, 50 °C for PMMA is a suitable temperature to maximize resolution as well as IgG1 recovery.

The IgG1 separation results using PMMA presented in Figure 3-2 and Figure 3-3 used a reaction time of 60 min for polymer growth, which was based on optimizations. The RPLC chromatogram for varying PMMA growth time is presented in Figure 3-5b and condition is described in Figure 3-5. Polymer layer must be thick enough to diminish the undesired negatively charged interactions from dissociated silanols on the surface with analytes. In accordance with he LC resolution and recovery, 60 min reaction time is the ideal. If the bare silica modified with BCC1 is used, there is no elution at all. Assumedly, IgG1 is trapped on column bonded phase since strong interaction between analyte and silanols. As building thicker layer of polymer, the resolution, peak width, peak shape, peak tailing are improved, indicating silanol effect is reduced. Hence, the initial improvement in separation with thickness. Further increasing the reaction time to 80 min worsens resolution and broadens peak width. One speculation is the polydispersity happened with polymerization time affects the separation. Nevertheless, multidimensional interactions will be introduced seriously with long polymer chains and cause tangling among analyte and polymers. The backpressure increases with the increase of polymer thickness in view of the decrease in porosity. The relation of backpressure and porosity can be calculated by the Kozeny-Carman equation.

$$\frac{P}{L} = \frac{180 \cdot \eta}{d_p^2} \cdot \frac{(1-\varepsilon)^2}{\varepsilon^3} \cdot \frac{Q}{\pi r^2}$$

The porosity is $\varepsilon$, the volume flow rate is $Q$, the column radius is $r$, and all other variables have their usual meanings. The 75:25 water/ACN (v/v) at 30 °C and Waters Acquity UPLC I-Class was used to measure the column backpressure. The porosity before and after polymerization was calculated by unretained peak, water injection. Then, the $d_p$ can be generated. The increase in $d_p$

and decrease in $\varepsilon$ for the polymer growth can be used to estimate the polymer thickness through the hydrodynmiac radius of the fluid channel corresponding to the particle size and porosity.

$$r_{hyd} = \frac{d_p}{3} \cdot \frac{\varepsilon}{1-\varepsilon}$$

The difference between before and after polymer growth, i.e. the initial hydrodynamic radius and final hydrodynamic radius generates the polymer thickness. Figure 3-5a shows the calculated polymer thickness with reaction time from 20 min to 80 min, which gives linear growth on polymerization. Other optimizations of other reaction conditions, such as monomer concentration, copper (II) concentration, solvent composition and temperature, all of which affect growth rate and polydispersity of the polymer, could also give improved LC performance. Fine tunings on reaction time may be needed to achieve even higher peak resolution. Figure 3-6 exhibits transmission electron microscopy (TEM) image of PMMA particles. The black sphere represents nonporous silica and grey area is polymer layers. The image was taken to show PMMA growth of 60 min on nonporous silica. The physical polymer thickness is approximately 30 nm, which is in agreement with the calculated result on 60 min reaction.

Effect of pH modifiers was investigated, which is highly related to the density of dissociated silanols, so that greatly impacts on the performance of column efficiency.[44, 46] In Figure 3-7, the FA concentration is varied from 0.75% to 0.1% and hence the pH is increased from 2.37 to 2.81 measured by pH meter. The decrease of LC resolution occurs when pH is higher than 2.6 (0.5% FA). Peak tailing and broadening appear from strong electrostatic interactions between IgG1 and silica surface. When pH is lower 2.4, peak tailing and peak width are improved as a result of less deprotonated silanols. Under 0.1% FA condition, PMMA column still resolves three major free thiol variants with the loss of only minor thiols information. This is a big improvement comparing to the result published using Agilent Diphenyl under 0.1% FA condition. They can barely separate the first and second major peaks only (resolution < 0.5).[31] It suggests that polymer-shell bonded phase is capable of shielding charge interactions better and keeping protein away from directly contact with silica surface.

After investigation on different FA concentration, pH has become a pivotal factor for RPLC separation for the purpose of protonating silanols. On the other hand, ion pairing effect by acidic modifier is another vital factor affecting RPLC separation. Hence, pH remains a constant in

this study to explore the function of ion pairing effect from TFA. Figure 3-7 signifies resolution has limited improvement if pH is lower than 2.46, mobile phases with different ratio of TFA and FA were adjusted at pH 2.46 carefully. The 0.5% FA and 0.031% TFA are both control experiments to compare RPLC resolution and peak selectivity, shown in Figure 3-8. TFA at 0.01% and 0.025% were blended in FA at 0.375% and 0.125%, respectively. The gradient method is same as method in Figure 3-7, 19-28% ACN in 30 min. However, 0.031% TFA requires stronger organic to elute IgG1 out of column (19-34% ACN in 50 min), recommending the increase of hydrophobicity from ion-pairing. Blue double-headed arrows and brown rectangles are labeled on chromatograms for peak selectivity measurement. (1) The shorter double-headed arrows stand for the peak distance between the first and second major peaks. The arrow length is the same across chromatograms. (2) The longer double-headed arrows measuring the peak distance of the first and the last major peaks. Same as (1), the arrow length is indistinguishable across all chromatograms. Both (1) and (2) point out the elevated concentration of TFA has negligible impact on chromatographic selectivity under the same pH value. (3) Noteworthily, the first minor peak (the peak right next to the first major peak) moves closer towards the first major peak from the top to bottom of chromatograms, with higher amount of TFA present. This result reveals TFA possibly masks the small hydrophobicity differences between peaks by reason of ion-pairing effect. With increasing percent of TFA, IgG1 retention time shift later, also advising TFA ion pairs IgG1. Notably, using PMMA bonded phase only requires 0.031% TFA for RPLC separation with neglect loss of resolution. The raw ESI-mass spectra show charge envelops along with chromatograms in the right column of Figure 3-8. Y-axis was normalized by the most intensive signal. The absolute ion abundance was listed along with each raw mass spectra. This value descends 10-fold from 0% to 0.031% TFA, which conveys how considerable ion suppression from TFA is. In this study, if pH value is low enough, RPLC resolution will be maintained regardless the presence or absence of TFA. Precisely, TFA makes RPLC separation worse in our cases.

There are less ion-pairing alternatives such as difluoroacetic acid (DFA) for protein RPLC/MS[47] for the sake of alleviating ion-suppression. Here we demonstrated some most common acidic modifier compositions for RPLC separation of Genentech IgG1 using our lab-made polymer-shell column online coupling with MS to differentiate ion abundance mass spectra. Figure 3-9 shows MS-compatible mobile phases from top to bottom: 0.5% FA, 0.125% FA + 0.025% TFA, 0.1% DFA and 0.1% TFA accordingly with same gradient steepness, 9% MPB over 30 min

and 15% MPB over 50 min for TFA. The results presented in Figure 3-9 used optimized PMMA column (60 min reaction time). 0.5% FA and 0.125% FA+0.025% TFA has similar LC resolution but retention time shifts 12 min with 0.025% TFA, suggesting strong ion pairing effect. Furthermore, TFA has a significant ESI suppression since ion abundance of 0.125% FA+0.025% TFA is 1/4 of 0.5% FA alone. Considering of 0.1% DFA, a widely used MS-compatible acidic modifier with relatively milder ion-pairing property gives good RPLC separation on intact IgG1 but again MS sensitivity is crucially lower than 0.5% FA. Also, DFA has 20% lower protein recovery than 0.5% FA. Using conventional mobile phase, 0.1% TFA, apparently performs the worst on intact IgG1 separation in terms of both LC resolution and MS sensitivity. Unsatisfactorily low peak recovery, wide peak wide, and deficient resolution are carried out using 0.1% TFA. Ion abundance of 0.1% TFA is three orders of magnitude lower than MS ion abundance of 0.5% FA. Therefore, 0.5% FA has been well-studied as a satisfactory acidic modifier for PMMA bonded phase.

## 3.5 Conclusions

In-house polymer-shell bonded phase performs extraordinarily online RPLC-MS analysis for IgG1 free thiols using 0.5% FA with pleasant of LC resolution and MS sensitivity. pH value is dominant to the reduction of detrimental electrostatic interaction between proteins and silanols on silica. TFA, strong ion-pairing reagent, deteriorates LC resolution including protein recovery, peak width, and peak shape. In our studies, pH is more important than ion-pairing. Therefore, it is promising to apply polymer-shell bonded phase to other protein LC/MS separation mode, such as HILIC/MS and HIC/MS.

## 3.6 Further studies

In Figure 3-2d, PMMA shows low protein recovery and wide peak width, which has opposite behavior to PBzMA and Agilent Diphenyl shown in Figure 3-2b and c. Hydrophobicity can be examined easily by water contact angle. Polymethyl methacrylate has water contact angle approximate 70°.[48, 49] Comparing to other popular RPLC surface, for example, C4 has contact angle 100°, C8 is 104°, C18 gives 110°, and even polystyrene has 94°.[50] Consequently, polymethylmethacrylate is relatively hydrophilic and might be solvated with increase amount of

organic hypothetically. In this aspect, analytes ion-paired with TFA would have higher possibility to be stuck into polymer brush. We tested PMMA columns with different reaction times, that is to say to test different polymer chain length to find out whether thinner polymer layer has less solvation effect or not and might improve LC resolution using TFA. However, PMMA thickness from 20 min to 80 min reaction time does not show any difference on peak recovery and resolution, shown in Figure 3-10.

Temperature is another key to improve protein recovery.[51] The dependence of resolution and recovery as a function of temperature from 40 °C to 80 °C was probed. 26-35% ACN over 30 min was used as the gradient, yet 60% ACN was added at the end of gradient to flush retained analytes out of column. The RPLC resolution becomes better with higher temperature (Figure 3-11). At 60 degree Celsius, clear 8 peaks can be obtained, which agrees with the RPLC separation using PBzMA under TFA in Figure 3-2c. In 40 and 50 °C chromatograms, the end of gradient (60% ACN) shots out IgG1 residues, possessing 280 nm absorbance. At this point, the mass transfer at lower temperature could be less efficient in the presence of TFA and hence IgG1 is trapped on the stationary phase. Higher organic use is required to elute IgG1. Selectivity then preserves the same trend as in Figure 3-3, lower temperature is, distinct peak distance is. As stated in Figure 3-12a, the plot in total peak area versus temperature was made in the basis of the all integrated IgG1 peaks from Figure 3-11 without the flushed protein residues. The trace flats out when temperature reaches 60 °C and above. After summation of washed peak from the end of gradient, the total peak areas across temperature from 40-70 °C are indistinguishable. This result further concludes higher temperature is necessary on PMMA bonded phase using TFA as an acidic modifier to attain full IgG1 recovery. As a consequence, 60 °C is the best option to balance resolution and recovery.

In comparison of temperature effect to Agilent column, the resolution and selectivity for 40 °C to 80 °C were evaluated in Figure 3-13. All chromatograms were selected the same time window and shifted along X-axis to align the first major peak. Only temperature higher than 75 °C gains the maximum protein recovery by Agilent Diphenyl. In contrast to PBzMA in Figure 3-2c, 50 °C reaches the greatest peak recovery, indicating that polymer results in faster mass transfer under lower temperature. Repeatedly, higher temperature reduces peak distance because of lessening difference in hydrophobicity by conformational changes.

## 3.7 References


1. Kaltashov, I. A.; Bobst, C. E.; Abzalimov, R. R.; Wang, G.; Baykal, B.; Wang, S., Advances and challenges in analytical characterization of biotechnology products: mass spectrometry-based approaches to study properties and behavior of protein therapeutics. *Biotechnol Adv* **2012,** *30* (1), 210-22.

2. Beck, A.; Wurch, T.; Bailly, C.; Corvaia, N., Strategies and challenges for the next generation of therapeutic antibodies. *Nature reviews immunology* **2010,** *10* (5), 345.

3. Rogstad, S.; Faustino, A.; Ruth, A.; Keire, D.; Boyne, M.; Park, J., A Retrospective Evaluation of the Use of Mass Spectrometry in FDA Biologics License Applications. *J Am Soc Mass Spectrom* **2017,** *28* (5), 786-794.

4. Wei, C.; Su, D.; Wang, J.; Jian, W.; Zhang, D., LC–MS Challenges in Characterizing and Quantifying Monoclonal Antibodies (mAb) and Antibody-Drug Conjugates (ADC) in Biological Samples. *Current Pharmacology Reports* **2018,** *4* (1), 45-63.

5. Chen, J.; Liu, Z.; Wang, F.; Mao, J.; Zhou, Y.; Liu, J.; Zou, H.; Zhang, Y., Enhancing the performance of LC-MS for intact protein analysis by counteracting the signal suppression effects of trifluoroacetic acid during electrospray. *Chem Commun (Camb)* **2015,** *51* (79), 14758-60.

6. Ecker, D. M.; Jones, S. D.; Levine, H. L., The therapeutic monoclonal antibody market. *MAbs* **2015,** *7* (1), 9-14.

7. Imai, K.; Takaoka, A., Comparing antibody and small-molecule therapies for cancer. *Nat Rev Cancer* **2006,** *6* (9), 714-27.

8. Morrow, T.; Felcone, L. H., Defining the difference: What makes biologics unique. *BIOTECHNOLOGY HEALTHCARE* **2004,** *1*, 24-26, 28-29.

9. Hansel, T. T.; Kropshofer, H.; Singer, T.; Mitchell, J. A.; George, A. J., The safety and side effects of monoclonal antibodies. *Nat Rev Drug Discov* **2010,** *9* (4), 325-38.

10. Esteva, F. J., Monoclonal Antibodies, Small Molecules, and Vaccines in the Treatment of Breast Cancer. *The Oncologist* **2004,** *9*, 4-9.

11. Zhan, M. M.; Hu, X. Q.; Liu, X. X.; Ruan, B. F.; Xu, J.; Liao, C., From monoclonal antibodies to small molecules: the development of inhibitors targeting the PD-1/PD-L1 pathway. *Drug Discov Today* **2016,** *21* (6), 1027-36.

12. Weiner, G. J., Building better monoclonal antibody-based therapeutics. *Nature reviews. Cancer* **2015,** *15* (6), 361-370.

13. Vidarsson, G.; Dekkers, G.; Rispens, T., IgG Subclasses and Allotypes: From Structure to Effector Functions. *Frontiers in Immunology* **2014,** *5*, 520.

14. Rosati, S.; Yang, Y.; Barendregt, A.; Heck, A. J., Detailed mass analysis of structural heterogeneity in monoclonal antibodies using native mass spectrometry. *Nature protocols* **2014,** *9* (4), 967.

15. Liu, H.; Chumsae, C.; Gaza-Bulseco, G.; Hurkmans, K.; Radziejewski, C. H., Ranking the susceptibility of disulfide bonds in human IgG1 antibodies by reduction, differential alkylation, and LC− MS analysis. *Analytical chemistry* **2010,** *82* (12), 5219-5226.

16. Liu, H.; May, K., Disulfide bond structures of IgG molecules. *mAbs* **2012,** *4* (1), 17-23.

17. Hmiel, L. K.; Brorson, K. A.; Boyne, M. T., 2nd, Post-translational structural modifications of immunoglobulin G and their effect on biological activity. *Anal Bioanal Chem* **2015,** *407* (1), 79-94.

18. Liu, H.; May, K., Disulfide bond structures of IgG molecules: structural variations, chemical modifications and possible impacts to stability and biological function. *MAbs* **2012,** *4* (1), 17-23.

19. Beck, A.; Wagner-Rousset, E.; Ayoub, D.; Van Dorsselaer, A.; Sanglier-Cianferani, S., Characterization of therapeutic antibodies and related products. *Anal Chem* **2013,** *85* (2), 715-36.

20. Riener, C. K.; Kada, G.; Gruber, H. J., Quick measurement of protein sulfhydryls with Ellman's reagent and with 4,4′-dithiodipyridine. *Analytical and Bioanalytical Chemistry* **2002,** *373* (4), 266-276.

21. Chumsae, C.; Gaza-Bulseco, G.; Liu, H., Identification and localization of unpaired cysteine residues in monoclonal antibodies by fluorescence labeling and mass spectrometry. *Analytical chemistry* **2009,** *81* (15), 6449-6457.

22. Xiang, T.; Chumsae, C.; Liu, H., Localization and Quantitation of Free Sulfhydryl in Recombinant Monoclonal Antibodies by Differential Labeling with $^{12}C$ and $^{13}C$ Iodoacetic Acid and LC-MS Analysis. *Analytical Chemistry* **2009,** *81*, 8101-8108.

23. Zhang, W.; Czupryn, M. J., Free sulfhydryl in recombinant monoclonal antibodies. *Biotechnology Progress* **2003,** *18*, 509-513.

24. Dillon, T. M.; Ricci, M. S.; Vezina, C.; Flynn, G. C.; Liu, Y. D.; Rehder, D. S.; Plant, M.; Henkle, B.; Li, Y.; Deechongkit, S.; Varnum, B.; Wypych, J.; Balland, A.; Bondarenko, P. V., Structural and functional characterization of disulfide isoforms of the human IgG2 subclass. *J Biol Chem* **2008,** *283* (23), 16206-15.

25. Wypych, J.; Li, M.; Guo, A.; Zhang, Z.; Martinez, T.; Allen, M. J.; Fodor, S.; Kelner, D. N.; Flynn, G. C.; Liu, Y. D.; Bondarenko, P. V.; Ricci, M. S.; Dillon, T. M.; Balland, A., Human IgG2 antibodies display disulfide-mediated structural isoforms. *J Biol Chem* **2008,** *283* (23), 16194-205.

26. Ren, D.; Pipes, G. D.; Hambly, D. M.; Bondarenko, P. V.; Treuheit, M. J.; Brems, D. N.; Gadgil, H. S., Reversed-phase liquid chromatography of immunoglobulin G molecules and their fragments with the diphenyl column. *J Chromatogr A* **2007,** *1175* (1), 63-8.

27. Newton, G. L.; Dorian, R.; Fahey, R. C., Analysis of Biological Thiols: Derivatization with Monobromobimane and Separation by Reverse-Phase High-Performance Liquid Chromatography. *Analytical Biochemistry* **1981,** *114*, 383-387.

28. Ren, D.; Pipes, G.; Xiao, G.; Kleemann, G. R.; Bondarenko, P. V.; Treuheit, M. J.; Gadgil, H. S., Reversed-phase liquid chromatography-mass spectrometry of site-specific chemical modifications in intact immunoglobulin molecules and their fragments. *J Chromatogr A* **2008,** *1179* (2), 198-204.

29. Zhang, T.; Zhang, J.; Hewitt, D.; Tran, B.; Gao, X.; Qiu, Z. J.; Tejada, M.; Gazzano-Santoro, H.; Kao, Y. H., Identification and characterization of buried unpaired cysteines in a recombinant monoclonal IgG1 antibody. *Anal Chem* **2012,** *84* (16), 7112-23.

30. Cheng, Y.; Chen, M. T.; Patterson, L. C.; Yu, X. C.; Zhang, Y. T.; Burgess, B. L.; Chen, Y., Domain-specific free thiol variant characterization of an IgG1 by reversed-phase high-performance liquid chromatography mass spectrometry. *Anal Biochem* **2017,** *519*, 8-14.

31. Liu, H.; Jeong, J.; Kao, Y.-H.; Zhang, Y. T., Characterization of free thiol variants of an IgG1 by reversed phase ultra high pressure liquid chromatography coupled with mass spectrometry. *Journal of Pharmaceutical and Biomedical Analysis* **2015,** *109*, 142-149.

32. Apffel, A.; Fischer, S.; Goldberg, G.; Goodley, P. C.; Kuhlmann, F. E., Enhanced sensitivity for peptide mapping with electrospray liquid chromatography-mass spectrometry in the presence of signal suppression due to trifluoroacetic acid-containing mobile phases. *Journal of Chromatography A* **1995,** *712* (1), 177-190.

33. Shou, W. Z.; Naidong, W., Simple means to alleviate sensitivity loss by trifluoroacetic acid (TFA) mobile phases in the hydrophilic interaction chromatography-electrospray tandem mass spectrometric (HILIC-ESI/MS/MS) bioanalysis of basic compounds. *J Chromatogr B* **2005,** *825* (2), 186-92.

34. Gilar, M.; Xie, H.; Jaworski, A., Utility of Retention Prediction Model for Investigation of Peptide Separation Selectivity in Reversed-Phase Liquid Chromatography: Impact of Concentration of Trifluoroacetic Acid, Column Temperature, Gradient Slope and Type of Stationary Phase. *Analytical Chemistry* **2010,** *82* (1), 265-275.

35. Nugent, K. D.; Burton, W. G.; Slattery, T. K.; Johnson, B. F.; Snyder, L. R., Separation of proteins by reversed-phase high-performance liquid chromatography: II. Optimizing sample pretreatment and mobile phase conditions. *Journal of Chromatography A* **1988,** *443*, 381-397.

36. Shibue, M.; Mant, C. T.; Hodges, R. S., The perchlorate anion is more effective than the trifluoroacetate anion as an ion-pairing reagent for reversed-phase chromatography of peptides. *Journal of Chromatography A* **2005,** *1080* (1), 49-57.

37. Garc´ıa, M. C.; Hogenboom, A. C.; Zappeya, H.; Irth, H., Effect of the mobile phase composition on the separation and detection of intact proteins by reversed-phase liquid chromatography–electrospray mass spectrometry. *journal of Chromatography A* **2002,** *957*, 187-199.

38. Poll, D. J.; Harding, D. R. K., Formic acid as a milder alternative to trifluoroacetic acid and phosphoric acid in two-dimensional peptide mapping. *Journal of Chromatography A* **1989,** *469*, 231-239.

39. Wang, S.; Xing, T.; Liu, A. P.; He, Z.; Yan, Y.; Daly, T. J.; Li, N., Simple Approach for Improved LC-MS Analysis of Protein Biopharmaceuticals via Modification of Desolvation Gas. *Anal Chem* **2019,** *91* (4), 3156-3162.

40. Chen, T. H.; Yang, Y.; Zhang, Z.; Fu, C.; Zhang, Q.; Williams, J. D.; Wirth, M. J., Native Reversed-Phase Liquid Chromatography: A Technique for LCMS of Intact Antibody-Drug Conjugates. *Anal Chem* **2019,** *91* (4), 2805-2812.

41. Horvath, C.; Melander, W.; Molnar, I.; Molnar, P., Enhancement of Retention by Ion-Pair Formation in Liquid Chromatography with Nonpolar Stationary Phases *Analytical Chemistry* **1977,** *49*, 2295-2305.

42. Shibue, M.; Mant, C. T.; Hodges, R. S., Effect of anionic ion-pairing reagent hydrophobicity on selectivity of peptide separations by reversed-phase liquid chromatography. *Journal of Chromatography A* **2005,** *1080* (1), 68-75.

43. Bobaly, B.; Toth, E.; Drahos, L.; Zsila, F.; Visy, J.; Fekete, J.; Vekey, K., Influence of acid-induced conformational variability on protein separation in reversed phase high performance liquid chromatography. *J Chromatogr A* **2014,** *1325*, 155-62.

44. Heinisch, S.; D'Attoma, A.; Grivel, C., Effect of pH additive and column temperature on kinetic performance of two different sub-2 mum stationary phases for ultrafast separation of charged analytes. *J Chromatogr A* **2012,** *1228*, 135-47.

45. Stackhouse, N.; Miller, A. K.; Gadgil, H. S., A high-throughput UPLC method for the characterization of chemical modifications in monoclonal antibody molecules. *J Pharm Sci* **2011,** *100* (12), 5115-25.

46. McCalley, D. V., Effect of buffer on peak shape of peptides in reversed-phase high performance liquid chromatography. *Journal of Chromatography A* **2004,** *1038* (1-2), 77-84.

47. Zhou, Y.; Zhang, X.; Fornelli, L.; Compton, P. D.; Kelleher, N.; Wirth, M. J., Chromatographic efficiency and selectivity in top-down proteomics of histones. *Journal of Chromatography B* **2017,** *1044*, 47-53.

48. Briggs, D.; Chan, H.; Hearn, M. J.; McBriar, D. I.; Munro, H. S., The Contact Angle of Poly(methyl methacrylate) Cast against Glass. *Langmuir* **1990,** *6*, 420-424.

49. Tokuda, K.; Ogino, T.; Kotera, M.; Nishino, T., Simple method for lowering poly(methyl methacrylate) surface energy with fluorination. *Polymer Journal* **2014,** *47* (1), 66-70.

50. Arkles, B., Hydrophobicity, Hydrophilicity and Silane Surface Modification. Gelest, Inc.: Morrisville, PA, 2006.

51. Fekete, S.; Veuthey, J. L.; Guillarme, D., New trends in reversed-phase liquid chromatographic separations of therapeutic peptides and proteins: theory and applications. *J Pharm Biomed Anal* **2012,** *69*, 9-27.

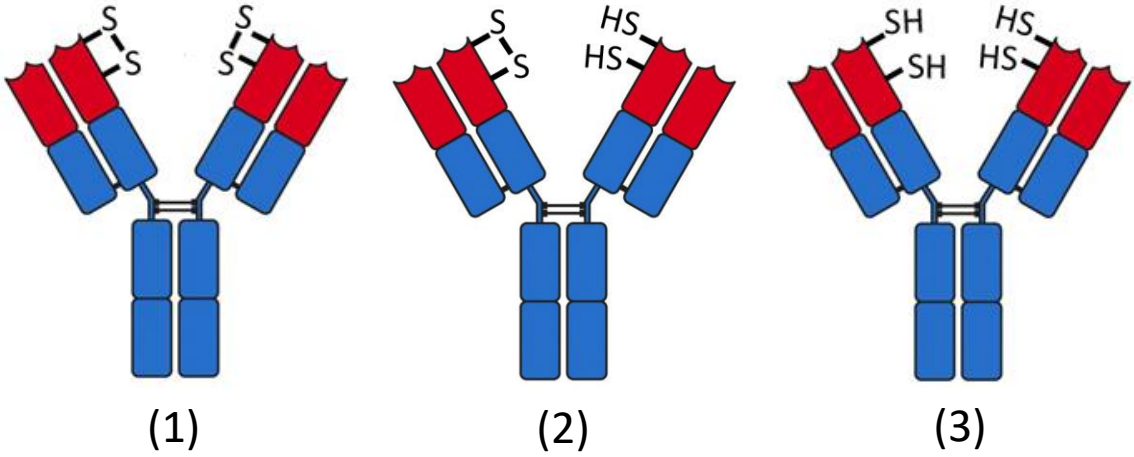


Figure 3-1 Three major free thiol variants of Genentech IgG1. Theoretically, mass of (2) is equal to mass of (1) + 2 Da and mass of (3) equals to (1) + 4 Da or (2) + 2 Da [Ref. 29].

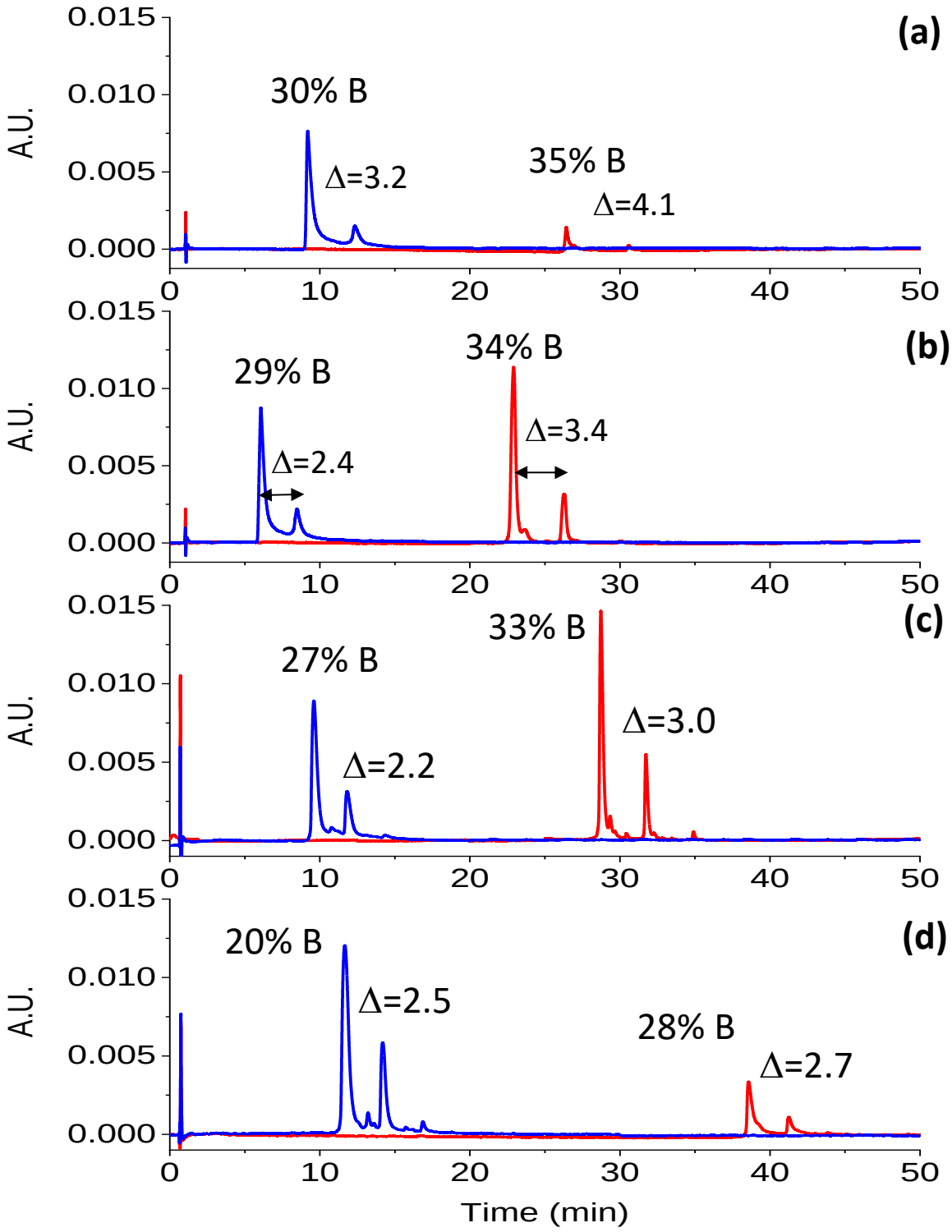


Figure 3-2 Chromatograms of IgG1 showing three main peaks: IgG1 with 0, 1 and 2 buried thiol sites. From top to bottom panels are: a) Diphenyl at 50 °C, b) Diphenyl at 75 °C, c) PBzMA at 50 °C, d) PMMA at 50 °C. Gradients with 0.5% FA (blue) and 0.1% TFA (Red). For all chromatograms: Δ 15%/ 50 min ACN in water, 0.1 mL/min, 2 µg injected, detection at 280 nm.

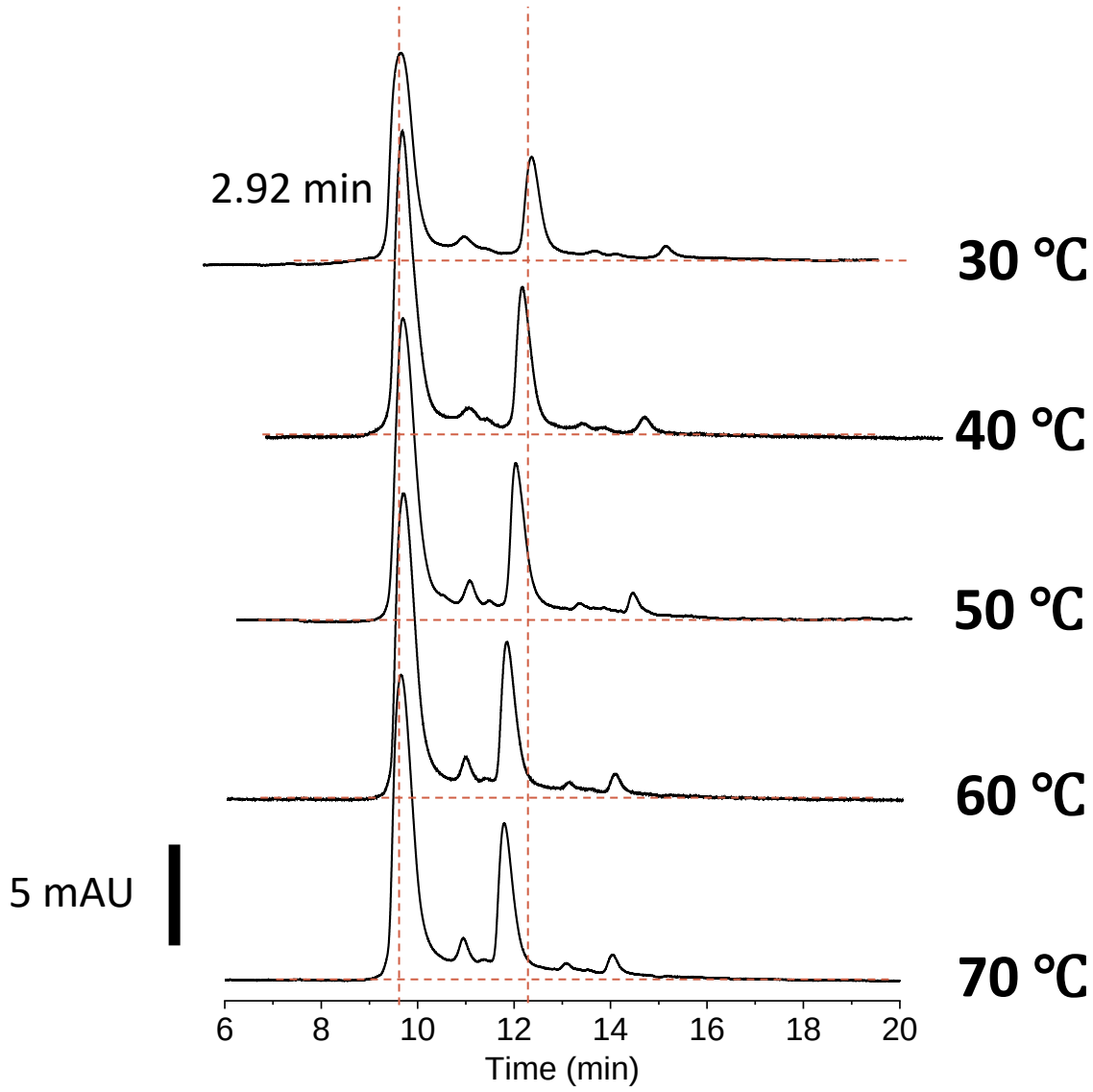


Figure 3-3 Dependence of resolution and recovery on temperature for PMMA brush layer. Chromatograms for temperatures from 30-70 °C for contact IgG1 separation on pMMA polymer-shell column. The gradient was 19-28% ACN with 0.5% FA in 30 min. Chromatograms are of the same Δt scale, but shifted along time axis to align the first peak. The dashed line indicates the distance between two largest peaks in 30 °C chromatogram.

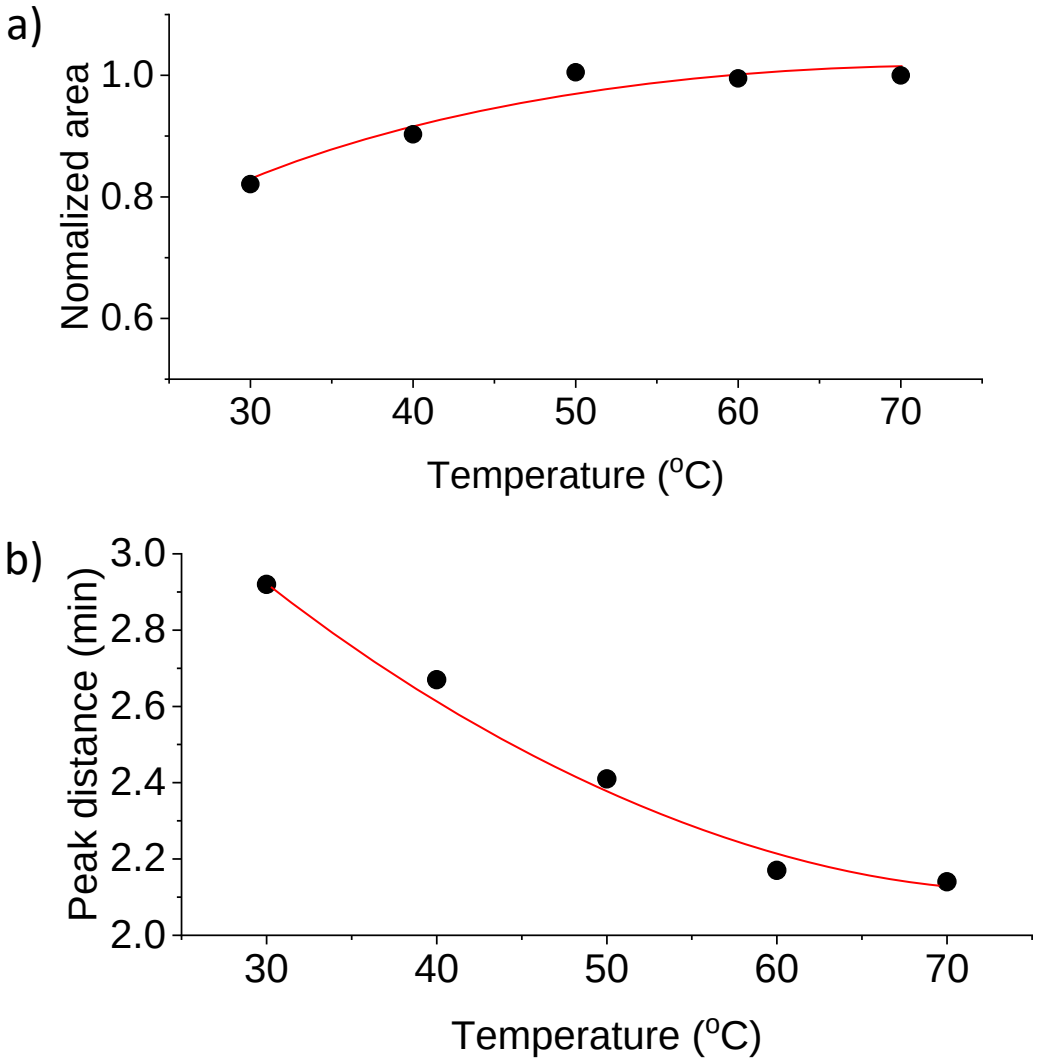


Figure 3-4 a) Plot of percent recovery, as determined from the chromatograms of Figure 3-3, in comparison with published data for the diphenyl silane bonded phase. b) Plot of the distance between peaks A and E, as a function of temperature.

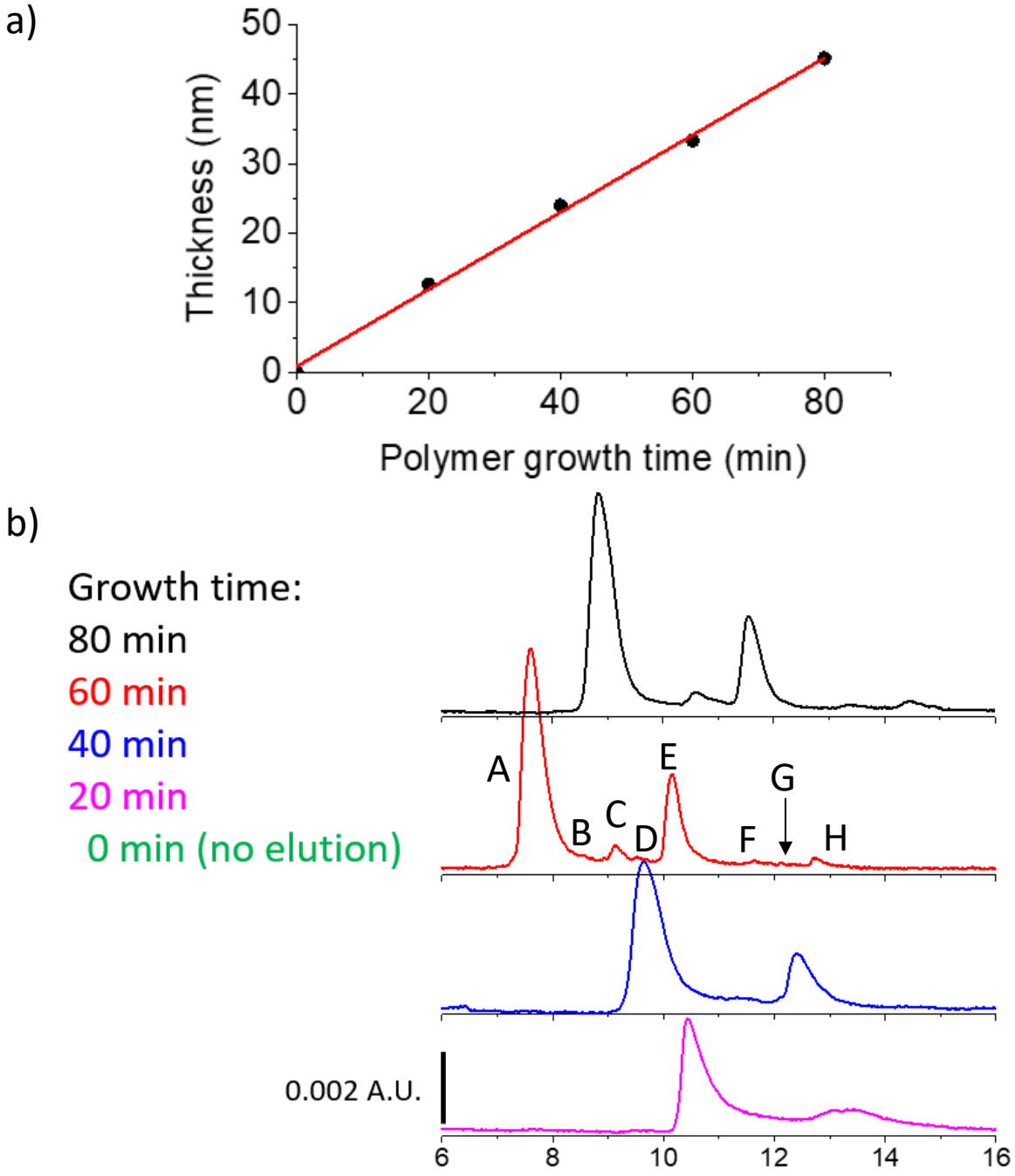


Figure 3-5 a) Plot of the polymer thickness, as a function of polymer growth time. b) RPLC chromatogram for varying PMMA growth time, showing that the 60 min growth time is optimal with respect to resolution. Polymer growth time is labeled in each panel. The gradient for columns of 20, 40, 60, and 80 min PMMA growth time were 20-29% ACN with 0.5% FA in 30 min, and the gradient for the column without polymers was 20-35% ACN with 0.5% FA in 50 min. Q: 100 µL/min at 50 °C; amount injected: 2 µg.

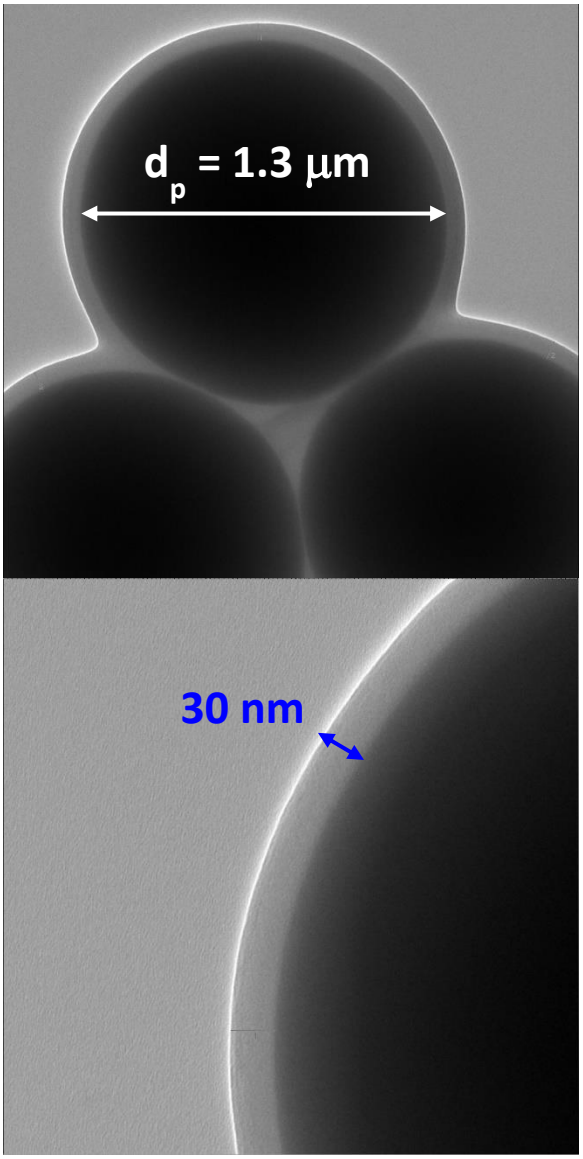


Figure 3-6 TEM image to show polymer-shell grown on nonporous silica by ATRP

pH = **2.37**
(0.75% FA)

pH = **2.46**
(0.5% FA)

pH = **2.61**
(0.25% FA)

pH = **2.81**
(0.1% FA)

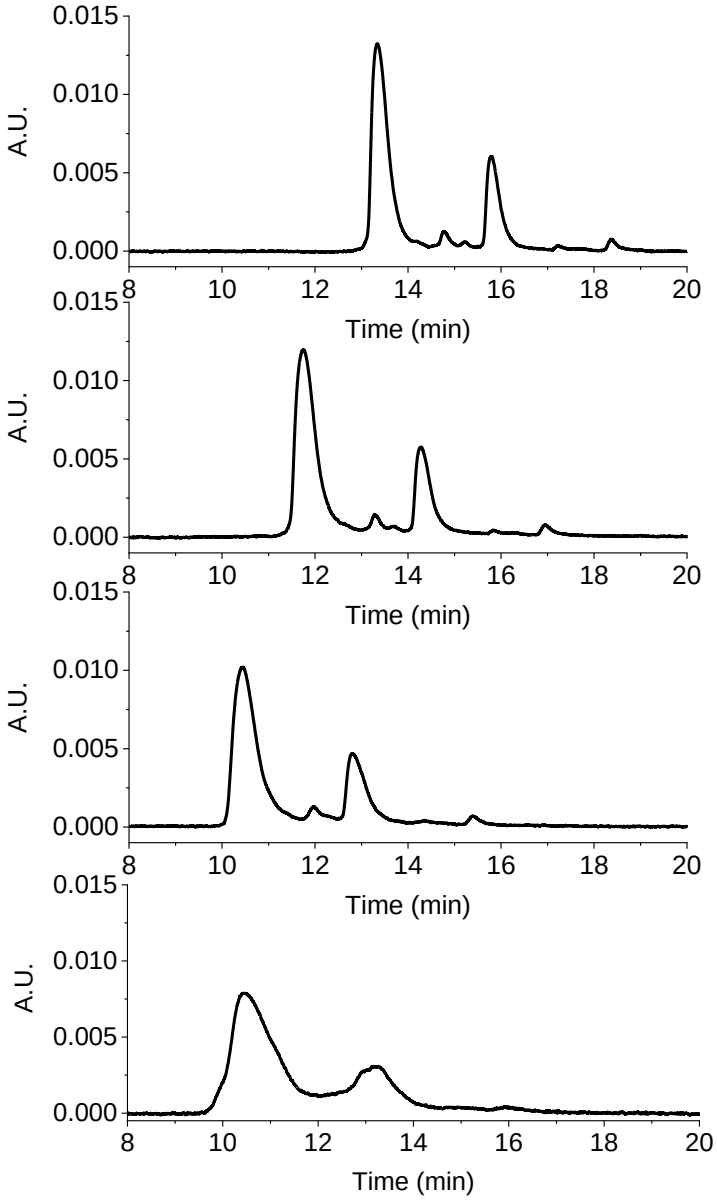


Figure 3-7 Chromatograms of intact IgG1 in different FA concentration in polymer-shell column. A gradient of 19-28% ACN in 30 min is used for polymer-shell column, 2 µg of intact IgG1 is injected onto both columns with 100 µL/min flow rate and 50 °C column temperature.

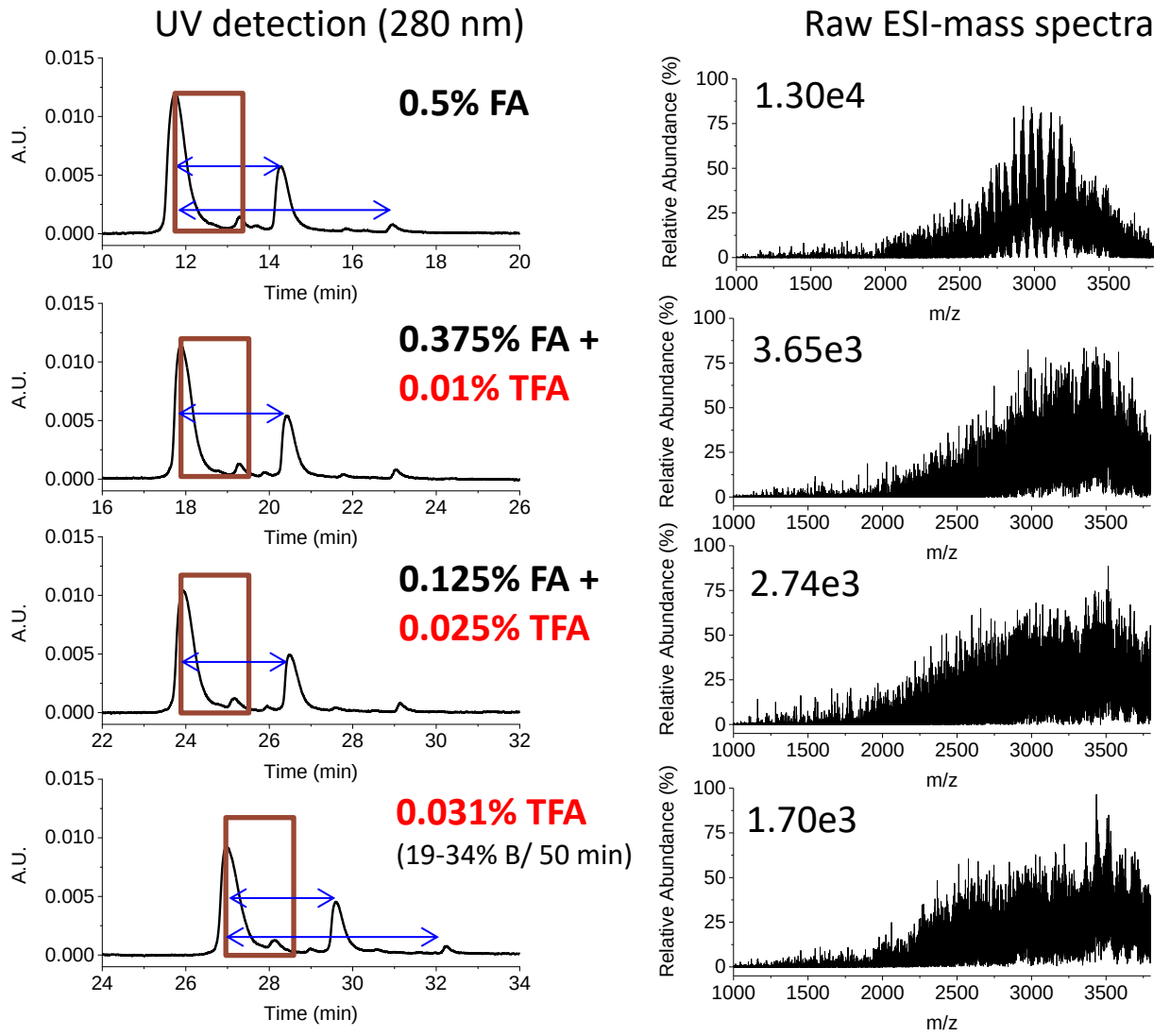


Figure 3-8 At constant pH 2.46 by increasing TFA and decreasing FA concentration. UV chromatograms (left) and MS raw mass spectra (right). The gradient was 19-28% B in 30 min with 100 µL/min at 50 °C. 19-34% B in 50 min was used for 0.031% TFA instead because TFA ion pairing made elution later than 28%.

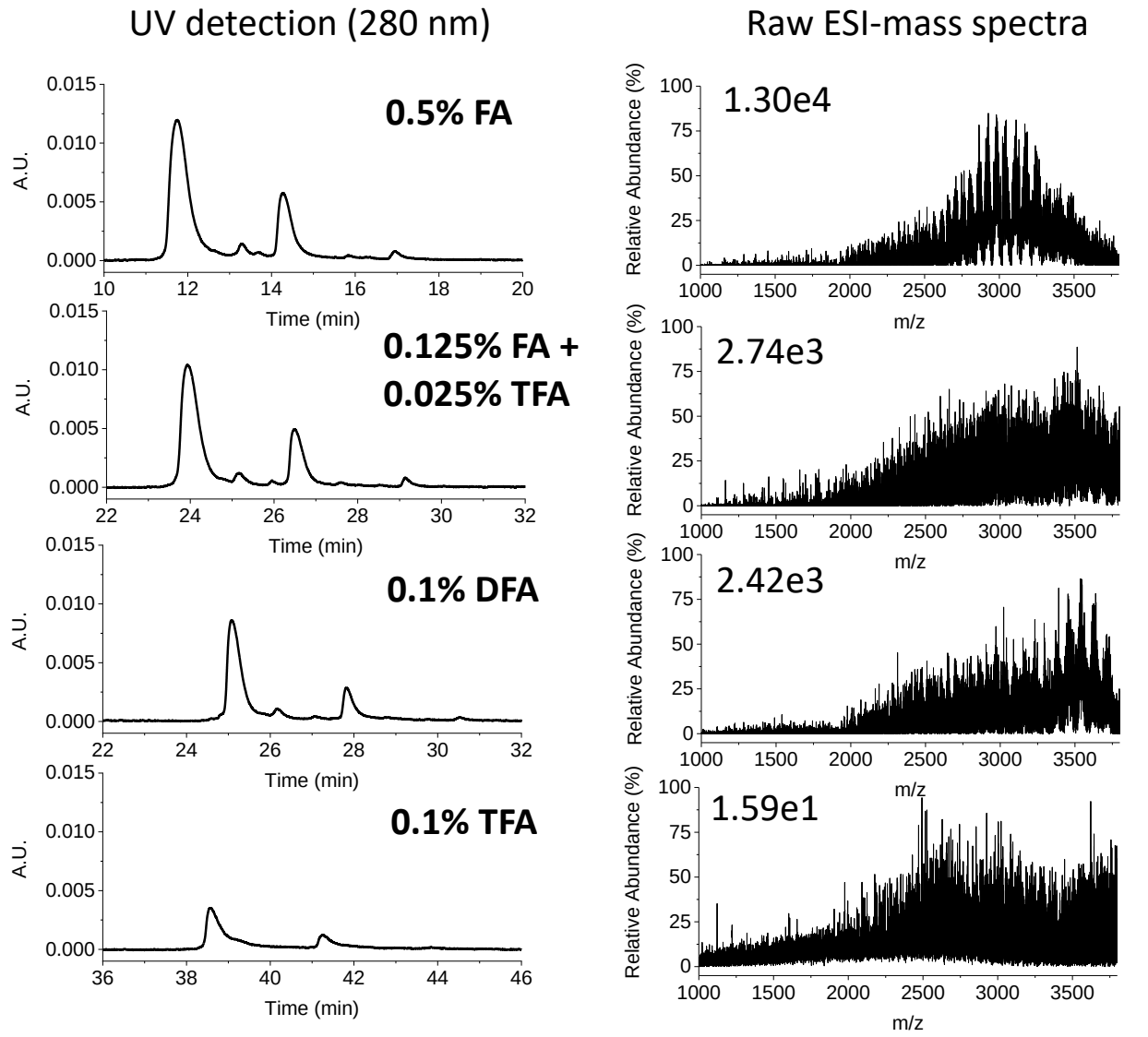


Figure 3-9 LC resolution (left) and MS sensitivity (right) for RPLC-MS of intact IgG1 for different acidic modifiers and combinations. The gradient was 9% B over 30 min, with a flow rate of 100 µL/min for first three RPLC methods and TFA method used 15% B over 50 min. Column temperature was 50 °C. IgG1 injected amount was 2 µg.

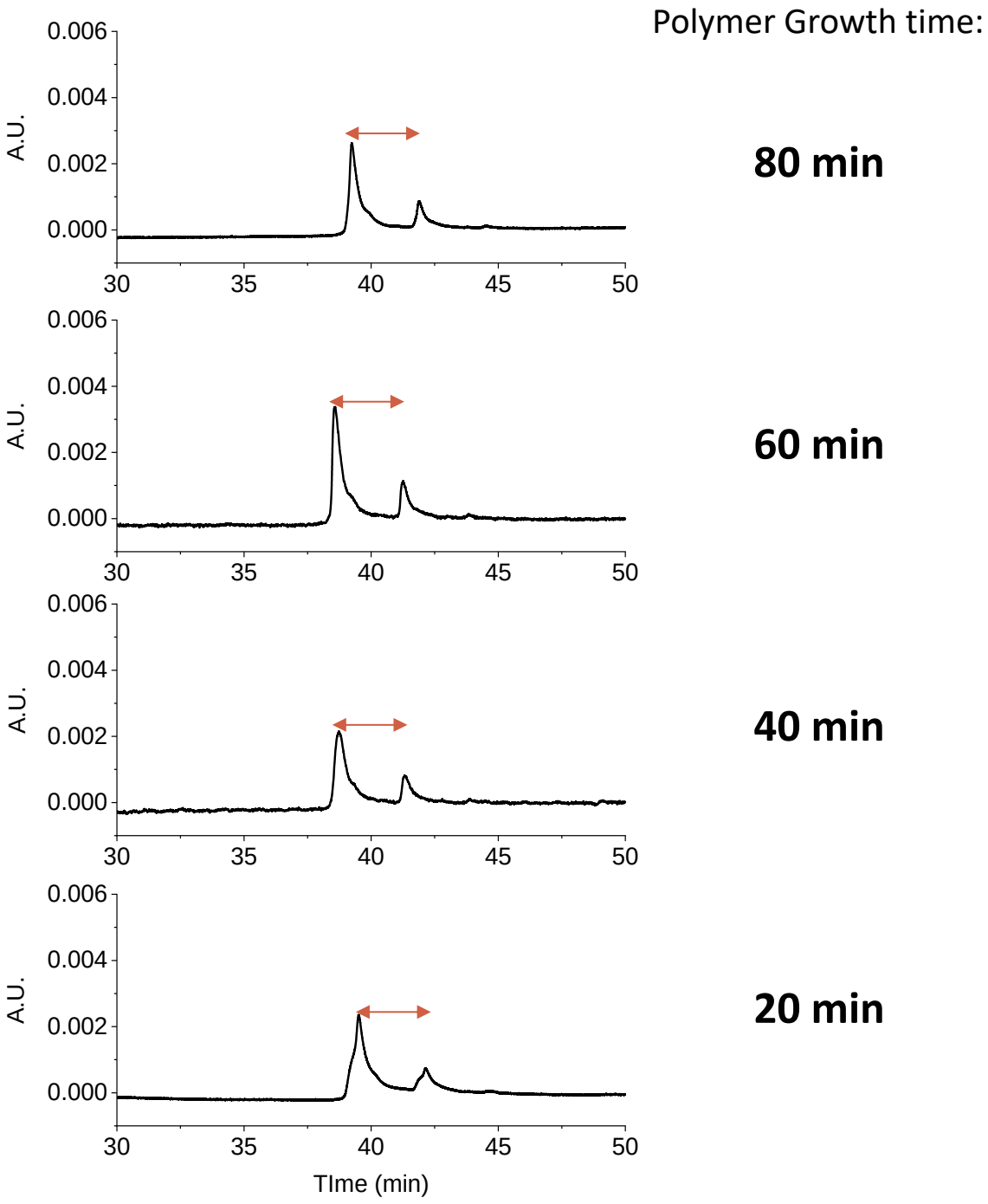


Figure 3-10 RPLC chromatograms of different PMMA growth time for separation of IgG1. Gradients was 19-34% ACN/ 50 min in water, 0.1 mL/min, 2 μg injected, detection at 280 nm.

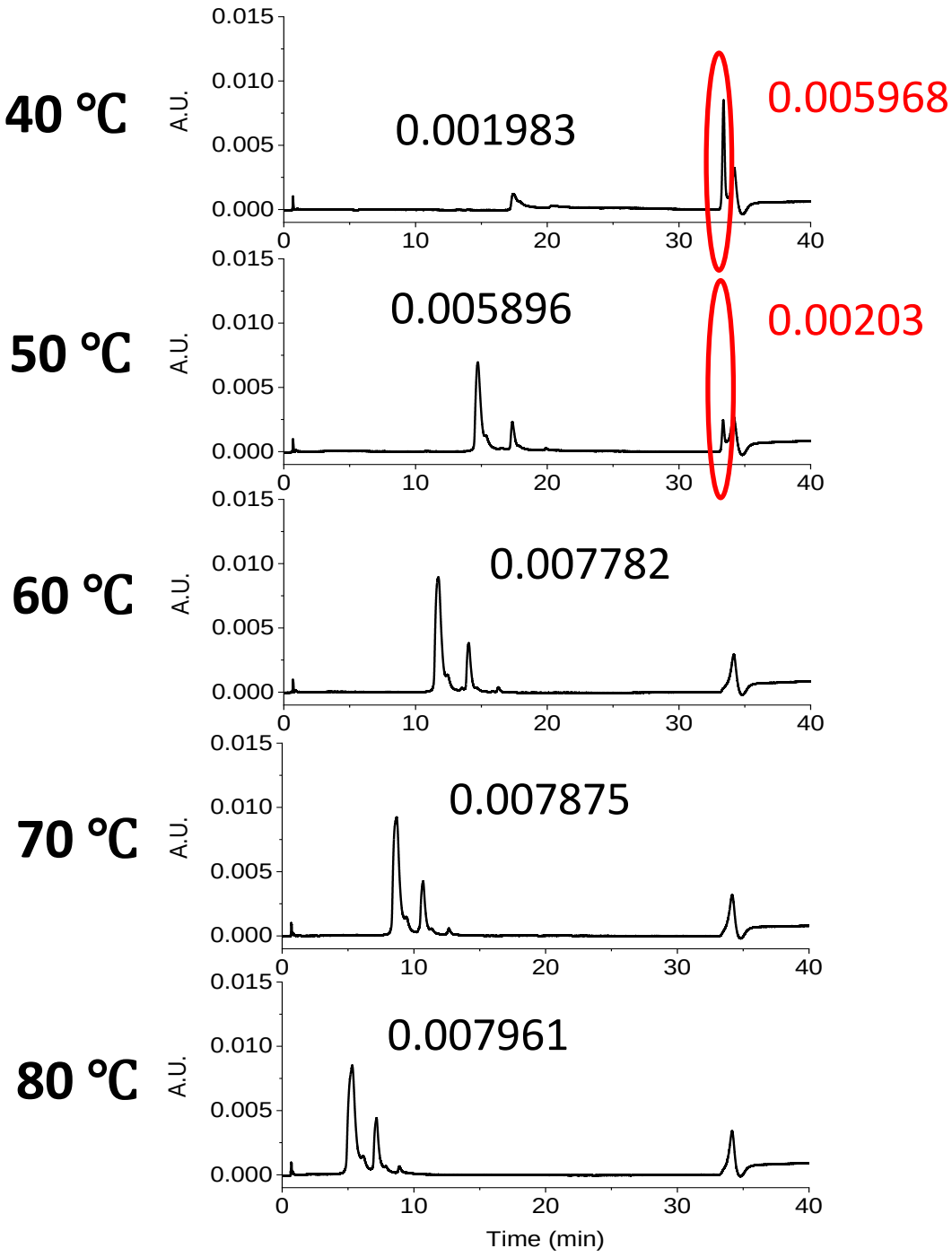


Figure 3-11 Dependence of resolution and recovery on temperature for PMMA brush layer. Chromatograms for temperatures from 40-80 °C for contact IgG1 separation on pMMA polymer-shell column. The gradient was 26-35% ACN with 0.1% TFA in 30 min. Selectivity shows same trace as Figure 3-4b, the higher temperature is, the lower peak distance.

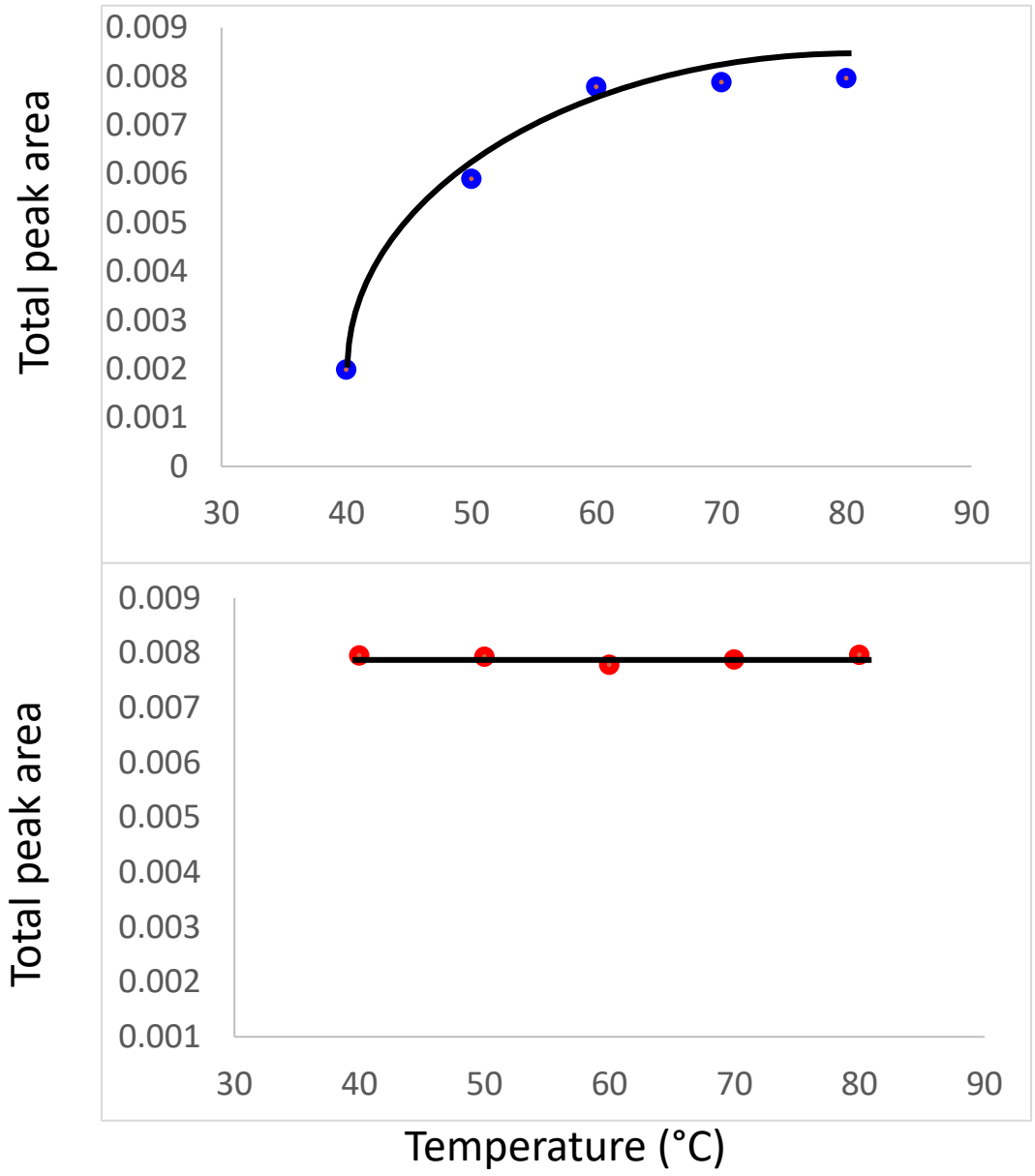


Figure 3-12 Plot of total peak area as a function of temperature, determined from the chromatograms of Figure 3-11. a) Before summation of the washing peak at the end of gradient b) After summation of the washing peak at the end of gradient.

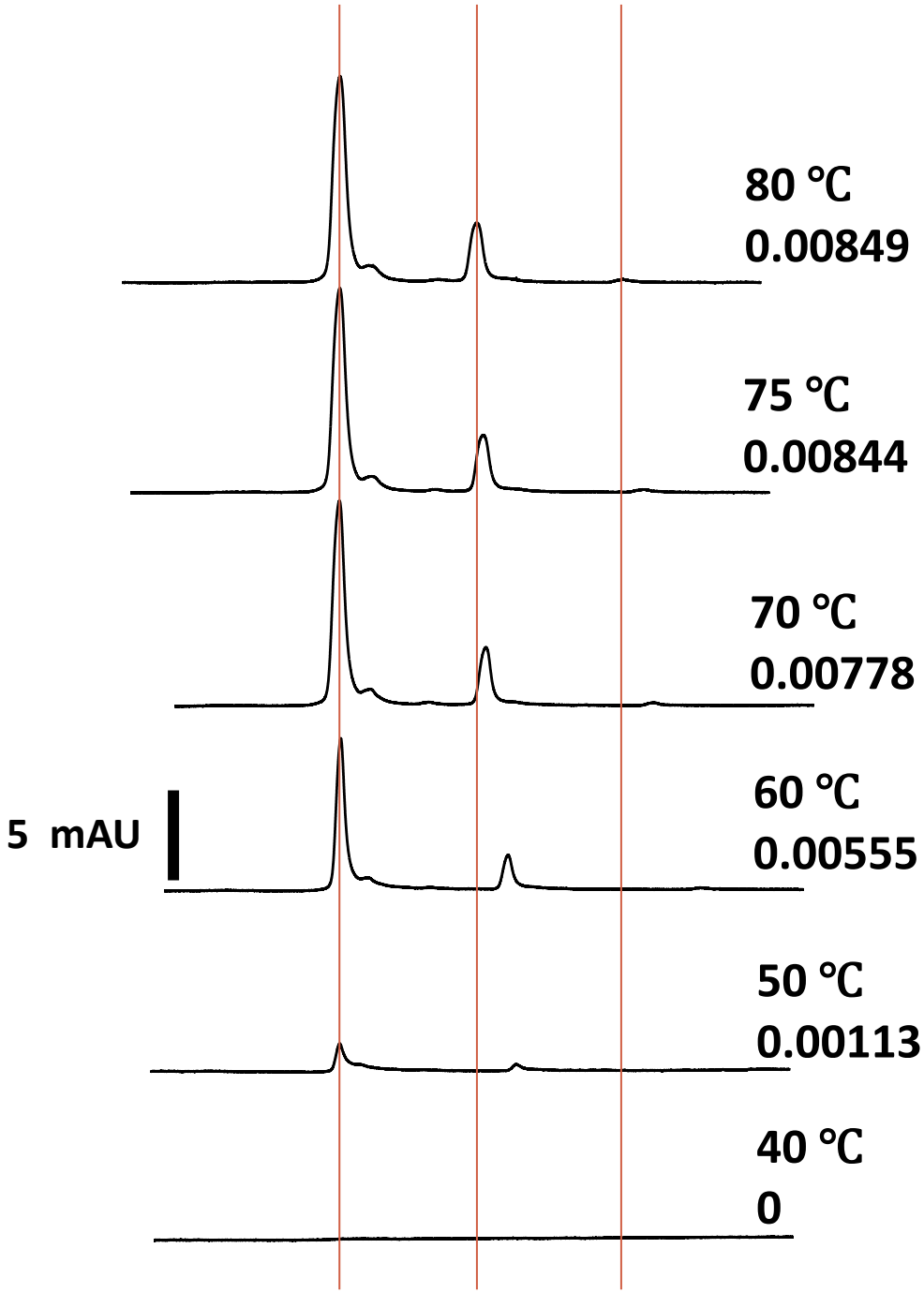


Figure 3-13 Dependence of resolution and recovery on temperature for Agilent AdvanceBio RP-mAb Diphenyl. Chromatograms for temperatures from 40-80 °C for separation of IgG1. The gradient was 31-46% ACN with 0.1% TFA in 50 min. Chromatograms are of the same Δt scale, but shifted along time axis to align the first peak. The solid line indicates the distance between three major peaks in 80 °C chromatogram.

# CHAPTER 4. THE PHENOMENON OF HYDRODYNAMIC CHROMATOGRAPHY

## 4.1 Abstract

Hydrodynamic chromatography (HDC) comes to the fore again recent years for size-based separations on colloidal particle and polymer latex. The advantage of HDC is analytes have experienced less shear force and hence have less potential to cause flow-induce degradation. At this point, it is beneficial to apply HDC on protein separation since conformation would not change via HDC method. In this chapter, we use protein samples to discuss essential theories and factors on HDC including selection of stationary phase, particle size, column length, and column inner diameter.

## 4.2 Introduction

Formulation development attracts drug makers' attention aggressively and has become a key process of biopharmaceutical drug development, which could have significant impacts on drug stability, solubility, and tonicity[1, 2]. The control of drug aggregation is always a primary concern during formulation process because it directly affects the shelf life and preservation of the drug.[3] There are several factors induce aggregation. For instance, temperature, pH, drug concentration, solvent, chemical modification, and structure of drug.[4] In this respect, analytical technique for the analysis of aggregation plays in a critical role.

There are several methods for the quantification and size-based characterization including size-exclusion chromatography (SEC), sodium dodecylsulfate polyacrylamide gel electrophoresis (SDS-PAGE), capillary electrophoresis (CE), light scattering, analytical ultracentrifugation (AUC) and other spectroscopic methods.[4, 5] Among mentioned analytical techniques, SEC is predominant and widely used for the qualitative and quantitative evaluation of protein aggregates. Three main advantages using SEC method: 1) It is a non-denaturing size-based separation method, which keeps protein on original conformation and preserves its biological function with different sizes.[5] 2) It is relatively high throughput and easier for experimental preparation. SEC also has relatively robustness on method validation.[6] 3) Peak fractions can be collected for extended characterizations.[7, 8] However, SEC has numbers of limitations. First of all, dynamic range is

limited, which has limitation of molecular mass that can be separated.[6] Not many columns are available for separating species larger than 300 kDa.[9] Moreover, peak capacity is substantially low since separation happens within one column volume.[10] The design of SEC traditionally use at higher flow rate, which conduct sample dilution substantially[10] and shear (flow-induce) degradation.[11, 12]

SEC is considered as a technique of separation by flow. Sharing with the same idea, hydrodynamic chromatography (HDC) is now recognized.[13] The theoretical foundation of HDC was established by DiMarzio and Guttman in 1969-1971.[14-17] They used polymer as a model to explain HDC separation in an open tube. In 1974, Small published the first HDC experimental result.[18] Small employed 4 packed columns in total around 4 meter with relatively hydrophobic packed materials to separate colloidal particles and polymer latexes on size based mechanism to study effects of type and size of packing bed as well as ionic strength of mobile phase. Following by the improvement of packing quality, the length of HDC column was shortened from 2-200 meters to 0.5-1 meter.[19, 20] Generally, HDC application is still limited due to the use of extremely long empty tube or compromising with packed bed but suffering from packing quality, and non-specific binding. Until these 10 years, only very limited number publications using HDC separation technique to nanoparticles or latex.[21-24] The estimated number on published HDC articles related to analyte separation based on size is probably less than 100 during these three decades. However, HDC using packed column has advantages superior to SEC. For example, packing bed in HDC in general uses non-porous particle, so back pressure is higher and only slower flow rate can be used, which minimize shear stress to possibly destruct native form of analyte. Traditionally, SEC separation time takes up to hours but HDC only requires few minutes, which dramatically saves time especially under industrial manner.

In this chapter, we discuss simple theories of HDC separation, packing quality and packing bed style effects including pore size and size of packing material, and mobile phase effect under acidic, neutral, and surfactant conditions. Our analytes are proteins, which is the first HDC separation on protein based on size. Also, analyte-surface interactions and limitations are addressed.

## 4.3 Materials and methods

### 4.3.1 Materials

Nonporous silica particles (500, 750, 1000, and 1500 nm) were purchased from Superior Silica (Tempe, AZ). Empty stainless-steel columns, 1.0 × 50 mm, 2.1 × 50 mm, 4.6 × 50 mm, 2.1 × 100 mm, reservoirs, 4.6 × 50 mm and 4.6 × 50 mm, and frits (0.5 µm pore diameter) were purchased from Isolation Technologies (Middleboro, MA). Stainless-steel tubing, ferrules, and internal nuts were all purchased from Valco Instruments (Houston, TX). Silanes, i.e., (chloromethyl)phenyl)dimethylchlorosilane (+99%), n-butyldimethylchlorosilane (+99%) and trimethylchlorosilane (+99%), were purchased from Gelest (Morrisville, PA). Methyl methacrylate (MMA, 99%), *N*,*N*-dimethylacrylamide (DMA), sodium dodecyl sulfate (≥99%), sodium ascorbate (≥99%), butylamine (99.5%), and ammonium acetate (≥99.99) were purchased from Sigma–Aldrich (St. Louis, MO). Other chemical used included copper(II) chloride ($CuCl_2$, 99%) from Acros Organics (Morris Plains, NJ), tris(2-dimethylaminoethyl)amine ($Me_6$TREN, +99%) from Alfa Aesar (Haverhill, MA), and formic acid (FA, 99.5%+, LC/MS grade), isopropanol (IPA), heptane, and acetonitrile (ACN) from Fisher Scientific (Hampton, NH). Ultrapure water was obtained from a Milli-Q system (MilliporeSigma, Darmstadt, Germany.)

Lyophilized lysozyme from chicken egg white was purchased from Sigma–Aldrich (St. Louis, MO). IgG4 were in-house made by Eli Lilly.

### 4.3.2 UHPLC column preparation

#### 4.3.2.1 Polymer column

The silica particles were modified as described earlier[25]. Briefly, the silica particles were calcined at 600 °C for 12 h, then annealed at 1050°C for 3 h, and rehydroxylated overnight in 10% $HNO_3$. Particles were then rinsed in ultrapure water and dried in a 60 °C vacuum oven. Freshly rehydroxylated silica particles were suspended in a dry toluene solution containing 2% (v/v) of (chloromethyl)phenyl)dimethylchlorosilane and 0.1% (v/v) of butylamine. The solution was refluxed for 3 h and then 2% (v/v) of trimethylchlorosilane was added for endcapping and refluxed for 3 h. The silylated, endcapped particles were then rinsed with dry toluene and allowed to dry in a 60 °C vacuum oven for 2 h.

For polymer growth, *N*,*N*-dimethylacrylamide was dissolved in 50:50 $H_2O$/IPA (v/v), respectively in a 50 mL round bottom flask for a final concentration of 2.5 M. Two other solutions were made: 1) a solution containing 40 mg of $CuCl_2$ and 80 μL $Me_6$TREN, and 2) a solution containing 20 mg sodium ascorbate. These were also prepared in 2.0 mL of their individual solvent. Afterwards, the Cu/$Me_6$TREN solution was added to the round bottom flask, followed by the sodium ascorbate solution. The resulting solution was poured into a plugged reservoir column of 4.6 mm × 150 mm. A 2.1 mm × 50 mm column was packed with 0.24 g of silylated, endcapped particles suspended in acetonitrile. The reservoir and column were connected in series. A high-pressure pump, LabAlliance Series 1500 HPLC Pump (Laboratory Alliance of Central New York, LLC, Syracuse, NY) was used for packing and modification. The reaction solution from the reservoir was pumped into the column starting at 170 μL/min until the reaction mixture dripped from the end of the column and counted flow time for 5 min and stop the flow for the rest of reaction time. Reaction time of *N*,*N*-dimethylacrylamide was total 60 min including 5 min flow and 65 min stop flow After reaction, the freshly packed column polydimethylacrylamide (PDMA) was rinsed with $H_2O$/IPA and $H_2O$/ACN for 20 min each at 100 μL/min.

#### 4.3.2.2 C4C1 column

The heating step and rehydroxylation step were mentioned above. Freshly rehydroxylated silica particles were suspended in a dry toluene solution containing 2% (v/v) of n-butyldimethylchlorosilane (C4) and 0.1% (v/v) of butylamine. The solution was refluxed for 3 h and then 2% (v/v) of trimethylchlorosilane (C1) was added for endcapping and refluxed for 3 h. The silylated, endcapped particles were then rinsed with dry toluene and allowed to dry in a 60 °C vacuum oven for 2 h.

For making C4C1 column, a 1.0 × 50 mm column was packed with 0.06 g; a 2.1 mm × 50 mm column was packed with 0.25 g; a 4.6 × 50 mm column was packed with 1.2 g; a 2.1 × 100 mm column was packed with 0.50 g of C4C1 particles. After weighing, C4C1 particles were suspended in 30:70 heptane/IPA (v/v) and slurry was poured into a plugged reservoir column of 4.6 mm × 150 mm for 1.0 × 50 mm column and 2.1 mm × 50 mm column, and 4.6 mm × 250 mm for 4.6 × 50 mm column and 2.1 mm × 100 mm column.

### 4.3.3 UHPLC

A Waters Acquity UPLC I-Class (Waters, Milford, MA) was used for hydrodynamic chromatography with no salt condition. Lab-made columns (polymer columns and C4C1 columns) were used as the analytical columns. Mobile phases and gradients used for elution were detailed along with the results.

## 4.4 Theory and design

SEC has been applied with stationary phase with pores since aggregation would be sterically hindered by pores and small analyte would be stagnant inside the pores.[11] On the contrary, HDC has been developed on non-porous stationary phase in order to maintain laminar flow.[13, 26] HDC separation occurs in the parabolic or named Hagen–Poiseuille flow profile under laminar flow conditions. The separation mechanism is shown in Figure 4-1. The liquid flow in the interstitial void space generates Poiseuille flow profile due to interaction of wall/packing material and mobile phase, which causes viscous forces. Therefore, mean velocity near wall/packing material is diminished, whereas center has highest mean velocity. When analytes pass through the limited void space, accessibility of this interface region becomes dominant and size-discriminating happens spontaneously. Because of Brownian diffusion, smaller analytes are accessible to more regions of void space and moves with relatively slower mean velocity. However, larger analytes are rejected from the sluggish regions near the wall/packing material and migrate consequently with the greater average velocity close to the center.[19, 27, 28] Therefore, larger analytes elute earlier than smaller analytes. Elution order in HDC is the same as in SEC. However, the separation mechanisms are different. Preferential sampling in SEC separation depends on pore volume, whereas preferential sampling in HDC is streamlines of flow (or to a preferential distribution of analyte between fluid mechanical phases).

We use expanded Van Deemter equation to study possible challenges for HDC.

$$H = A + \frac{B}{\nu} + C_m\nu + C_p\nu + C_s\nu$$

Where H represents plate height and $\nu$ is linear velocity. The A term can be considered as packing quality, which corresponds to multiple pathways that a solute could find. The B term is longitudinal diffusion, which describes a solute continuously diffuses away from their concentrated band center

along with the direction of flow travel. Solutes spend less time in the column, the less B term occurs. C term relates to equilibrium time at millisecond scale of a solute required between mobile phase and stationary phase, called resistance to mass transfer. C term is then expanded into three factors, $C_m$, $C_p$, and $C_s$. Under easier way to understand the function of three C terms, the term $C_m$ accounts for the mass transfer in mobile and $C_s$ is in charge of the mass transfer in stationary phase. The $C_p$ term only arises from porous or superficially porous particles, in which a solute passes in and out from stationary pores. In our case, we are using non-porous particles, so the $C_p$ term is zero. Our analytes are proteins that has negligible longitudinal diffusion, normally within a order of $10^{-6}$ or $10^{-7}$. Hence, the B term can be neglect. The $C_s$ however is tricky owing to non-specific interactions between proteins and stationary phase. Ideally, both SEC and HDC separations should not have analyte-surface interaction to cause non-specific binding and restrict the separation resolution. In the view of complexity of protein structures and large molecules, analyte-surface interaction is inevitable.[29-31] On those accounts, Van Deemter equation is re-written as following.

$$H = A + C_m v + C_s v$$

In Dr. Wirth lab, we have patented method of packing chromatographic columns.[32] We are able to uniformly pack columns with porosity ($\varepsilon$) lower than theoretical minimum (0.4) in Giddings book.[33] As scanning electron microscope (SEM) images and calculated porosity shown in our publications[34-38], the silica particles are well-arranged to form crystals with a face-center cubic (FCC), which shows opalescence in blue color. Our lab invented packing method produces porosity range typically 0.26 to 0.40. The average of porosity in our lab for stainless steel is typically 0.36 and capillary gives even better packing to have $\varepsilon$ lower than 0.3. In this point of view, the A term ascribes to the increase of plate height can be minimized. In contrast to long open tubes, well-packed stationary phase generates well-ordered pore sizes. The interstitial spaces from packing medium can be considered as short channels, so a collection of all these channels could be regarded as a long open tube in which HDC phenomenon arises (Figure 4-2).

## 4.5 Results and discussions

We solved the packing issue of the A term, now $C_m$ and $C_s$ terms are investigated using different stationary phases and mobile phases. Recently, our group published a separation of large proteins, up to 1.2 megaDalton by packed capillary electrophoresis (pCE) since pore sizes are well-

controlled.[38] Proteins will not be trapped by small pores transiently from wide distribution of pore sizes to slow down separation speed. Preferably, HDC should be explicated using packed capillary. Nevertheless, sodium dodecyl sulfate (SDS) is not nanoLC-friendly, stainless steel column using UHPLC system is an alternative. In the best scenario to generate similar results from packed capillary to packed stainless steel column, 350 nm bare silica particles should be used. Because of the limitation of packing quality and pore size on column frits (0.5 μm), 500 nm particle is the smallest size we could use to pack a stainless-steel column Porosity was calculated by unretained water injection peak in Figure 4-3, which gives $\varepsilon = 0.37$. The calculated $\varepsilon$ is smaller than 0.4, indicating uniformed packing was obtained. HDC phenomenon has been first proved by applying capillary electrophoresis condition to liquid chromatography shown in Figure 4-3. In all cases throughout this chapter, lysozyme (~14 kDa) and Eli Lilly IgG4 (~150 kDa) were used. Notebaly, the elution order in Figure 4-3 gives IgG4 (red) first, lysozyme (blue), and the last water injection (black), which exactly matches the elution order from large analytes to small analytes. Nevertheless, the resolution is slightly less than 1, which shows not good resolution and low peak capacity. According to the recoded video to calculate a physical peak width of protein ladder, the average physical peak width using CE is approximately 0.8 mm. Then, physical peak width using stainless steel column with UHPLC can be calculated in Figure 4-3 with subtraction of system void volume, 8.2 μL, which yields the average physical peak width at approximation 5.0 mm. The average physical peak width using stainless steel column with UHPLC is roughly 6-fold greater than using CE due to larger void volume using a wider bore column and resulting in band broadening. Undoubtedly, the limitation of HDC under stainless steel column with UHPLC system will be peak capacity. Moreover, the wider peak width is, the lower resolution is.

Figure 4-3a shows HDC separation using 0.1% formic acid (FA) and 1% SDS under different volumetric flow rate. Obviously, resolution is independent of flow rate that similar resolution between lysozyme and IgG4 were attained from 20 μL/min to 60 μL/min. This result agrees with an overview of HDC conditions published by Edam's group.[22] No matter lysozyme or IgG4 peaks, full width of half maximum (FWHM) are slightly larger than FWHM of water injection peak, attributing to undesired analyte-surface interaction. When SDS was reduced to 0.1%, lysozyme gets stuck on stationary phase and IgG4 elutes later than water injection (Figure 4-3b). Presumably, SDS pairs on protein surface by hydrophobic interactions and increases protein hydrophobicity. In contrast to hydrophobic protein surface, bare silica particles are hydrophilic

due to high density of silanols, so hydrophobic proteins become slippery to hydrophilic stationary phase. Moreover, negatively charged SDS turns protein net charge into negative, so negatively charged proteins is repulsive from negatively charged silanols. Thus, 2% SDS was tested to prove the role of SDS in HDC separation. Figure 4-3c gives slightly better resolution than Figure 4-3a. Although peak width in 2% SDS is also slightly wider than 1% SDS, the resolution is improved and approaches to 1. With increasing on flow rate, a second peak emerges. It could be due to protein conformational change with increasing on back pressure.[39, 40] However, mass spectrometry (MS) characterization is not possible in this case because of in the presence of SDS. Fortunately, HDC separation takes place using acidic modifier and SDS. Nonetheless, SDS is not compatible with MS, substituted stationary phases and mobile phase modifiers need to further investigate.

On the purpose of removing SDS, proteins become relatively hydrophilic, so hydrophobic stationary phase is an approach to avoid hydrogen bonding interactions or hydrophilic interactions. Bare silica surface modified with butyl group (C4) was first applied to HDC separation. To compromise back pressure limit by exploring effects of column length, column inner diameter, and particle size, 1500 nm C4 stationary phase packed in a 2.1 × 100 mm was regarded as a standard. In Chapter 3, we addressed that dissociated silanol is a crucial factor to retain proteins on stationary phase. 0.5% FA was used to protonate silanols as much as possible. To further avoid protein-surface interactions, 50% ACN was applied. Flow rate was first screened to study the relation between protein peak shape and back pressure in Figure 4-4. The chromatographic result is similar as Figure 4-3 that resolution does not improve by varying flow rate. Instead, resolution shown in Figure 4-4 is actually worse than resolution shown in Figure 4-3 because FA is a weak acid and a weak ionic strength acidic modifier. Silanols are dissociated and carries negative charge to induce uninvited protein-silanol interactions. Likewise, a second peak shows up with increase of flow rate. In spite of not acceptable resolution, at least, HDC occurs using C4 surface with MS-compatible conditions.

C4 particle size, column length and inner diameter were then probed in Figure 4-5. HDC chromatograms of 1500 nm C4, 750 nm C4, and 500 nm C4 give similar retention time in water injection, addressing packing quality is consistent with different particle sizes. However, IgG4 peak gets closer to lysozyme peaks when smaller particle was used. Unfortunately, this result is opposite to previous published article that smaller particle size achieves better resolution under CE condition.[38, 41] Hypothetically, greater surface area from smaller particle size contributes to

stronger undesired protein-surface interactions. Interestingly, protein peaks separate further away from water injection while using smaller particle size. In this aspect, both mobile phase composition and stationary phase have to investigate deeply. By decreasing void volume through shorter and thinner columns, as expected, the resolution is worse. This consequence indicates that HDC requires certain amount of void volume to yield better parabolic separation flow profile. In this respect, wider column will be the next step to test rather than using even longer column due to packing quality.

Formic acid has pKa (3.75) closes to silanols (pKa = 4.5), so isolated silanols are possibly charged. Trifluoroacetic acid (TFA) replaces FA for examination on silanol effect and 2.1 × 100 mm packed with 750 nm C4 particles were applied. HDC chromatogram in Figure 4-6 reveals peak width of lysozyme and IgG4 is comparable to peak width of water injection. Besides, comparing to the same column under FA condtion shown in Figure 4-5, intact IgG4 under TFA gives homogeneous structure with only one peak without split. Alike RPLC separation using commercially alkyl column mentioned in Chapter 3, TFA has better LC resolution than FA.

TFA produced better peak shape, resolution, and narrower peak width using 750 nm C4 column, pointing out strong protein-surface interactions from C4 bonded phase. Throughout Chapter 2 and 3, we expressed that polymer brush layer can keep protein away from silica surface and shield electrostatic interaction from dissociated silanols. As a result, polydimethylacrylamide (PDMA) was chosen to perform HDC separation instead. The preliminary result shown in Figure 4-7, describes a baseline resolution between lysozyme and water injection. Despite the resolution between IgG4 and lysozyme is still smaller than 1, which is similar as the best resolution shown in Figure 4-3. It is a good sign of using polymer-shell bonded phase.

## 4.6 Conclusions and further plans

In this work, HDC phenomenon is proved using lysozyme and IgG4. Even though none of separation in this HDC chapter achieves baseline resolved, it is still a promising method that could be possibly applied to protein separation based on size differences. What exciting aspect is there is not yet any application of HDC on protein separations. One drawback in this discovery is all separation methods denature proteins. Therefore, protein cannot preserve its sphere structure and might experience longer time to pass through pores. The native state under salt condition may be

a potential direction to not only maintain protein non-denaturing structure but also reduce undesired protein-silanol interactions.

## 4.7 References


1. Frokjaer, S.; Otzen, D. E., Protein drug stability: a formulation challenge. *Nat Rev Drug Discov* **2005,** *4* (4), 298-306.

2. Kamerzell, T. J.; Esfandiary, R.; Joshi, S. B.; Middaugh, C. R.; Volkin, D. B., Protein-excipient interactions: mechanisms and biophysical characterization applied to protein formulation development. *Adv Drug Deliv Rev* **2011,** *63* (13), 1118-59.

3. Ohtake, S.; Kita, Y.; Arakawa, T., Interactions of formulation excipients with proteins in solution and in the dried state. *Adv Drug Deliv Rev* **2011,** *63* (13), 1053-73.

4. Mahler, H. C.; Friess, W.; Grauschopf, U.; Kiese, S., Protein aggregation: pathways, induction factors and analysis. *J Pharm Sci* **2009,** *98* (9), 2909-34.

5. Fekete, S.; Beck, A.; Veuthey, J. L.; Guillarme, D., Theory and practice of size exclusion chromatography for the analysis of protein aggregates. *J Pharm Biomed Anal* **2014,** *101*, 161-73.

6. Arakawa, T.; Ejima, D.; Li, T.; Philo, J. S., The critical role of mobile phase composition in size exclusion chromatography of protein pharmaceuticals. *J Pharm Sci* **2010,** *99* (4), 1674-92.

7. Muneeruddin, K.; Thomas, J. J.; Salinas, P. A.; Kaltashov, I. A., Characterization of small protein aggregates and oligomers using size exclusion chromatography with online detection by native electrospray ionization mass spectrometry. *Anal Chem* **2014,** *86* (21), 10692-9.

8. Boing, A. N.; van der Pol, E.; Grootemaat, A. E.; Coumans, F. A.; Sturk, A.; Nieuwland, R., Single-step isolation of extracellular vesicles by size-exclusion chromatography. *J Extracell Vesicles* **2014,** *3*.

9. Hong, P.; Koza, S.; Bouvier, E. S., Size-Exclusion Chromatography for the Analysis of Protein Biotherapeutics and their Aggregates. *J Liq Chromatogr Relat Technol* **2012,** *35* (20), 2923-2950.

10. Bouvier, E. S. P.; Koza, S. M., Advances in size-exclusion separations of proteins and polymers by UHPLC. *TrAC Trends in Analytical Chemistry* **2014,** *63*, 85-94.

11. Barth, H. G.; Boyes, B. E.; Jackson, C., Size Exclusion Chromatography and Related Separation Techniques. *Analytical Chemistry* **1998,** *70*, 251R-278R.

12. Barth, H. G.; Carlin, F. J., A Review of Polymer Shear Degradation in Size-Exclusion Chromatography. *Journal of Liquid Chromatography* **2006,** *7* (9), 1717-1738.

13. Striegel, A. M.; Brewer, A. K., Hydrodynamic chromatography. *Annu Rev Anal Chem (Palo Alto Calif)* **2012,** *5*, 15-34.

14. DiMarzio, E. A.; Guttman, C. M., Separation by flow. *POLYMER LETTERS* **1969,** *7*, 267-272.

15. Guttman, C.; DiMarzio, E., Seperation by Flow. II. Application to Gel Permeation Chromatography. *Macromolecules* **1970,** *3* (5), 681-691.

16. DiMarzio, E. A.; Guttman, C. M., Separation by Flow. *Macromolecules* **1970,** *3* (2), 131-146.

17. DiMarzio, E. A.; Guttman, C. M., Separation by flow and its application to gel permeation chromatography. *JOURNAL OF CHROMATOGRAPHY* **1971,** *55*, 83-97.

18. H, S., Hydrodynamic Chromatography. *Journal of Colloid and Interface Science* **1974,** *48*, 147-161.

19. Small, H.; Langhorst, M. A., Hydrodynamic Chromatography. *ANALYTICAL CHEMISTRY* **1982,** *54*, 892A-898A.

20. Revillon, A., Alternatives to Size Exclusion Chromatography. *Journal of Liquid Chromatography* **1994,** *17* (14-15), 2991-3023.

21. Brewer, A. K.; Striegel, A. M., Hydrodynamic chromatography of latex blends. *J Sep Sci* **2010,** *33* (22), 3555-63.

22. Edam, R.; Eeltink, S.; Vanhoutte, D. J.; Kok, W. T.; Schoenmakers, P. J., Hydrodynamic chromatography of macromolecules using polymer monolithic columns. *J Chromatogr A* **2011,** *1218* (48), 8638-45.

23. Gray, E. P.; Bruton, T. A.; Higgins, C. P.; Halden, R. U.; Westerhoff, P.; Ranville, J. F., Analysis of gold nanoparticle mixtures: a comparison of hydrodynamic chromatography (HDC) and asymmetrical flow field-flow fractionation (AF4) coupled to ICP-MS. *Journal of Analytical Atomic Spectrometry* **2012,** *27* (9).

24. Philippe, A.; Schaumann, G. E., Evaluation of hydrodynamic chromatography coupled with UV-visible, fluorescence and inductively coupled plasma mass spectrometry detectors for sizing and quantifying colloids in environmental media. *PLoS One* **2014,** *9* (2), e90559.

25. Huang, X.; Wirth, M. J., Surface-Initiated Radical Polymerization on Porous Silica. *Anal. Chem.* **1997,** *69* (22), 4577-4580.

26. Guillaume, Y.-C.; Robert, J.-F.; Guinchard, C., A Mathematical Model for Hydrodynamic and Size Exclusion Chromatography of Polymers on Porous Particles. *analytical Chemistry* **2001,** *73*, 3059-3064.

27. Small, H.; Saunders, F. L.; Solc, J., Hydrodynamic chromatography - A new approach to particle size analysis. *Advances in Colloid end interface Science,* **1976,** *6*, 237-266.

28. STEGEMAN, G.; KRAAK, J. C.; HOPPE, H., Hydrodynamic and size-exclusion chromatography of polymers on porous particles. *Journal of Chromatography* **1991,** *550*, 721-739.

29. Lou, J.; Harinath, V., Effects of Molecular Weight and Flow Rate on Stress-Induced Migration of Polystyrene. *Journal of Liquid Chromatography & Related Technologies* **2009,** *27* (18), 2819-2835.

30. Goyon, A.; Sciascera, L.; Clarke, A.; Guillarme, D.; Pell, R., Extending the limits of size exclusion chromatography: Simultaneous separation of free payloads and related species from antibody drug conjugates and their aggregates. *J Chromatogr A* **2018,** *1539*, 19-29.

31. Adrover, A.; Cerbelli, S.; Giona, M., Taming axial dispersion in hydrodynamic chromatography columns through wall patterning. *Physics of Fluids* **2018,** *30* (4).

32. Wirth, M. J.; Kodithuwakkuge, S. R.; Yerneni, C.; Birdsall, R. E.; Kodithuwakkuge, T. R. Method of packing chromatographic columns. US9504936B2, 2016.

33. Giddings, J. C., *Unified Separation Science*. Wiley-Interscience: New York City, NY, 1991; p 65.

34. Huckabee, A. G.; Yerneni, C.; Jacobson, R. E.; Alzate, E. J.; Chen, T. H.; Wirth, M. J., In-column bonded phase polymerization for improved packing uniformity. *J Sep Sci* **2017,** *40* (10), 2170-2177.

35. Wei, B.; Rogers, B. J.; Wirth, M. J., Slip flow in colloidal crystals for ultraefficient chromatography. *J Am Chem Soc* **2012,** *134* (26), 10780-2.

36. Wu, Z.; Wei, B.; Zhang, X.; Wirth, M. J., Efficient separations of intact proteins using slip-flow with nano-liquid chromatography-mass spectrometry. *Anal Chem* **2014,** *86* (3), 1592-8.

37. Njoya, N. K.; Birdsall, R. E.; Wirth, M. J., Silica colloidal crystals as emerging materials for high-throughput protein electrophoresis. *AAPS J* **2013,** *15* (4), 962-9.

38. Ragland, T. S.; Gossage, M. D.; Furtaw, M. D.; Anderson, J. P.; Steffens, D. L.; Wirth, M. J., Electrophoresis of megaDalton proteins inside colloidal silica. *Electrophoresis* **2019,** *40* (5), 817-823.

39. Mozhaev, V. V.; Heremans, K.; Frank, J.; Masson, P.; Balny, C., High Pressure Effects on Protein Structure and Function. *PROTEINS: Structure, Function, and Genetics* **1996,** *24*, 81-91.

40. Engen, J. R., Analysis of protein conformation and dynamics by hydrogen/deuterium exchange MS. *Anal Chem* **2009,** *81* (19), 7870-5.

41. Birdsall, R. E.; Koshel, B. M.; Hua, Y.; Ratnayaka, S. N.; Wirth, M. J., Modeling of protein electrophoresis in silica colloidal crystals having brush layers of polyacrylamide. *Electrophoresis* **2013,** *34* (5), 753-60.

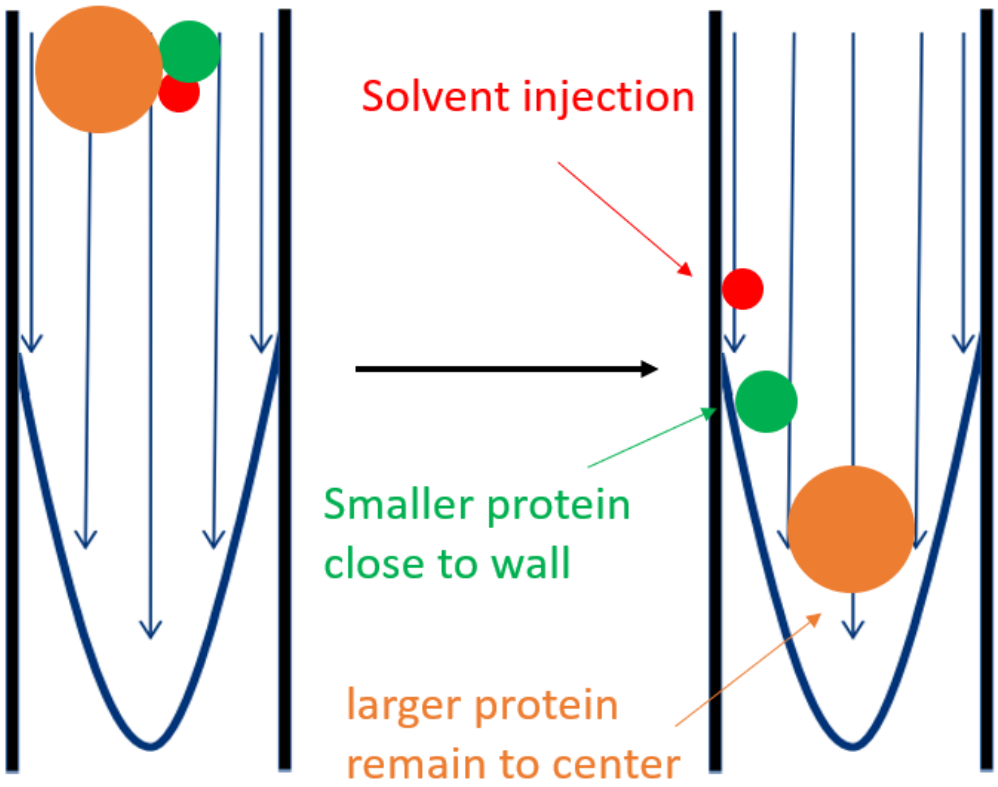


Figure 4-1 A depicted mechanism of hydrodynamic chromatography (HDC) separation. Arrows indicate the direction of streamline flow. Longer arrows have higher velocity and shorter arrows have relatively low velocity. A protein mixer flows laminarly with a parabolic flow profile. The sample mixer contains a larger protein (orange), a smaller protein (green), and buffer solvent to store protein (red). The larger protein stays the center of the flow, experiencing a faster velocity, whereas the smaller protein experiences slower velocity. Buffer, in general, is composed of small molecule, and thus flows near the walls.

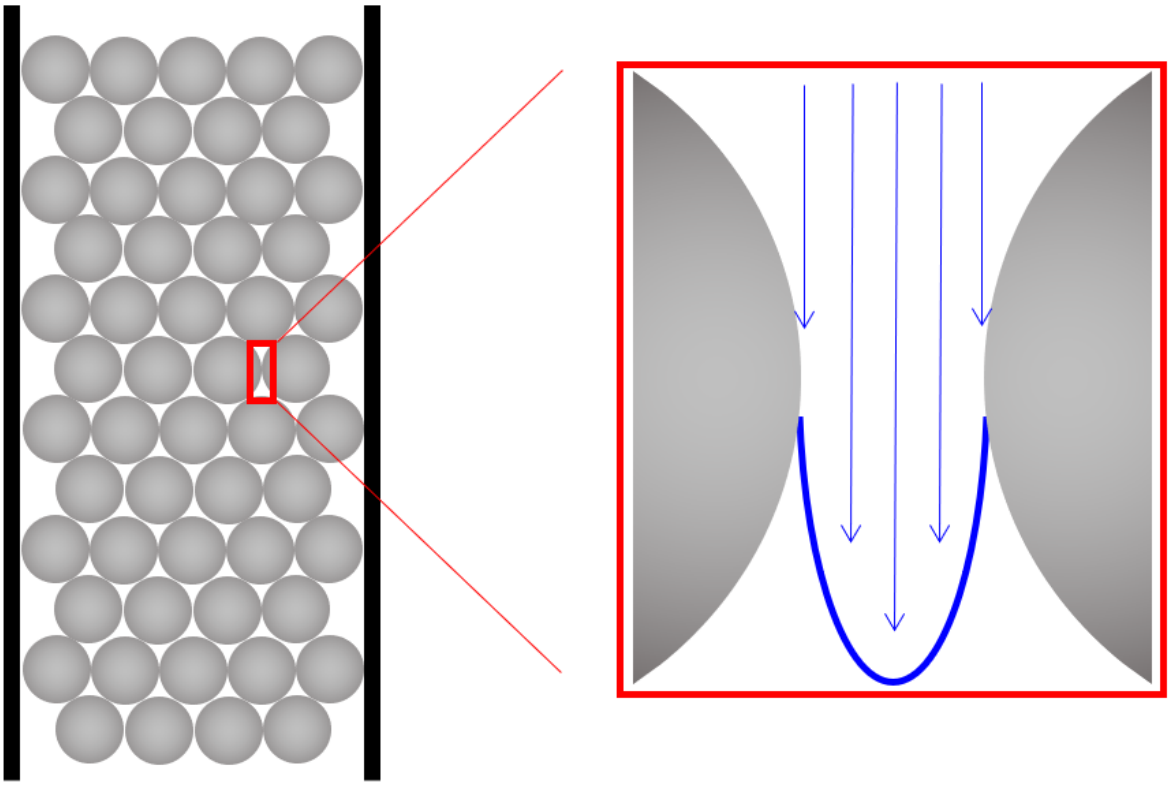

Figure 4-2 Grey sphere represents packing particles and black color lines are walls. Under laminar flow (blue parabolic flow profile), each interstitial space from a well-packed stationary phase can be considered as an open channel where HDC is performed.

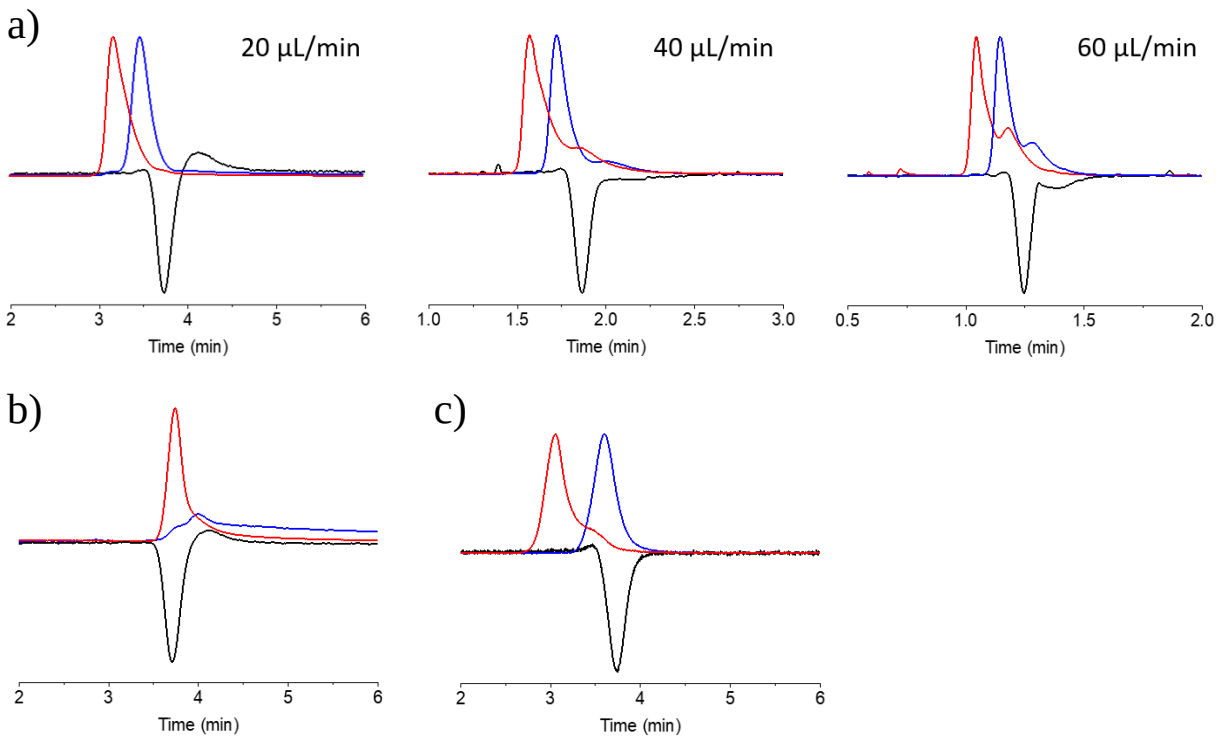


Figure 4-3 HDC separation using 500 nm base silica particles packed in a 2.1 × 50 mm stainless steel column. Blue chromatogram is lysozyme, red represents Eli Lilly intact IgG4, and black is water injection. Separation condition was 100% $H_2O$ isocratically with 0.1% FA and a) 1% SDS b) 0.1% SDS. C) 2% SDS. Flow rate was varied at 30 °C. Detection wavelength was 280 nm for proteins and 230 nm for water injection in order to see a up-side down peak. The UV absorbances are normalized by peak height to obtain a fair resolution comparison.

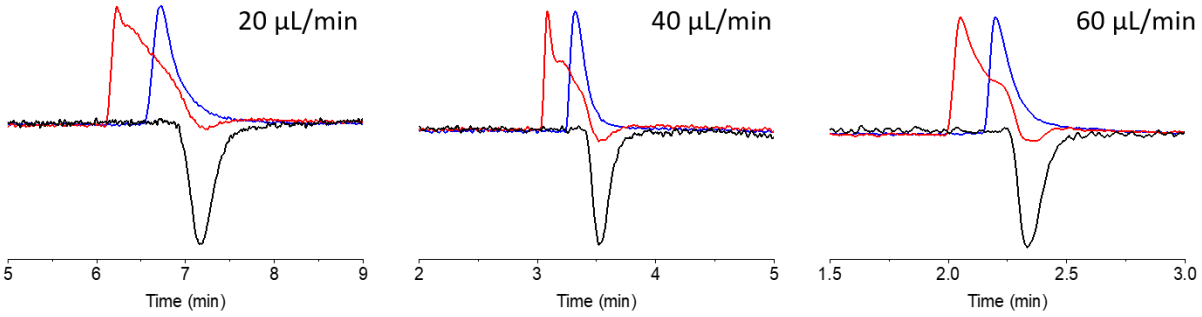


Figure 4-4 1500 nm C4 column (2.1 × 50 mm stainless steel column) was used for HDC separation under MS-compatible conditions. Lysozyme (blue), IgG4 (red), and water injection (black) were examined. Separation condition was 50:50 $H_2O$/ACN (v/v) isocratically with 0.5% FA at 30 °C. Flow rate was varied from 20 µL/min to 60 µL/min. Detection wavelength was 280 nm for proteins and 230 nm for water injection in order to see a up-side down peak. The UV absorbances are normalized by peak height to obtain a fair resolution comparison.

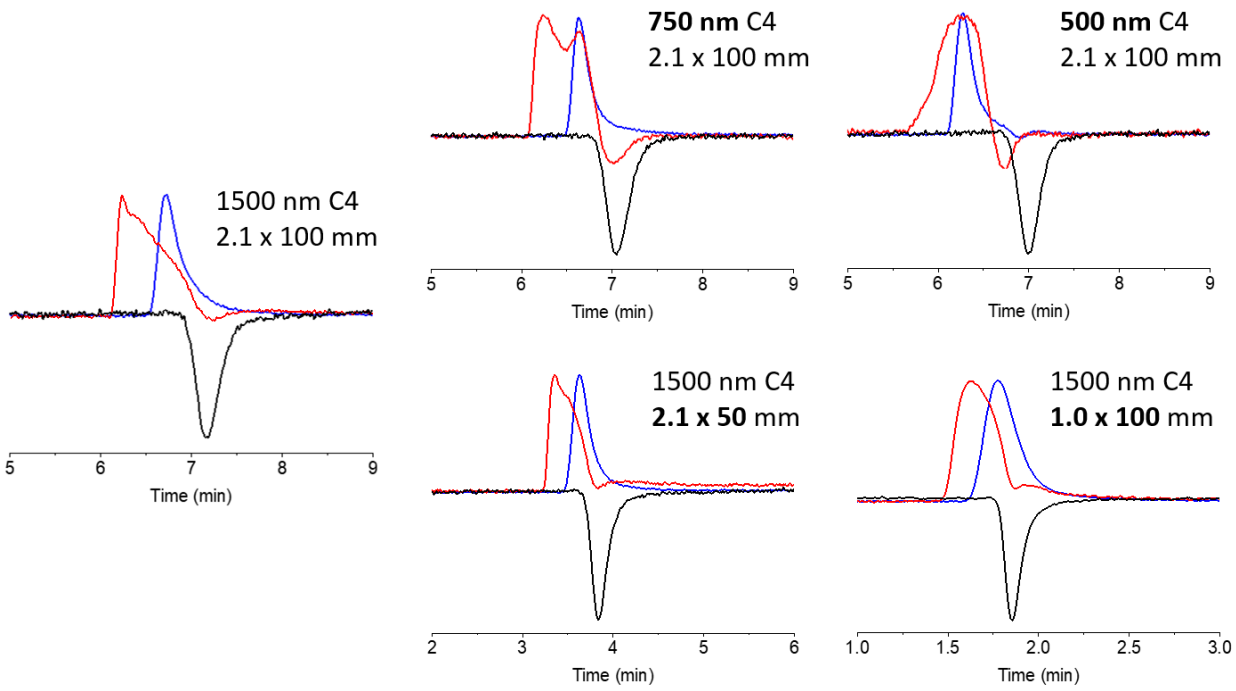


Figure 4-5 Different C4 particle sizes were packed in 2.1 × 50 mm stainless steel columns. In addition, 1500 nm C4 particles were pack in stainless steel columns with length and inner diameter. Elution method and order are same as Figure 4-4. The UV absorbances are normalized by peak height to obtain a fair resolution comparison.

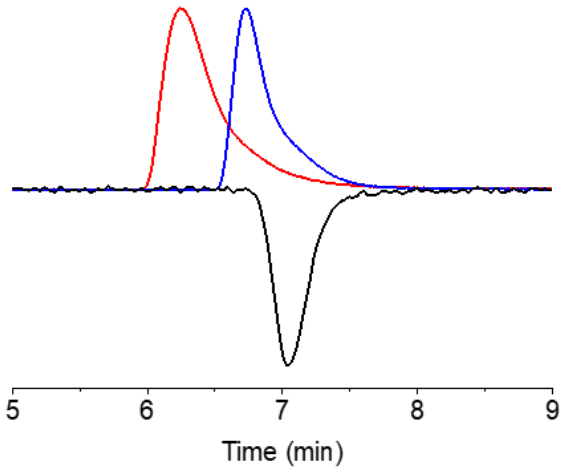


Figure 4-6 750 nm C4 column (2.1 × 100 mm stainless steel column) was used for HDC separation. Samples were the same as Figure 4-5. Separation condition was isocratic 50:50 $H_2O$/ACN (v/v) with 0.1% TFA at 30 °C. Otherwise noted.

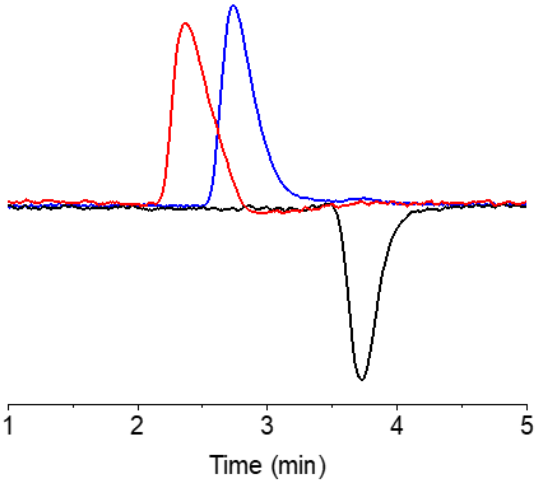


Figure 4-7 1500 nm BCC1 particle was packed in 2.1 × 50 mm stainless steel columns, then modified with monomer dimethylacrylamide (DMA). Samples, elution method and order are same as Figure 4-4. The UV absorbances are normalized by peak height to obtain a fair resolution comparison.

# CHAPTER 5. CONCLUSIONS AND FUTURE DIRECTIONS

## 5.1 Conclusions

The most pivatol moment began with why liquid chromatograpy (LC) and mass spectrometry (MS) stand on exclusive sides. Better chromatographic resolution is, worse mass spectrometry sensitivity is. However, combining LC and MS becomes a marvelous analytical technique. Therefore, we started improving chromatographic peak tailing and noticed that “active silanols” plays a critical role on influencing LC separation. The interesting part is no actually reasonable evidence to explain whether molecule-silanol interaction is good or bad until we saw molecules got stuck, then desorbed and started eluting again monitored by fluorescence microscopy. Afterwards, we decided to take a lot of time to study how to polish silica surface including calcining, annealing, and rehydroxylating. Chromatogram confirmed that peak tailing was remarkably reduced. Nevertheless, No matter how good the polishing process is, silanols never go away. When analytes are shifted gear from small molecules to proteins even large proteins, LC resolution becomes worse again due to strong electrostatic interactions from dissociated silanols with amino groups on proteins. As a result, this dissertation discussed the development of polymer-shell bonded phases, where a thick polymer brush layer is built on silica surface. Two major reasons are adopted on this design: 1) High-dense polymer brush layer keeps proteins away from silica surface to reduce protein exposure on silica surface as well as protein-silanol interactions. 2) Electric field generated by negatively charged silanols will interfere elution. Precisely, it increases protein retention time on the stationary phase. Therefore, thicker polymer layer prevents proteins from sensing surface charges.

Our group has developed polymer-shell bonded phases for hydrophobic interaction chromatography (HIC-MS) of prorteins and antibody-drug conjugates (ADCs), hydrophilic interaction liquid chromatography (HILIC-MS) of glycoproteins, reversed-phase liquid chromatography (RPLC-MS) of proteins and monoclonal antibodies (mAbs) including immunoglobulin G (subclasses: IgG1, IgG2, and IgG4), and cation exchange chromatography (CEX-MS) & anion exchange chromatography (AEX-MS) of proteins, mAbs, and ADCs. All listed LC separation methods are undergoing and avoiding trade-off between LC resolution and

MS sensitivity. The polymer stationary phases perform extraordinarily using LC-MS analysis and will be investigated more in the future for protein separations.

## 5.2 Future directions

In Chapter 2, we saw monoclonoal antibodies without drug (D0) is barely retained, which proves that our polymethylmethacrylate bonded phase has negligible interaction with mAb, as our expectation that designing retention only for attached drug and column surface. However, this result could be pro and con. The pro is non-covalent bound mAbs from ADCs will not suffer from adsorption-desorption processes, which avoid dissociating and denaturing. The con is D0 overlaps with excipient, which affect MS quantification and calculation on average drug-to-antibody ratio. We can design a copolymer bonded phase to increase retention time slightly or conjugate affinity property to stationary phase to increase only interaction between mAb and chromatographic surface to retain D0.

In Chapter 3, the RPLC application shows mainly on IgG1 separation. Actually, IgG2 has more complicated disulfide bond scrambling. It is worthy to design polymer shell bonded phase to distinguish IgG2 disulfides. In this regard, benzylmethacrylate monomer has been utilized for IgG2 disulfide separation. However, it is about a new start on this monomer, a matter of time is needed to optimize polymerization. If we could have IgG2 sample from industries, that will be wonderful to understand what they concern about.

In Chapter 4, HDC is not a freshly new LC method, but due to its impractical applications and limitations, people pay less attention on it. In this chapter, we just started exploring HDC and proved HDC theory. Apparently, peak capacity and resolution are big concerns so far. The more investigation on surface development is required. Another direction is our packed capillary separated bovine serum albumin (BSA) using isocratic 25/75 ACN/water (v/v) with 0.1% TFA to generate an unbelievable physical peak sigma only 20 μm (physical peak width, 80 μm). Hence, if we pack a 5 cm capillary, based on 80 μm peak width, there will be tremendous peak capacity and excellet resolution.

# VITA

In 2008, Tse-Hong (Aaron) Chen was graduated in National Chuung Hsing with bachelor degree major in Chemistry. In 2012, Aaron started Master's career under Prof. Rui Zhang's lab in Department of Chemistry at Western Kentucky University. During this time, Aaron was inspired by his advisor/mentor to further pursue a PhD degree.

In 2015, Aaron joined the PhD program under Prof. Mary Wirth's research group in Department of Chemistry at Purdue University and major in Analytical Chemistry. In Dr. Wirth's lab, Tse-Hong developed several polymer-shell bonded phases to improve online LC coupled with MS and achieve high LC resolution and MS sensitivity. Furthermore, Aaron devoted his research objectives to HPLC/UHPLC-MS method development to pharmaceutical proteins, monoclonal antibodies, and antibody-drug conjugates. After graduation in 2019, Tse-Hong decided to work as a scientist in Formulation Development Group at Regeneron and continue to pursue the science in the field of chromatography and mass spectrometry.

# PUBLICATIONS

analytical chemistry

Article

Cite This: *Anal. Chem.* 2019, 91, 2805−2812

pubs.acs.org/ac

## Native Reversed-Phase Liquid Chromatography: A Technique for LCMS of Intact Antibody−Drug Conjugates

Tse-Hong Chen,[†] Yun Yang,[†] Zhaorui Zhang,[‡] Cexiong Fu,[‡,⊥] Qunying Zhang,[‡] Jon D. Williams,[§] and Mary J. Wirth*[,†]

[†]Department of Chemistry, Purdue University, 560 Oval Drive, West Lafayette, Indiana 47907, United States

[‡]Process Analytical Chemistry, AbbVie, Inc. 1 N. Waukegan Road, North Chicago, Illinois 60064, United States

[§]Discovery Structural Chemistry, AbbVie, Inc. 1 N. Waukegan Road, North Chicago, Illinois 60064, United States

Supporting Information

**ABSTRACT:** The synthesis of antibody−drug conjugates (ADCs) using the interchain cysteines of the antibody inherently gives a mixture of proteins with varying drug-to-antibody ratio. The drug distribution profiles of ADCs are routinely characterized by hydrophobic interaction chromatography (HIC). Because HIC is not in-line compatible with mass spectrometry (MS) due to the high salt levels, it is laborious to identify the constituents of HIC peaks. An MS-compatible alternative to HIC is reported here: native reversed phase liquid chromatography (nRPLC). This novel technique employs a mobile phase 50 mM ammonium acetate for high sensitivity in MS and elution with a gradient of water/isopropanol. The key to the enhancement is a bonded phase giving weaker drug−surface interactions compared to the noncovalent interactions holding the antibody−drug conjugates together. The hydrophobicity of the bonded phase is varied, and the least hydrophobic bonded phase in the series, poly(methyl methacrylate), is found to resolve the intact constituents of a model ADC (Ab095-PZ) and a commercial ADC (brentuximab vedotin) under the MS-compatible conditions. The nRPLC-MS data show that all species, ranging from drug-to-antibody ratios of 1 to 8, remained intact in the column. Another desired advantage of the nRPLC is the ability of resolving multiple positional isomers of ADC that are not well-resolved in other chromatographic modes. This supports the premise that lower hydrophobicity of the bonded phase is the key to enabling online nRPLC-MS analysis of antibody−drug conjugates.

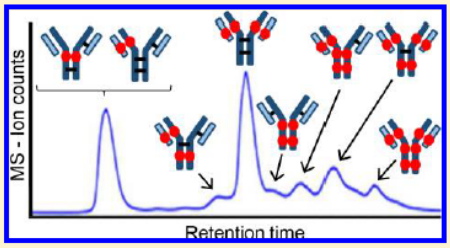




Antibody−drug conjugates (ADCs) are highly selective and potent chemotherapeutics for the treatment of different types of cancer, inspired by Paul Ehrlich.[1] An ADC consists of a recombinant monoclonal antibody (mAb) covalently conjugated with a drug via a hydrophilic linker. The mechanism exploits specific binding of tumor-expressed antigens and delivers covalently conjugated cytotoxic payloads to cancer cells selectively over nonmalignant cells, resulting in greater efficacy and minimized systemic toxicity. Four ADCs are currently on the market: Adcetris (brentuximab vedotin) from Seattle Genetics for the treatment of relapsed Hodgkin's lymphoma and systemic anaplastic large-cell lymphoma, Kadcyla (trastuzumab emtansine) from Genentech for the treatment of metastatic breast cancer,[2−4] Mylotarg (gemtuzumab ozogamicin) from Pfizer for acute myeloid leukemia, and Besponsa (inotuzumab ozogamicin) also from Pfizer for acute lymphoblastic leukemia. More than 60 ADCs have been advanced into clinical trials for cancer treatment,[3] and there are currently more than 65 ADCs in clinical evaluation to target different hematologic malignancies and solid tumors.[3,5] The vast majority of the cytotoxic warheads of the ADCs currently in clinical trials are conjugated to either lysine or cysteine residues on the antibody,[6−8] with most using cysteine residues.[9] Drug loading in the ADCs is an important design parameter that needs to be characterized.[10]

Liquid chromatography separation of cysteine-conjugated ADCs to characterize the drug loading distribution is the topic of this paper. Taking IgG1, for example, a common conjugation approach entails partial reduction of four interchain disulfide bonds to generate up to eight reactive thiol groups.[11−13] This conjugation scheme yields a mixture of species ranging from 0 to 8 drugs per antibody, which is a broad distribution. The different drug loadings have been reported to affect the pharmacokinetics, stability, and clearance of ADCs.[14−18] Native SEC-MS is a rapid technique for determining the distribution of drug loads, where the SEC serves to desalt the sample rather than separate the components and relies solely on MS for characterization and quantitation.[19] The technique skews the distribution toward

Received: October 12, 2018
Accepted: January 20, 2019
Published: January 21, 2019





DOI: 10.1021/acs.analchem.8b04699
*Anal. Chem.* 2019, 91, 2805−2812

lower drug load due to ion suppression and suboptimal recovery of species with higher drug load.[20] Pretreatment by enzymatic cleavage of the hydrophobic drug from the ADC, which leaves the hydrophilic linker attached as a tag, reduces the skewing but does not eliminate it.[21] Consequently, chromatographic separations are used for quantitative ADC characterization. Reversed-phase liquid chromatography coupled to mass spectrometry (RPLC-MS) is used to determine the average drug-to-antibody ratio (DAR) by separating the denatured subunits of the reduced ADC,[22] but this approach loses information about the drug load distribution.[23] Hydrophobic interaction chromatography (HIC) is a nondenaturing separation[24−26] that is currently the gold standard for resolving the drug distribution of ADCs.[27] A gradient of decreasing salt concentration is used for elution,[28,29] and the high initial concentration and low volatility of the salts prevent its direct coupling to mass spectrometry for peak identification.[30−34]

The Ge and Alpert groups were the first to show that HIC-MS of intact proteins is possible with volatile salts.[26,35] In their papers, MS-compatible ammonium acetate salt was used, with a gradient decreasing from 1 M to 20 mM, concurrent with a gradient of increasing acetonitrile in water from 0 to 50%. Because $NH_4OAc$ has kosmotropic properties weaker than those of the typical HIC salts of $(NH_4)_2SO_4$ and $Na_2HPO_4$, they used a bonded phase with increased hydrophobicity, and their results demonstrated that the proteins maintained their native forms. HIC-MS has not yet been reported for intact ADCs.

The considerations for HIC-MS of ADCs are different from those of natural proteins. The conjugated drug of an ADC is far more hydrophobic than the solvent-exposed surface of a native protein, as demonstrated by the elution time increasing with increasing drug load in HIC of ADCs. In light of this, the concept behind our work is that a fixed, low concentration of MS-compatible salt, e.g., 50 mM $NH_4OAc$, might give retention of ADCs on hydrophobic columns because less salting-out would be needed. If so, the question then is whether a mild organic additive, isopropanol, can be made to desorb the ADC from the stationary phase without dissociating the noncovalently bound subunits of the antibody. The strategy is to decrease the hydrophobicity of the bonded phase so that less organic component is needed for elution, thereby avoiding the dissociation of the antibody into subunits.[36] This is the opposite of the strategy used by Chen and coworkers[26,35] because ADCs present a different problem than mAbs, which are more hydrophilic than ADCs. The other difference from the prior work is that the salt concentration is fixed at low level while the organic component is increased, which would make this a reversed-phase separation. Hence, the proposed new method is a nondenaturing version of reversed-phase liquid chromatography (RPLC), and we refer to it as native reversed-phase liquid chromatography (nRPLC).

The purpose of this work is to test the idea that a bonded phase with sufficiently low hydrophobicity would enable a new technique, nRPLC-MS, for separating intact ADCs and determining their molecular weights by in-line coupled mass spectrometry. The method is evaluated using both a model ADC and a commercial ADC, where each ADC has a drug mimic or drug coupled to cysteines of the mAb using a hydrophilic linker.

## MATERIALS AND METHODS

**Materials.** Nonporous silica particles (1500 nm) were purchased from Superior Silica (Tempe, AZ). Empty stainless-steel columns (2.1 mm ID, 50 mm length), reservoirs (4.6 mm ID, 150 mm), and frits (0.5 $\mu$m pore diameter) were purchased from Isolation Technologies (Middleboro, MA). Stainless-steel tubing, ferrules, and internal nuts were all purchased from Valco Instruments (Houston, TX). Silanes, i.e., (chloromethyl)phenyl)dimethylchlorosilane (+99%) and trimethylchlorosilane (+99%), were purchased from Gelest (Morrisville, PA). Methyl methacrylate (MMA, 99%), sodium ascorbate (≥99%), butylamine (99.5%), $NH_4OAc$ (99.99%), ammonium sulfate ($(NH_4)_2SO_4$, ≥99%), sodium phosphate ($Na_3PO_4$, 96%), and ammonium hydroxide were purchased from Sigma-Aldrich (St. Louis, MO). Other chemicals used included trifluoroacetic acid (TFA, 99%), difluoroacetic acid (DFA, 98%), and copper(II) chloride ($CuCl_2$, 99%) from Acros Organics (Morris Plains, NJ), tris(2-dimethylaminoethyl)amine ($Me_6$TREN, + 99%) from Alfa Aesar (Haverhill, MA), and formic acid (FA, 99.5%+, LC/MS grade), acetonitrile (ACN), and 2-propanol (IPA) from Fisher Scientific (Hampton, NH). Ultrapure water was obtained from a Milli-Q system (MilliporeSigma, Darmstadt, Germany).

IgG1 Ab095 was conjugated with drug-linker mimic PZ in-house at AbbVie (North Chicago, IL) as a model ADC. Brentuximab vedotin was obtained from Seattle Genetics. Both ADCs were prepared at 1 mg/mL in $NH_4OAc$ or $(NH_4)_2SO_4$ with final concentration 0.8−1.0 M.

**UHPLC Column Preparation.** The silica particles were modified as described earlier.[37] Briefly, the silica particles were calcined at 600 °C for 12 h, then annealed at 1050 °C for 3 h, and rehydroxylated overnight in 1.0 M $HNO_3$. Particles were then rinsed in ultrapure water and dried in a 60 °C vacuum oven. SEM showed that the particles decreased in diameter to 1.2 $\mu$m from the heating steps. Freshly rehydroxylated silica particles were suspended in a dry toluene solution containing 2% (v/v) of (chloromethyl)phenyl)dimethylchlorosilane and 0.1% (v/v) of butylamine. The solution was refluxed for 3 h and then rinsed with dry toluene. The particles were then end-capped by suspending in another dry toluene solution containing 2% (v/v) of trimethylchlorosilane and 0.1% (v/v) of butylamine and refluxed for 3 h. The silylated, end-capped particles were then rinsed with dry toluene and allowed to dry in a 60 °C vacuum oven for 2 h.

For polymer growth, each monomer was dissolved in 50:50 $H_2O$/IPA (v/v) in a 50 mL round-bottom flask for a final concentration of 2.5 M. Two other solutions were made: (1) a solution containing 40 mg of $CuCl_2$ and 80 $\mu$L of $Me_6$TREN and (2) a solution containing 20 mg of sodium ascorbate. These were also prepared in 2.0 mL of 50:50 $H_2O$/IPA. Afterward, the Cu/$Me_6$TREN solution was added to the round-bottom flask, followed by the sodium ascorbate solution. The resulting solution was poured into a plugged reservoir column of 4.6 × 150 mm. A 2.1 × 50 mm column was packed with 0.24 g of silylated, end-capped particles suspended in acetonitrile. The reservoir and column were connected in series. A high-pressure pump, LabAlliance Series 1500 HPLC Pump (Laboratory Alliance of Central New York, LLC, Syracuse, NY) was used for packing and modification. The reaction solution from the reservoir was pumped into the column starting at 200 $\mu$L/min until the reaction mixture dripped from the end of the column. The flow rate was then



DOI: 10.1021/acs.analchem.8b04699
Anal. Chem. 2019, 91, 2805−2812

lowered to 100 μL/min, and the polymerization reaction was allowed to proceed for a range of reaction times from 40 to 85 min for optimization. After reaction, the freshly packed column poly(methyl methacrylate) (PMMA) was rinsed with water for 20 min at 100 μL/min.

**UHPLC.** The columns and mobile phases for the various separations are summarized in Table 1.

**Table 1. Summary of HPLC Columns and Their Applications Herein**

| column | application | mobile phase A; B |
|---|---|---|
| Thermo MabPac RP | RPLC, reduced ADC | $H_2O$ + 0.1% DFA; ACN + 0.1% DFA |
| Supelco Bioshell A400 | RPLC, nonreduced ADC | $H_2O$ + 0.1% FA + 0.015% TFA; ACN + 0.1% FA + 0.015% TFA |
| Thermo-HIC butyl | HIC, ADC (Purdue) | 50 mM $Na_3PO_4$ + 1 M $(NH_4)_2SO_4$, pH 7; 50 mM $Na_3PO_4$ + 30% IPA, pH 7 |
| Tosoh TSKgel Butyl | HIC, ADC (AbbVie) | 25 mM $Na_3PO_4$ + 1.5 M $(NH_4)_2SO_4$, pH 7; 25 mM $Na_3PO_4$ + 25% IPA, pH 7 |
| PMMA, nonporous | nRPLC, ADC | 50 mM $NH_4OAc$, pH 7; 50 mM $NH_4OAc$ + 50% IPA, pH 7 |

A Thermo Accela UHPLC system (Thermo-Scientific, Waltham, MA, United States) was used for the development of nRPLC separations at the Purdue lab. Lab-made nRPLC columns (2.1 × 50 mm, 1.2 μm nonporous silica particles coated with various polyalkyl methacrylates were used as the analytical columns. A commercial column, MabPac HIC-Butyl (4.6 × 100 mm, 5 μm nonporous), from Thermo Scientific (Waltham, MA) was used under both HIC and nRPLC conditions for comparison because both have polymeric surfaces. UV absorbance wavelength was set to 280 nm. The column temperature was 30 °C, and the injection volume was 3 μL.

A TSKgel Butyl-NPR column (4.6 × 35 mm, 2.5 μm, Tosoh, King of Prussia, PA) was used for HIC at the AbbVie site, with an Agilent 1200 HPLC (Agilent, Santa Clara, CA). The system is routinely used for HIC separations of ADCs to calculate DAR. With the mobile phase given in Table 1, the gradient started with 90% MPA, decreased to 75% MPA in 2 min followed by a gradient to 0% MPA in 10 min, and was held for 2 min before re-equilibrium. The flow rate was 0.8 mL/min, and column temperature was set to 25 °C.

**LC-MS.** For RPLC-MS of the reduced ADC, this was generated in the Purdue lab by adding 1,4-dithiothreitol (DTT), a Thermo Accela UHPLC was used with a Thermo MabPac RP column (2.1 × 50 mm, 4 um, supermacroporous polymer particles) (Thermo-Scientific, Waltham, MA, United States), and the column was coupled to a Thermo LTQ Velos mass spectrometer (Thermo-Scientific, Waltham, MA, United States). With the mobile phase given in Table 1, the gradient started with 27% with MPB2, increased to 43% MPB2 in 15 min, and returned to 27% MPB2 for re-equilibrium. Flow rate was 0.2 mL/min, and column temperature was 80 °C. Peak identities were assigned by matching deconvoluted masses with theoretical masses.

For RPLC-MS of the nonreduced ADC (no DTT), a Supelco Bioshell A400 Protein C4 column (2.1 × 100 mm, 3.4 μm, Sigma-Aldrich, St. Louis, MO) was used in the AbbVie lab. With the mobile phase given in Table 1, the gradient started with 90% MPA3, ramped to 69% MPA3 in 1 min followed by a decrease to 52% MPA3 in 13 min and returned to original condition for re-equilibrium. Flow rate was 0.3 mL/min, and column temperature was 70 °C. The ADC samples were analyzed using an Acquity UPLC H-Class coupled to a Synapt G2 Si mass spectrometer (Waters, Milford, MA). Peak identities were assigned by matching deconvoluted masses with theoretical masses.

For online nRPLC-MS analysis, the poly(methyl methacrylate) (PMMA) column made in the Purdue lab was used at AbbVie, where the LC-MS system was a Waters Acquity UPLC H-Class coupled to a Xevo G2 qTOF mass spectrometer (Waters, Milford, MA). With the mobile phase given in Table 1, the gradient started with 0% MPB4, held for 2 min, ramped to 15% MPB4 in 3 min followed by a gradient to 50% MPB4 in 15 min and held at 50% MPB4 for 6 min before re-equilibrium. Flow rate was reduced to 0.07 mL/min. Column temperature was 30 °C. For MS condition, capillary voltage was 3.00 kV. Sample cone voltage was 85 V, trap collision energy was set to 60 V, source temperature was 140 °C, and desolvation temperature was 500 °C. The high sampling cone voltage was used to improve resolution and sensitivity in raw MS spectra, but this more prone to cause in-source fragmentation

## RESULTS AND DISCUSSION

A model ADC was synthesized by AbbVie, with the chemical structure of the linker and drug portions depicted in Figure 1a.

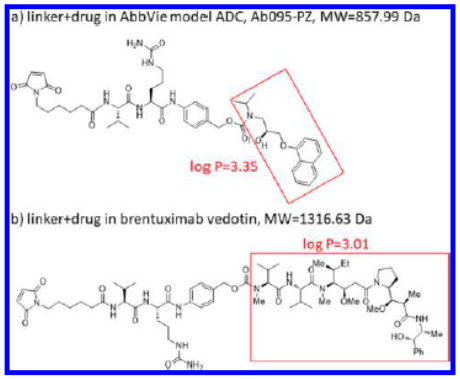


**Figure 1.** Chemical structures of linker-drug combination for (a) the AbbVie model ADC, Ab095-PZ and (b) brentuximab vedotin. Each drug or drug mimic part is in the red square, and its hydrophobicity is expressed by log *P*, where *P* represents the octanol/water partition coefficient.

The structure is similar to that of the commercial ADC, Brentuximab, also studied here, with its structure depicted in Figure 1b. These are both cysteine-conjugated ADCs using a similar, typical hydrophilic linker with coupling to the mAb cysteines via the maleimide group. The figure shows that the drug mimic for the AbbVie model ADC and the drug for brentuximab vedotin are quite hydrophobic, each with a log *P* in excess of 3, where *P* is the partition coefficient for octanol/water.

ADCs can be characterized with respect to their average DAR by fully reducing the ADCs with DTT and then separating the subunits by RPLC. Sketches to indicate labeling



DOI: 10.1021/acs.analchem.8b04699
Anal. Chem. 2019, 91, 2805−2812

for intact ADCs and the various subunits are given in Figure 2a. The RPLC chromatogram for the reduced AbbVie model

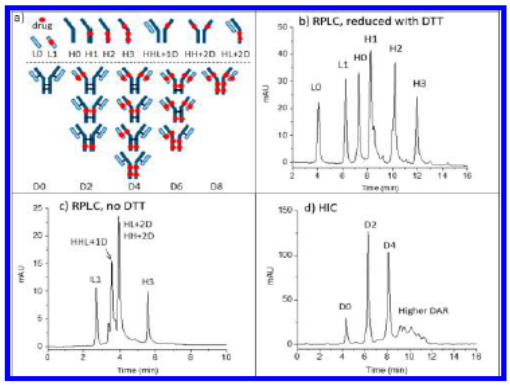


**Figure 2.** (a) Sketches explain abbreviations for peak assignments. (b) RPLC of the model ADC after reduction with DTT. (c) RPLC of the model ADC without DTT. (d) HIC of the intact ADC with tentative peak assignments. Condition are in the Supporting Information.

ADC Ab095-PZ is shown in Figure 2b. The mass spectrum of each peak (Supplementary Figure S1) was used to assign each of the six peaks to the subunit, as labeled in the chromatogram. The first two peaks are light chains without (L0) or with (L1) one drug+linker, and the latter four peaks are heavy chains with 0, 1, 2, and 3 drug+linker attachment(s). The average DAR calculated from the relative peak areas is 3.9. The RPLC chromatogram of Ab095-PZ without DTT reduction (i.e., nonreduced RPLC) is shown in Figure 2c. The peak assignments from MS show that the model ADC was only partially reduced during the conjugation process, as expected. The results demonstrate that in conventional RPLC, without interchain disulfide bond linkages, the ADC dissociates into subunits. The value of this chromatogram is that it can be later compared to that for native RPLC with DTT absent. The HIC chromatogram of Ab095-PZ, using a commercial HIC-Butyl column and typical HIC salt gradient, is shown in Figure 2d. As is common practice, an isopropanol gradient was superimposed on the salt gradient to attain full elution of the ADC constituents. The species with higher drug loading gave multiple peaks, and this is shown later to be due to partial resolution of positional isomers. Mass spectrometry cannot be used to identify the peaks of Figure 2d because the conventional HIC salts suppress ionization and cause adduct formation, as discussed earlier. One can make tentative peak assignments based on typical drug loading profile for ADCs with an average DAR of 3.9, as indicated in Figure 2d.

The proposed strategy described earlier to enable native RPLC-MS is to use no more than 50 mM $NH_4OAc$. This amount of salt is normally reached at the end of a salt gradient for online HIC-MS;[25,26,38] therefore, there is now little value in even running a salt gradient in RPLC mode. Despite this low level of salt, the same commercial HIC column as used for the HIC of Figure 2d (Thermo MabPac HIC-Butyl column) was found to give virtually no elution of the ADC, as shown in Supplemental Figure S2; the retention to the column is too strong for elution. This indicates that the lower kosmotropic power of 50 mM $NH_4OAc$ gives more retention than the higher kosmotropic power of 50 mM sodium phosphate of Figure 2d. The strong retention with 50 mM $NH_4OAc$ is attributed to irreversible adsorption of the hydrophobic drug rather than to salting out of the intact ADC. The HIC stationary phase, which is said to be made of butyl groups, is thus too hydrophobic for use with isocratic 50 mM $NH_4OAc$, i.e., the hydrophobic interactions between ADC and bonded phase surface are stronger than the intramolecular hydrophobic interactions within the ADC. This inspires the proposed strategy to make the bonded phase less hydrophobic so that the free energy barrier for protein desorption is lower than the free energy barrier for protein denaturation.

Native RPLC chromatograms of model ADC Ab095-PZ using isocratic 50 mM $NH_4OAc$ with a gradient of 0−50% isopropanol are shown in Figures 3a−d for a series columns

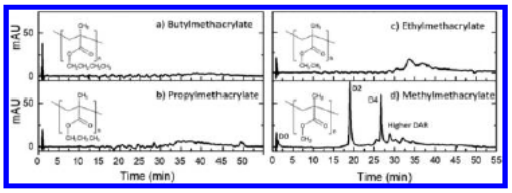


**Figure 3.** Native RPLC (nRPLC) of AbbVie model ADC with varying hydrophobicity of bonded phase, as denoted by the structures. Gradient conditions are A: 50 mM $NH_4OAc$, pH 7, B: 50 mM $NH_4OAc$, 50% IPA, pH 7, 0−100%B/40 min, 100%B/5 min, 100 $\mu$L/min, 30 °C. The same tentative labels as for the HIC chromatogram of Figure 2d are made due to the similarity.

with decreasing bonded phase hydrophobicity, including polymethyl-, polyethyl-, polypropyl-, and poly(butyl methacrylate). The recovery and resolution are progressively higher with lower hydrophobicity, consistent with less denaturation of the ADCs lower mobile phase strength. Poly(methyl methacrylate), with the lowest hydrophobicity, gives a chromatogram similar to that of the native HIC chromatogram of Figure 2d, suggesting that intact ADCs are indeed eluted under mild organic phase content without dissociation. The chromatogram is quite different from than that of the denaturing RPLC case of Figure 2c, again arguing that the ADCs are not dissociated.

The downside of the nRPLC separation of the ADCs in Figure 3 is that the native antibody, i.e., the species having no conjugated drug, D0, has low retention. This is an inherent outcome of the nRPLC strategy, where the designed retention mechanism is based on the hydrophobic interaction between the exposed/or partially exposed hydrophobic drug with the bonded phase. To increase the retention of D0 species, some mixed-mode copolymer could potentially be used with minimal effect on retention of the hydrophobic drug.

Mass spectrometry is used to test whether the constituents of the ADC peaks are intact vs dissociated under nRPLC conditions for the column with poly(methyl methacrylate) grown for 70 min. Figure 4a shows the nRPLC chromatogram for the AbbVie model ADC using the poly(methyl methacrylate) column, now with the gradient adjusted for faster elution. The peaks are labeled in detail based on the mass of the most prevalent protein for each peak. The raw mass spectral data are given in Figure 4b. By extracting high



DOI: 10.1021/acs.analchem.8b04699
Anal. Chem. 2019, 91, 2805−2812

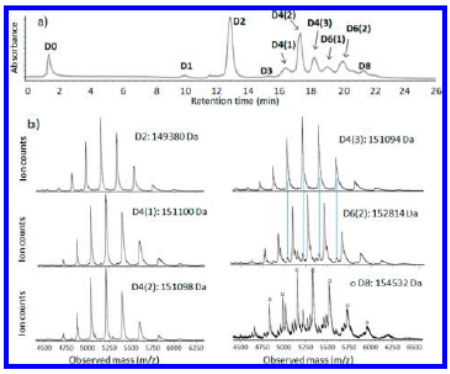


**Figure 4.** (a) nRPLC of the AbbVie model ADC Ab095-PZ, with peaks labeled based on the mass spectra. Gradient: 0 to 4.5% IPA/water over 3 min, then 4.5 to 50% IPA/water over 20 min. Detection at 280 nm. (b) Raw mass spectra for peaks as labeled, with the molecular weight based on deconvoluted mass spectra for peak ID. The blue lines show that extra peaks are from overlap.

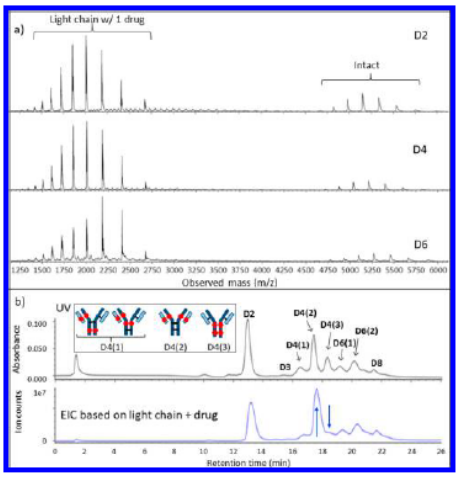


**Figure 5.** Evidence that light chain dissociates in MS source for AbbVie model ADC. (a) Full-range raw mass spectra show large signals for light chain+drug, but no significant signals for ADC minus light chain+drug. (b) Chromatogram with UV detection (top) and EIC based on light chain+drug (bottom). The blue arrows point to two peaks that changed intensities, and the inset depicts the structures for the isomers consistent with these intensity changes.

mass range (extracted in chromatogram not shown), it was confirmed that the unconjugated species (D0) was barely retained and was nearly coeluting with the injection peak. The small peak in the chromatogram of Figure 4a eluting at 10 min was identified as D1. In Figure 4b, the first mass spectrum assigned the peak at 13 min as D2 based on deconvoluted mass, which gives the mass (149 380 Da) corresponding to that expected for D2 (theoretical mass: 147 640 + 2 × 859). There are three peaks for D4, labeled as D4(1), D4(2), and D4(3) in the order of elution, and Figure 2a showed that there are theoretically four positional isomers for D4. Of note, the positional isomers of D4 that result from conjugation of the upper vs lower cysteine pairs in the hinge region likely coelute because they are only subtly different in structure. Similarly, D6 gives two peaks when there are expected to be three, but again, as illustrated in Figure 2a, two cases differ only by position on the heavy chain (upper hinge cysteine conjugation vs lower hinge cysteine conjugation). It is novel for a HIC column to resolve different D4 and D6 isoforms from one another, and the separation on this poly(methyl methacrylate) under nRPLC mode could be advantageous in process understanding and quality control. The mass spectrum of the larger of the two D6 peaks is given in Figure 4b. It shows some peak overlap with D4, as indicated by the light blue lines in Figure 4b. The mass spectrum of the peak labeled D8 indicates it to be mainly D8 with some overlap from D5, D6, and D7. No peaks due to fragments were observed. It is noteworthy that all ADC mass spectra demonstrated a native-like charge envelope distribution with charge state from 24 to 33, which further supports the conclusion of native RPLC.

Representative mass spectra of model ADC over a wider range of mass-to-charge ratio ($m/z$) are given in Figure 5a. All spectra show strong signals from a heretofore unexpected L1 fragment (light chain plus drug), despite the absence of corresponding species (ADC minus L1) in the higher mass range for intact ADC. This at first seems to contradict the claim of intact ADC elution during the discussion of Figure 4 for the higher mass range. Our conclusion is that this L1 signal in Figure 5 arises from two circumstances: (1) in-source fragmentation of the ADC after elution due to the rather high sampling cone voltage and (2) a greater ionization efficiency of the L1 fragment to make its signal appear disproportionately strong compared to that of the intact ADC. If the signal strength were proportional to abundance, there would be a significant amount of ADC-L1 detectable in the higher range of $m/z$. Therefore, the large peaks for L1 must be due to greater ionization efficiency. In addition, if L1 dissociated from the ADC on the column, the EIC based on L1 would not be correlated with the UV chromatogram. The only reasonable way for the subunits of the ADC to travel together throughout the separation is for the ADC to be intact. An extracted ion chromatogram (EIC) for the L1 fragment is shown in Figure 5b, in comparison with the same chromatogram using UV detection. It is clear that the chromatograms closely track one another for the two different modes of detection. Further, the exceptions prove the rule: the blue arrows in Figure 5b show a D4 peak that is increased and a D4 peak that is decreased for EIC of L1. These are consistent with the expectation that one D4 should have two L1 species and one should have none. The inset images in Figure 5b depict the structures of the positional isomers. D4(2) has twice as many light chains with drug compared to D4(1), which would make its signal increase for EIC of L1. Likewise, D4(3) has no light chain with drug; hence, signal would decrease for EIC of L1. The EIC supports the conclusion that L1 dissociated postcolumn and all ADCs remained intact throughout the nRPLC separation. It is remarkable that D8, with fully reduced interchain disulfide bonds between subunits, eluted intact.

The native RPLC-MS strategy was also tested for a commercial ADC, brentuximab vedotin, which is a well-



DOI: 10.1021/acs.analchem.8b04699
Anal. Chem. 2019, 91, 2805−2812

characterized commercial ADC with an average DAR of 4.0, comparable to that of the AbbVie model ADC.[39] HIC was performed to compare DAR profiles of the two ADCs. The results are provided in Figure 6, confirming that the DAR

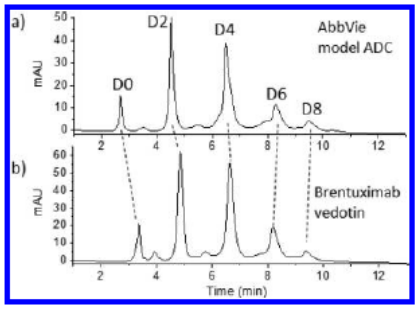


**Figure 6.** HIC separation of (a) model ADC and (b) commercial ADC Brentuximab vedotin. The dashed lines illustrate that the greater hydrophobicity of the mAb itself for Brentuximab vedotin. Tosoh TSKgel Butyl-NPR, 4.6 × 35 mm, 2.5 μm. MPA: 1.5 M ammonium sulfate, 25 mM sodium phosphate pH 7.0; MPB: 25 mM sodium phosphate pH 7.0 with 25% IPA; flow rate: 0.8 mL/min; column temp: 25 °C.

profiles of these two ADCs are qualitatively similar. The chromatograms show that the D0 peak elutes later for brentuximab vedotin, indicating that the brentuximab (mAb of brentuximab vedotin) sequence is more hydrophobic than that of the AbbVie model ADC. This is offset by the drug of brentuximab vedotin being less hydrophobic than the drug-linker of the AbbVie model ADC, with its lower octanol/water partition coefficient, log $P$ = 3.01, for MC-VC-MMAE compared to that of the AbbVie model drug, log $P$ = 3.35. The elution times of peaks with higher drug load in HIC are similar in both chromatograms: 10 min.

The nRPLC chromatogram for brentuximab vedotin, using the same poly(methyl methacrylate) column and separation conditions as for the AbbVie model ADC, is given in Figure 7a.

The chromatogram is similar to that for the AbbVie model ADC, with differences in relative peak heights and a small extra peak before D6. The D0 species is now slightly retained in nRPLC, owing to the greater hydrophobicity of the mAb that was noted using HIC. All ADC peaks elute somewhat earlier in nRPLC for brentuximab vedotin, consistent with the lower hydrophobicity of the drug. The mass spectra, detailed in Figure 7b, show that the D2 peak and the first D4 peak, D4(1), are intact, with no loss of L1. The other two D4 peaks, D4(2) and D4(3), show some loss of one or two light chains with drug (D4-L1 and D4-2xL1), in addition to the intact forms being observed. Overall, the results show that it is much easier to lose L1 from brentuximab vedotin than it is from the AbbVie model ADC.

As was done with the AbbVie model ADC to distinguish on-column vs in-source dissociation, Figure 8a shows representative mass spectra over wider range of $m/z$ for brentuximab vedotin. The relative signals from the L1 fragment are much stronger than those of the AbbVie model ADC, again illustrating the greater ease of loss of L1 for brentuximab vedotin. To determine whether L1 dissociated on-column or in-source, the EIC for the L1 fragment is shown in Figure 8b, in comparison with the same chromatogram using UV

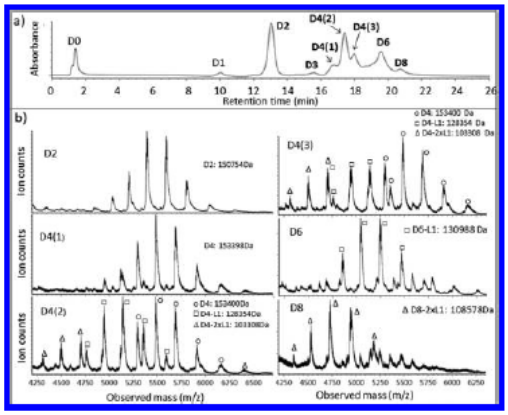


**Figure 7.** nRPLC and mass spectra for commercial ADC: brentuximab vedotin. (a) nRPLC with detection at 280 nm. Conditions same as those in Figure 4. (b) Raw mass spectra for D2, D4(1,2,3), D6, and D8, with the molecular weight based on deconvoluted mass spectra.

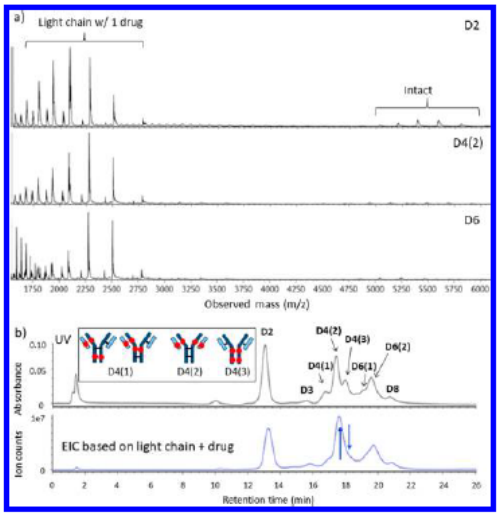


**Figure 8.** LCMS data for brentuximab vedotin, analogous to Figure 5. (a) Full-range raw mass spectra show even stronger signals for light chain+drug than observed for the AbbVie model ADC. (b) Chromatogram for UV detection (top) approximately tracks that of EIC for signal of light chain+drug, again indicating light chain+drug dissociated after separation. Again, the blue arrows show two peaks that changed intensities, and the inset depicts the structures for the D4 isomers that are consistent with these changes.

detection. As with the case for the AbbVie model ADC, the UV and extracted ion chromatograms closely track one another. The lack of an L1 background across the chromatogram confirms that all of the ADCs remain intact throughout the course of the nRPLC separation. As with the AbbVie model ADC, the L1 fragment signal is more pronounced in the D4(2) position than the latter peak D4(3), indicated by the blue arrows. As with the case for the AbbVie model ADC, the



DOI: 10.1021/acs.analchem.8b04699
Anal. Chem. 2019, 91, 2805−2812

relative abundances of the L1 fragment peaks are likely associated with same two factors: (a) the L1 molar ratio in the positional isomer: 1, 2, and 0, for D4(1), D4(2), and D4(3), respectively; and (b) strength of the noncovalent interaction between L1 and heavy chain in the MS source. These two factors reflect on the L1 fragment peak abundance in the order of D4(2) > D4(1) ≫ D4(3). The comparison of EIC and UV chromatograms again supports the conclusion that nRPLC elutes intact brentuximab vedotin species. The greater loss of L1 in the source for brentuximab vedotin relative to the AbbVie model ADC indicates that the noncovalent interactions between light and heavy chains are weaker for brentuximab vedotin than that of the AbbVie model ADC Ab095-PZ.

## ■ CONCLUSIONS

A novel protein chromatography technique intersecting HIC and RPLC modes was developed, termed native reverse-phase liquid chromatography, nRPLC. nRPLC employs the solvent elution model and MS compatibility of RPLC while preserving the native form of protein and ADC as in HIC. This new nRPLC technique is an alternative to HIC for ADCs when in-line coupling of MS is desired by virtue of using only 50 mM $NH_4OAC$. The nRPLC method eluted intact ADCs for both a model ADC from AbbVie and a commercial ADC from Seattle Genetics. Key to this chromatographic advance was lower hydrophobicity of the bonded phase to make drug−surface hydrophobic interactions weaker than the intramolecular hydrophobic interactions that maintain the noncovalent complexes. Inherent to this strategy of designing retention only for interactions between the attached drug and chromatographic surface is that the D0 species has little retention at this stage in column development. The column gives partial resolution of positional isomers, thereby providing additional characterization beyond what is typically obtained using HIC. The lesser number of peaks in HIC permits full resolution of the ADC based on drug loading, which enables precise calculation of DAR. With its greater resolution of positional isomers that currently overlap, nRPLC will be a companion rather than a replacement for HIC until resolution is improved. Longer nRPLC columns, refinement of polymer growth conditions, and optimization of separation conditions could lead to sufficient resolution to determine DAR while also characterizing positional isomers. To our knowledge, this is the first time that intact ADCs made from reduced cysteines have been separated based on DAR using an MS-compatible mobile phase.

## ■ ASSOCIATED CONTENT

### Supporting Information

The Supporting Information is available free of charge on the ACS Publications website at DOI: 10.1021/acs.analchem.8b04699.

Conditions for conventional chromatography in Figure 2; Figure S1a, RPLC chromatogram for AbbVie model ADC after reduction with DTT; Figure S1b, raw mass spectra and deconvoluted mass spectra for each peak in the chromatograms of part a; Figure S2, nRPLC of model ADC using a commercial HIC column (PDF)

## ■ AUTHOR INFORMATION


### Corresponding Author

*E-mail: mwirth@purdue.edu; Phone: +1-765-494-5328.

### ORCID

Mary J. Wirth: 0000-0003-2538-6985

### Present Address

⊥C.F.: Shire Pharmaceutical, Lexington, MA 02421, United States.


### Notes

The authors declare the following competing financial interest(s): The corresponding author (M.J.W.) is part owner of a company, bioVidria, that has licensed the technology described in this paper.

## ■ ACKNOWLEDGMENTS

This work was supported by a grant from the National Institutes of Health, R01GM121910.

## ■ REFERENCES


(1) Hughes, B. *Nat. Rev. Drug Discovery* **2010**, *9* (9), 665−7.
(2) Thomas, A.; Teicher, B. A.; Hassan, R. *Lancet Oncol.* **2016**, *17* (6), e254−e262.
(3) Beck, A.; Goetsch, L.; Dumontet, C.; Corvaia, N. *Nat. Rev. Drug Discovery* **2017**, *16* (5), 315−337.
(4) Polakis, P. *Pharmacol. Rev.* **2016**, *68* (1), 3−19.
(5) Lambert, J. M.; Berkenblit, A. *Annu. Rev. Med.* **2018**, *69*, 191−207.
(6) Tsuchikama, K.; An, Z. *Protein Cell* **2018**, *9* (1), 33−46.
(7) Flygare, J. A.; Pillow, T. H.; Aristoff, P. *Chem. Biol. Drug Des.* **2013**, *81* (1), 113−21.
(8) Peters, C.; Brown, S. *Biosci. Rep.* **2015**, *35* (4), No. e00225.
(9) Jain, N.; Smith, S. W.; Ghone, S.; Tomczuk, B. *Pharm. Res.* **2015**, *32* (11), 3526−3540.
(10) Hamblett, K. J.; Senter, P. D.; Chace, D. F.; Sun, M. M. C.; Lenox, J.; Cerveny, C. G.; Kissler, K. M.; Bernhardt, S. X.; Kopcha, A. K.; Zabinski, R. F.; Meyer, D. L.; Francisco, J. A. *Clin. Cancer Res.* **2004**, *10* (20), 7063−7070.
(11) Behrens, C. R.; Ha, E. H.; Chinn, L. L.; Bowers, S.; Probst, G.; Fitch-Bruhns, M.; Monteon, J.; Valdiosera, A.; Bermudez, A.; Liao-Chan, S.; Wong, T.; Melnick, J.; Theunissen, J. W.; Flory, M. R.; Houser, D.; Venstrom, K.; Levashova, Z.; Sauer, P.; Migone, T. S.; van der Horst, E. H.; Halcomb, R. L.; Jackson, D. Y. *Mol. Pharmaceutics* **2015**, *12* (11), 3986−98.
(12) Sanderson, R. J.; Hering, M. A.; James, S. F.; Sun, M. M. C.; Doronina, S. O.; Siadak, A. W.; Senter, P. D.; Wahl, A. F. *Clin. Cancer Res.* **2005**, *11*, 843−852.
(13) Sun, M. M. C.; Beam, K. S.; Cerveny, C. G.; Hamblett, K. J.; Blackmore, R. S.; Torgov, M. Y.; Handley, F. G. M.; Ihle, N. C.; Senter, P. D.; Alley, S. C. *Bioconjugate Chem.* **2005**, *16*, 1282−1290.
(14) Ducry, L. *Antibody-Drug Conjugates*; Humana Press: New York City, NY, 2013; Vol. *1045*.
(15) Shen, B. Q.; Xu, K.; Liu, L.; Raab, H.; Bhakta, S.; Kenrick, M.; Parsons-Reponte, K. L.; Tien, J.; Yu, S. F.; Mai, E.; Li, D.; Tibbitts, J.; Baudys, J.; Saad, O. M.; Scales, S. J.; McDonald, P. J.; Hass, P. E.; Eigenbrot, C.; Nguyen, T.; Solis, W. A.; Fuji, R. N.; Flagella, K. M.; Patel, D.; Spencer, S. D.; Khawli, L. A.; Ebens, A.; Wong, W. L.; Vandlen, R.; Kaur, S.; Sliwkowski, M. X.; Scheller, R. H.; Polakis, P.; Junutula, J. R. *Nat. Biotechnol.* **2012**, *30* (2), 184−9.
(16) Adem, Y. T.; Schwarz, K. A.; Duenas, E.; Patapoff, T. W.; Galush, W. J.; Esue, O. *Bioconjugate Chem.* **2014**, *25* (4), 656−64.
(17) Boswell, C. A.; Mundo, E. E.; Zhang, C.; Bumbaca, D.; Valle, N. R.; Kozak, K. R.; Fourie, A.; Chuh, J.; Koppada, N.; Saad, O.; Gill, H.; Shen, B. Q.; Rubinfeld, B.; Tibbitts, J.; Kaur, S.; Theil, F. P.; Fielder, P. J.; Khawli, L. A.; Lin, K. *Bioconjugate Chem.* **2011**, *22* (10), 1994−2004.




DOI: 10.1021/acs.analchem.8b04699
*Anal. Chem.* 2019, 91, 2805−2812

(18) Lyon, R. P.; Bovee, T. D.; Doronina, S. O.; Burke, P. J.; Hunter, J. H.; Neff-LaFord, H. D.; Jonas, M.; Anderson, M. E.; Setter, J. R.; Senter, P. D. *Nat. Biotechnol.* **2015**, *33* (7), 733−5.
(19) Valliere-Douglass, J. F.; McFee, W. A.; Salas-Solano, O. *Anal. Chem.* **2012**, *84* (6), 2843−2849.
(20) Firth, D.; Bell, L.; Squires, M.; Estdale, S.; McKee, C. *Anal. Biochem.* **2015**, *485*, 34−42.
(21) Chen, J.; Yin, S.; Wu, Y. J.; Ouyang, J. *Anal. Chem.* **2013**, *85* (3), 1699−1704.
(22) Wiggins, B.; Liu-Shin, L.; Yamaguchi, H.; Ratnaswamy, G. *J. Pharm. Sci.* **2015**, *104* (4), 1362−72.
(23) Fekete, S.; Veuthey, J. L.; Beck, A.; Guillarme, D. *J. Pharm. Biomed. Anal.* **2016**, *130*, 3−18.
(24) Alpert, A. J. *J. Chromatogr. A* **1986**, *359*, 85−97.
(25) Xiu, L.; Valeja, S. G.; Alpert, A. J.; Jin, S.; Ge, Y. *Anal. Chem.* **2014**, *86* (15), 7899−906.
(26) Chen, B.; Peng, Y.; Valeja, S. G.; Xiu, L.; Alpert, A. J.; Ge, Y. *Anal. Chem.* **2016**, *88* (3), 1885−91.
(27) Wiggins, B.; Liu-Shin, L.; Yamaguchi, H.; Ratnaswamy, G. *J. Pharm. Sci.* **2015**, *104* (4), 1362−1372.
(28) McCue, J. T. *Methods Enzymol.* **2009**, *463*, 405−414.
(29) Queiroz, J. A.; Tomaz, C. T.; Cabral, J. M. S. *J. Biotechnol.* **2001**, *87*, 143−159.
(30) Rippel, G.; Szepesy, L. *J. Chromatogr. A* **1994**, *664*, 27−32.
(31) Machold, C.; et al. *J. Chromatogr. A* **2002**, *972*, 3−19.
(32) Xia, F.; Nagrath, D.; Garde, S.; Cramer, S. M. *Biotechnol. Bioeng.* **2004**, *87* (3), 354−63.
(33) To, B. C.; Lenhoff, A. M. *J. Chromatogr. A* **2007**, *1141* (2), 235−43.
(34) Baca, M.; De Vos, J.; Bruylants, G.; Bartik, K.; Liu, X.; Cook, K.; Eeltink, S. *J. Chromatogr. B: Anal. Technol. Biomed. Life Sci.* **2016**, *1032*, 182−188.
(35) Chen, B. F.; Lin, Z. Q.; Alpert, A. J.; Fu, C. X.; Zhang, Q. Y.; Pritts, W. A.; Ge, Y. *Anal. Chem.* **2018**, *90* (12), 7135−7138.
(36) Bobaly, B.; Beck, A.; Veuthey, J. L.; Guillarme, D.; Fekete, S. *J. Pharm. Biomed. Anal.* **2016**, *131*, 124−132.
(37) Huang, X.; Wirth, M. J. *Anal. Chem.* **1997**, *69* (22), 4577−4580.
(38) Valeja, S. G.; Xiu, L.; Gregorich, Z. R.; Guner, H.; Jin, S.; Ge, Y. *Anal. Chem.* **2015**, *87* (10), 5363−5371.
(39) Janin-Bussat, M. C.; Dillenbourg, M.; Corvaia, N.; Beck, A.; Klinguer-Hamour, C. *J. Chromatogr. B: Anal. Technol. Biomed. Life Sci.* **2015**, *981*, 9−13.



DOI: 10.1021/acs.analchem.8b04699
*Anal. Chem.* 2019, 91, 2805−2812